Labeled Mimics of *N*-Acetyl-D-Fucosamine

By

Michael R. Evans

Submitted in Partial Fulfillment of the Requirements

for the Degree of

Master of Science

in the

Chemistry

Program

YOUNGSTOWN STATE UNIVERSITY

May, 2008

Labeled Mimics of *N*-Acetyl-D-Fucosamine

Michael R. Evans

I hereby release this thesis to the public. I understand that this thesis will be made available from the OhioLINK ETD Center and the Maag Library Circulation Desk for public access. I also authorize the University or other individuals to make copies of this thesis as needed for scholarly research.

Signature:

_____
Michael R. Evans   Date

Approvals:

_____
Dr. Peter Norris   Date
Thesis Advisor

_____
Dr. John A. Jackson   Date
Committee Member

_____
Dr. Nina V. Stourman   Date
Committee Member

_____
Dr. Peter J. Kasvinsky   Date
Dean of Graduate Studies and Research

Thesis Abstract

The synthesis of *N*-acetyl-D-fucosamine and derivatives will be attempted from inexpensive commercially available starting materials. The final products contain medicinally important markers such as fluorine, which can be viewed easily by examining ^{19}F nuclear magnetic resonance spectra. Protective group chemistry will have a major role in this work and enables the selective introduction of markers into *N*-acetyl-D-fucosamine derivatives. Another crucial chemical process includes inverting the stereochemistry at *C*-4 of the precursor, namely *N*-acetyl-D-glucosamine. 1-D and 2-D nuclear magnetic resonance studies will be used to verify regiochemical and stereochemical outcomes of reactions.

Carbohydrates such as *N*-acetyl-D-fucosamine and its derivatives mimic the types of molecules found in the capsular polysaccharides of bacteria such as *Staphylococcus aureus*. If incorporated into the bacterium's capsular polysaccharides, this should modify the capsular polysaccharides possibly allowing the human immune system to recognize the bacterium. Therefore, these types of compounds are likely candidates for antibiotics against such bacteria.

Acknowledgements

I would like to begin by thanking Dr. Norris for giving me this great opportunity and for pushing me to always try my hardest. I do not think I would have realized my potential if I had would have never met him. I want to also thank Dr. Jackson for helping me with everything and for his comic relief. I would also like to thank the Norris group for all their help and support. I would especially like to thank Ryan, Jen, and Brian for being great friends and also going to the movies a lot and seeing people dressed as pirates. I would also like to thank Beagle for the "extreme" time at Denny's and also for being a good friend.

I would especially like to thank my Dad, Mom, and my brother for always believing that I could achieve anything that I wanted to do. I am honored and privileged to have such a caring and compassionate family as I do. My family has made a lot of sacrifices for my education and I am forever in debt to them. Last and most importantly I would like to thank my wife Kari. She has always been there for me and supported me through the good and the bad times. She has also sacrificed many things for me to go to graduate school which I greatly appreciate. I am looking forward to spending the rest of my life with her and also to creating a lot of memories to replace any that were lost.

Table of Contents

      1.   *O*-Glycoside Synthesis

      2.   Attempted Fluorination of *O*-Glycosides

List of Tables

List of Schemes

List of Equations

List of Figures

Introduction

       Carbohydrates are among the most abundant constituents of plants and animals[1] and have played many important roles in major civilizations such as the manufacturing of beer and wine by alcoholic fermentation of grain starch and grape sugar, which was well documented on the walls of ancient Egyptian tombs, to the isolation of sucrose from the juice of sugarcane dating back to fourth century Chinese civilization. Another important process still in use today is the manufacture of paper from wood pulp achieved around the first century by the Chinese civilization and which constituted a marked improvement over the then-available Egyptian papyri.[2] It was not until the nineteenth century that Emil Fischer did his groundbreaking research that started one of the most important and useful fields of chemistry.[3] The name "carbohydrate" arose from the belief that each substance of this type consisted solely of the elements of carbon and water and had a molecular formula that could be expressed as $C_x(H_2O)_y$.[1,2,4,5] Carbohydrates have many other uses besides being manipulated by humankind. They serve as sources of energy (sugars), and as stores of energy (starch and glycogen) and are the supporting tissue of plants (cellulose).[1] In the arthropods, a major constituent of the exoskeleton (shell) is chitin, a polymer of 2-acetamido-2-deoxy-D-glucose.[4] Very many other biological functions are performed by carbohydrate materials; in particular, they play many roles as recognition compounds, for example between cells, as antigens and as blood group substances. They have many key roles, often in association with proteins in, for example, bacterial cell walls, mammalian cartilage tissue and some enzymes.[6] In addition to being biologically important, carbohydrates serve many important roles in modern industry. These include the food industry, which uses huge amounts of starch in various degrees of

purity in the manufacture of baked goods and pastas, and of gums in food processing; the textile industry, which, despite the advent of synthetics, is still dependent to a large extent on cellulose; the pharmaceutical industry, particularly in the areas of antibiotics such as amphotericin B (Figure 1), intravenous solutions, and vitamin C; and the chemical industry, which produces and markets several pure sugars and their derivatives.[2]
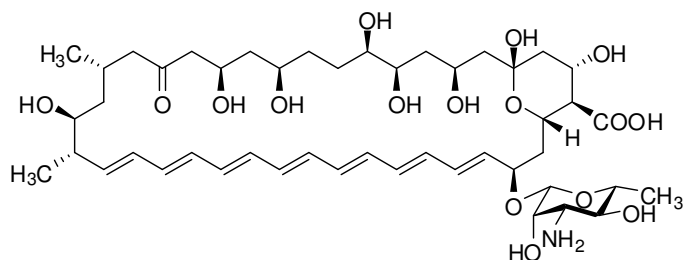
Figure 1: Example of antifungal pharmaceutical Amphotericin B.

Synthetic organic chemists use carbohydrates for many reasons. Readily available natural carbohydrates, such as D-glucose, prove to be relatively inexpensive. They also help solve an ever increasing demand for stereoselectivity. Making a synthesis enantioselective can be a simple or difficult task, but regardless it requires introduction of optical activity from a natural source, either through a chiral auxiliary in an enantioselective reaction or by using a chiral starting material.[7] As previously mentioned, carbohydrates play a vital role in a broad range of applications thus making them prime targets for many different syntheses. Even though there are many advantages to using carbohydrates, there are also disadvantages. The main disadvantages are the employment of tedious functional group interconversions and protection/deprotection strategies.[7] This can become tiresome to a chemist but there are many ways developed to

do functional group interconversions and protection/deprotection schemes to try and alleviate the typical problems with carbohydrate chemistry.
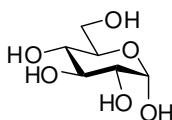
Figure 2: α-D-Glucose, example of a monosaccharide.

Carbohydrates are traditionally considered in three different groups: monosaccharides (Figure 2), oligosaccharides, and polysaccharides. Monosaccharides are the simple sugars which cannot be hydrolyzed to smaller molecules and from which the two other groups are obtained by formation of glycosidic linkages.[8] The term *sugar* has been used to mean sucrose by the general public, glucose by the medical profession, and mono- to oligosaccharides by chemists.[2-4,6] Monosaccharides can first be divided into two main groups according to whether their acyclic form possesses an aldehyde- or keto-group designated as *aldose* and *ketose* respectively (Figure 3). They can be further classified according to the number of carbon atoms the molecule contains. Trioses have the general formulae ($C_3H_6O_3$), tetroses ($C_4H_8O_4$), pentoses ($C_5H_{10}O_5$), and hexoses ($C_6H_{12}O_6$), etc. with subdivisions being made according to functional groups which may also be present.[8]
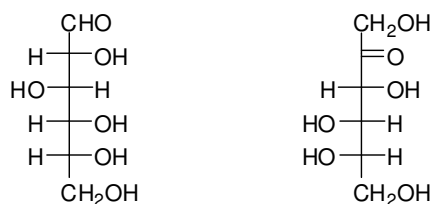
Figure 3: Examples of aldose (D-Glucose, left) and ketose (L-Fructose, right).

Further classification among monosaccharides involves assigning different notations based on the configuration of the molecule as according to the *Rosanoff convention*.[6] The D and L convention is used to differentiate between enantiomers of a sugar. This convention employs observing the furthest chiral centre from the most oxidized carbon and is designated as having a D configuration if the hydroxyl group is on the right hand side of a Fischer projection and if the hydroxyl is on the left hand side the molecule it is designated as having an L configuration (Figure 3). Another configuration exists because monosaccharides have the ability to exist in cyclic and acyclic forms. The cause of this is the unique functional moiety centered about C-1. In solution a cyclic hemiacetal such as D-glucose converts to the acyclic form and is represented in its straight chain form (**A** in Figure 4). Four different combinations can be formed through the cyclization of the acyclic form. The α- and β-anomers are determined by the position of the hydroxyl at C-1 otherwise known as the anomeric carbon. If the hydroxyl is positioned below the ring (**B** and **C**) the relative configuration about the anomeric carbon is said to be α anomer and if it is above the ring (**D** and **E**) the relative configuration is designated as the β anomer. The only exception to this convention is when the sugar is in the L configuration. Freudenberg developed a convention that if the hydroxyl at the anomeric centre was pointed downward in Haworth formulae (below the ring on a chair form) and had a configuration of L then the anomeric centre was designated as the β-anomer and likewise if the hydroxyl was pointing up in a Haworth formulae (above the ring on the chair form) the relative configuration was designated as the α-anomer.[6]
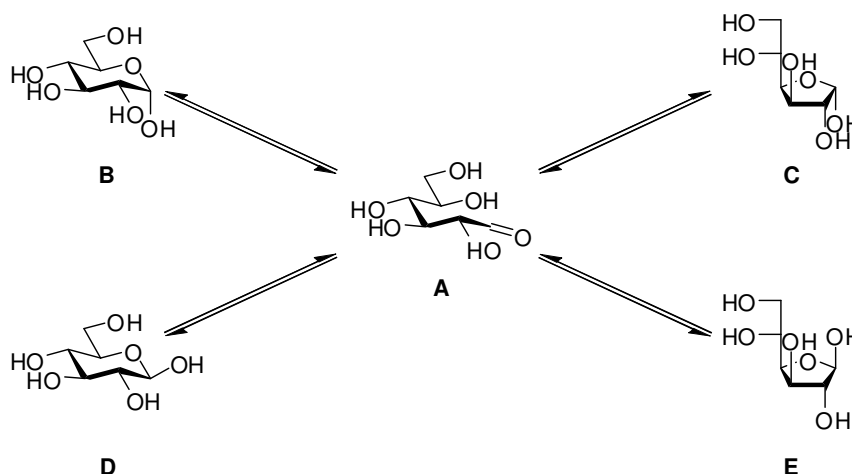
Figure 4: Examples of α and β anomers for 5- and 6-membered rings for D-glucose.

The pyranose (**B** and **D**) and furanose (**C** and **E**) forms are not static as represented in Figure 4 but exist with different conformations. The pyranose ring has many recognized conformers including two chairs, six boats, twelve half-chairs, and six skews. The principle conformations of the furanose ring are the envelope and the twist form.[5] The compounds discussed herein adopt the chair conformation in the pyranose form and this will therefore be the only conformation covered. There are two main chair conformations for the pyranose ring and these are designated $^4C_1$ and $^1C_4$ (Figure 5). The conformer is designated a notation according to which carbon atom is above and below the plane of the chair. The carbon atom above the plane is written in superscript on the left side of C and the atom that is below the plane is written in subscript on the right side of the C. Thus the conformer on the left (Figure 5) has carbon 4 above the plane and carbon 1 below the plane and is written as $^4C_1$. Likewise, the conformer on the right has carbon 4 below the plane of the ring and carbon 1 above the plane and is designated $^1C_4$. The preferred conformer depends on the groups attached and closely relates to basic cyclohexane conformational analysis. This steric effect is a combinatorial effect due to

either favorable or unfavorable diaxial interactions caused by the attached substituents or because of the stability of the substituents being in the axial or equatorial conformation. The conformer that will be discussed later will take the form of $^4C_1$.
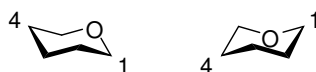
Figure 5: The $^4C_1$ (left) and $^1C_4$ (right) pyranose chair conformers.

Another effect with sugars influences the configuration about the anomeric centre and is appropriately named the *anomeric effect*. The anomeric effect is not governed by sterics but rather by stereoelectronic factors. Carbohydrates ($X = O$-alkyl, O-aryl, O-acyl, halide, etc.) prefer the illustrated conformation (Figure 6, left) and the extent of this preference decreases in solvents of increasing polarity and increases with increase in the electronegativity of X. The effect, identified by Edward and studied extensively by Lemieux, apparently is caused mainly by interaction between the axial lone pairs of electrons on the ring oxygen atoms and the antibonding σ*-orbital of the C–X bond. This leads to shortening of the bond connecting the ring oxygen atom to the anomeric centre and lengthening of the C–X bond in the case of anomers having the X group axial relative to the respective bond lengths in the equatorial anomer. Variations of just this kind have been found by X-ray and neutron diffraction analyses of many carbohydrates and have been predicted by theoretical studies applied to model systems such as dimethoxymethane in different conformations.[6] The less stable configuration (Figure 6, right) is the β-anomer and exhibits electrostatic repulsion between the lone pair electrons of the ring oxygen atom and the bonding σ-orbital electrons of the C–X bond. Figure 6 is a representation of the D configuration and not the L configuration. The stability of

each anomer can easily be compared by utilizing nuclear magnetic resonance (NMR) spectroscopy and integrating the α- and β-signals and comparing the ratio of one relative to the other. In an aqueous solution, 2-acetamido-2-deoxy-D-glucose exhibits a 61:39% mixture of α- to β-anomers respectively.[9] Even though the α-anomer exhibits 1,3-diaxial interactions, the anomeric effect is still thermodynamically favorable exemplifying how strong this effect is. Upon acetylation and chlorination at the anomeric carbon, 2-acetamido-3,4,6-tri-*O*-acetyl-α-D-glucopyranosyl chloride exhibits 96% of the α-anomer and was solved by NMR spectroscopy. This was done using the H-1 and H-2 coupling constant (found as 3.8 Hz) showing the α-anomer to be major.[10] When the anomeric proton is in the *gauche* orientation compared to H-2, the coupling constant is relatively small and around 3–4 Hz. When it is in the *anti* orientation with respect to H-2 the coupling constant is larger and around 7–8 Hz.

Figure 6: Example of anomeric effect.

The compounds that are formed when two or more monosaccharides are joined together are classified as oligosaccharides. More specifically oligosaccharides contain anywhere from 2–10 monosaccharides joined together *via* glycosidic linkages.[11] Oligosaccharides are grouped into simple (or true) oligosaccharides, which on depolymerization yield monosaccharides only, and conjugate oligosaccharides, which are linked to nonsaccharides such as peptides and lipids and on depolymerization yield monosaccharides and aglycons. The simple oligosaccharides are further classified

according to the degree of polymerization, into disaccharides, trisaccharides, tetrasaccharides, etc.; whether they are composed of one or more types of monosaccharides, into *homo-* and *hetero*-oligosaccharides; and finally whether they do or do not possess a hemiacetal function at one terminus of the molecule, into reducing and non-reducing oligosaccharides.[2]
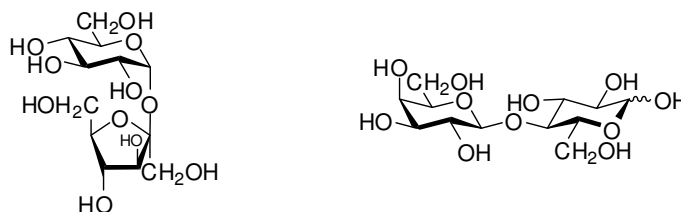
Figure 7: Examples of disaccharides sucrose and lactose.

The most common oligosaccharides are sucrose and lactose. Sucrose (Figure 7, left) is a *hetero*-oligosaccharide composed of D-glucose and D-fructose. Lactose (Figure 7, right) is also a *hetero*-oligosaccharide composed of D-glucose and D-galactose.

As mentioned previously, carbohydrates serve many more roles other than nutritional value. A major role that oligosaccharides play an important part in is biological activity. There is evidence in Nature to confirm that carbohydrates are indeed involved in dynamic biological messages and thus lead to cell differentiation and cell-cell recognition processes. Moreover, it has been discovered that oligosaccharides of even short sequences are used for carrying important biological information. For example, human blood groups are differentiated by relatively simple changes in oligosaccharide structure (Figure 8).[11]
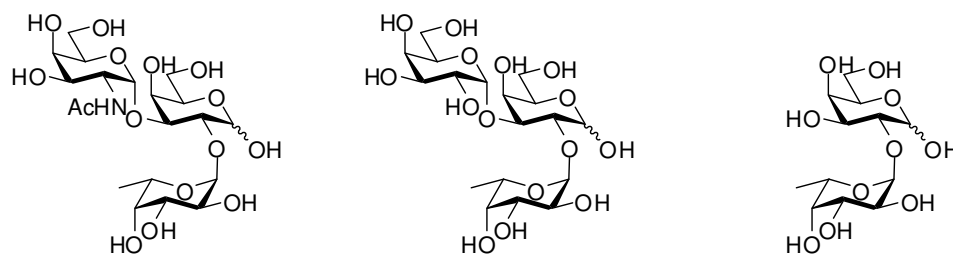
Figure 8: Examples of oligosaccharides, Human Blood Groups A, B, and H.

Biologically, oligosaccharides have been found to play other important roles such as using the highly sulfated oligosaccharide Heparin (Figure 9) for blood clotting in addition to key biological processes involving lectins. Lectins are found on the surface of all cell membranes, for example liver cells, macrophages, and epithelial and tumor cells, and can interact with oligosaccharides present on surrounding cells. Hence they play key roles in molecular recognition. Oligosaccharide:lectin binding plays a fundamental role in the conception of human life. Union of the egg and sperm is of low probability, but the chances of fertilization are improved by chemoattractants produced by the egg which attract the sperm. Oligosaccharides present on the surface of the sperm cells allow the sperm to interact with lectins on the egg's surface and initiate fertilization of the egg. These oligosaccharides interact by specific recognition of α-galactosyl and α-fucosyl end-groups by the spermatozoa receptors. It is interesting that once the egg has been fertilized, it then releases an enzyme which cleaves the oligosaccharides from the surface of the sperm cells so that further fertilization is discouraged.[11]
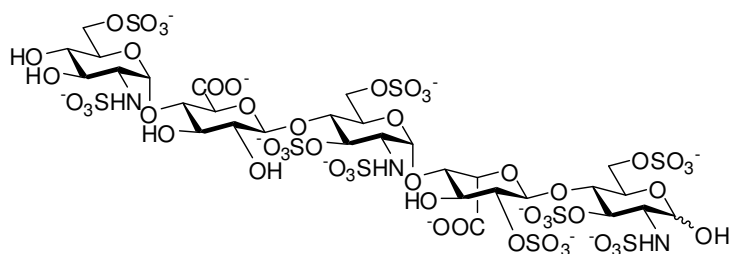
Figure 9: Example of oligosaccharide; Heparin.

Polysaccharides are natural macromolecules occurring in almost all living organisms, constituting one of the largest groups of natural compounds classified thus far, and function either as an energy source or as structural units in the morphology of the living material in which they are endogenous. Examples of polysaccharides possessing structural functions are cellulose (Figure 10, top), a polymer of D-glucose which is probably the most abundant naturally occurring organic substance and is the structural material of plants; and chitin (Figure 10, bottom), a polymer of 2-acetamido-2-deoxy-D-glucose which is the major organic component of the exoskeleton (shells) of insects, crabs, lobsters, etc.[8]
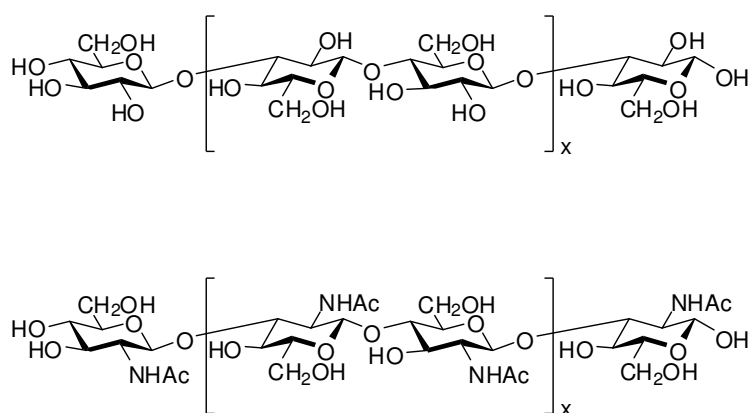
Figure 10: Example of polysaccharides; cellulose and chitin.

The term "glycan" (derived from glycose, meaning a simple monosaccharide), is another word for polysaccharide, but a more specific term is obtained by using the configurational prefix of the parent sugar with the suffix –an to signify a polymer. Further specificity is achieved by inclusion of the D- or L-configuration, as appropriate, for example, D-glucan from D-glucose. Polysaccharides which, on hydrolysis, yield only one type of monosaccharide are called *homo*glycans, whereas those which can be hydrolyzed to more than one type of monosaccharide are called *hetero*gylcans, with designatory prefixes of di-, tri-, etc., for the number of monosaccharide types involved.[8]

As stated previously carbohydrates exist in almost every facet of Biology ranging from structural features of plants and shellfish to cell-to-cell recognition factors and also play many roles in bacteria. The opportunistic bacteria *Staphylococcus aureus* (*S. aureus*) is a Gram-positive bacterium that causes a wide range of diseases and infections in humans and animals. Infections caused by *S. aureus* can prove to be lethal if left untreated. *S. aureus* is a major cause of wound infections and has the invasive potential to induce osteomyelitis, endocarditis, and bacteremia, leading to secondary infections in any of the major organ systems.[12] *S. aureus* has also been found to cause a severe, but rare, flesh eating infection called *necrotizing fasciitis*. Usually, *necrotizing fasciitis* is a synergistic polymicrobial infection that occurs in patients with coexisting factors such as diabetes, vascular disease, alcoholism, intravenous drug abuse or other causes for altered immune function. This case of *necrotizing fasciitis* was found to be monomicrobial *S. aureus*-induced showing how virulent the bacterium can be.[13] Though some humans are a natural reservoir for *S. aureus* most infections caused by *S. aureus* originate from being hospitalized. Carriage rates are 25% to 50%; higher rates in the general population are

observed in injection drug users, persons with insulin-dependent diabetes, patients with dermatologic conditions, patients with long-term indwelling intravascular catheters, and health-care workers.[14] The virulence of *S. aureus* is essentially the side effect of the bacterium succumbing to adverse environments. This constellation of bacterial products allows staphylococci to adhere to eukaryotic membranes, resist opsonophagocytosis, lyse eukaryotic cells, and trigger the production of a cascade of host immunomodulating molecules.[12]

One of the most dramatic syndromes caused by *S. aureus* after bacteremia is acute bacterial endocarditis leading to septic shock or disseminated intravascular coagulation.[15] The mortality rate in such cases ranges from 40 to 80%, depending on the age of the infected person. Frequent complications include high fever, pulmonary abscesses, meningitis, glomerulonephritis, specific arthritis, etc.[15] Many antibiotic resistant strains of *S. aureus* have emerged ever since antibiotics were used to defend against the bacterium. A thorough discussion of some of the antibiotics used to treat against *S. aureus*, their typical biological targets, and their mechanism of action will give insight into the current resistant *S. aureus* strains.

Antibiotics generally target enzymes that are vital to the survival of bacteria. Such targets include, but are not limited to, cell wall synthesis, the cytoplasmic membrane, nucleic acid synthesis, and ribosome function. The peptidoglycan is the one polymer found in the cell walls of both Gram-positive and negative bacteria that is considered to be essential for survival of bacteria growing in hypotonic environments: many lines of evidence suggest that its removal or interference with its synthesis results in loss of rigidity and leads to cell death. The strength and rigidity of the peptidoglycan

results from a basic framework composed of oligosaccharide backbone chains linked together in an irregular manner by short branched peptide chains of 7-12 amino acid residues. One of the enzymes that assemble this important structure is the transpeptidase. The transpeptidase carries out the hydrolysis of a peptide bond of the terminal D-Ala residue of the D-Ala-D-Ala substrate and makes a crosslink with a free amino group bonded to the peptidoglycan. Penicillin, more generally known as a β-lactam (Figure 11), mimics the D-Ala-D-Ala substrate and irreversibly binds the transpeptidase ceasing the production of the rigid peptidoglycan structure. Other penicillin-sensitive enzymes include D,D-carboxypeptidases, L,D-carboxypeptidases/ transpeptidases, and endopeptidases.[16] Penicillin was originally isolated biologically from a strain of *Penicillium notatum*. The mechanism of the production of the β-lactam-thiazolidine ring nucleus common to all penicillins can be conceived of as a condensation product of L-cystine and D-valine. Indeed, these two amino acids are the precursors of the nucleus even though valine enters the biosynthetic path as the L form.[17]
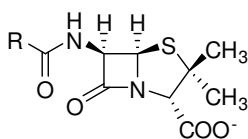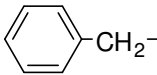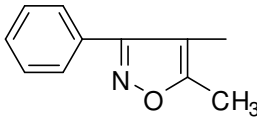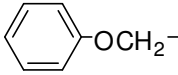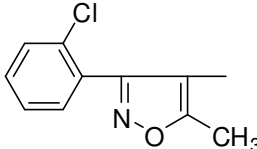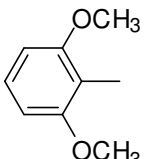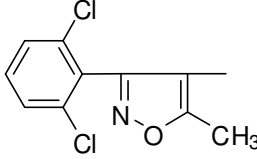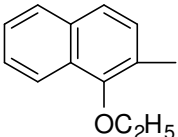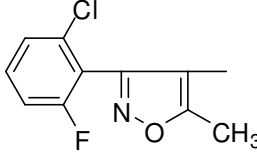
Figure 11: General structure of the penicillin family.

Studies have shown that there is a correlation between the overuse of antibiotics and the emergence of bacteria that show signs of resistance to antibiotics.[18,19] Others believe that resistant bacteria will inevitably develop and have produced resistance genes long before the 'antibiotic era'.[20,21] One constant factor with both arguments is that bacteria are becoming resistant to a growing number of antibiotics used to treat

infections. Bacteria have developed a mechanism of evading β-lactam antibiotics by producing a β-lactamase, of which several different types exist.[22] The β-lactamase hydrolyzes the peptide bond of the β-lactam ring rendering it incapable of inhibiting their target enzymes. To combat this emerging resistance, different groups (Table 1) were placed off of the β-lactam ring to prevent it from being cleaved by the β-lactamase but still capable of inhibiting the target enzyme. To date over 40 structurally different β-lactam molecules are available in 73 formulations.[23] Benzyl penicillin is considered the original penicillin with popular derivatives such as methicillin, oxacillin, cloxacillin, and flucloxacillin.

Table 1: Various penicillins showing respective R groups.

Cephalosporins are also a β-lactam family of antibiotic that closely resemble the family of penicillins but are slightly different by the fused β-lactam/dihydrothiazine ring system.[16] Both exhibit the same basic structure-activity relationships by mimicking the D-Ala-D-Ala moiety and differences of the 'R' group on the general structure of cephalosporins yields many different compounds.
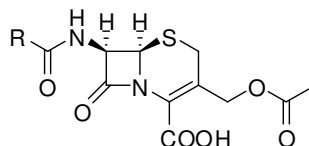
Figure 12: General structure of cephalosporins.

The emergence of high levels of penicillin resistance followed by the development and spread of strains resistant to the semisynthetic penicillins (methicillin, nafcillin, and oxacillin), macrolides, tetracyclines, and aminoglycosides has made therapy of staphylococcal disease a global challenge.[24] Although the emergence of penicillin resistant *S. aureus* was documented in 1944, only three years after penicillin had been introduced, the bacterium was 85% to 90% resistant to penicillin by the late 1950's to early 1960's. In only six years, 25% of the bacteria became resistant to penicillin. Methicillin was introduced in 1961 and, in less than one year, *S. aureus* showed signs of being resistant. It took 25-30 years for 25% of *S. aureus* to show signs of resistance becoming widely known as methicillin resistant *Staphylococcus aureus* (MRSA).

The most effective antibiotic thus far has been vancomycin. It took 40 years for the advent of a resistant strain of *S. aureus* to vancomycin.[14] Similar to β-lactams, it also affects cell wall synthesis by inhibiting the transpeptidase responsible for the peptide cross-linking of the polysaccharide backbone and the transglycosylase reaction that

polymerizes the polysaccharide backbone, and it does so by binding to D-Ala-D-Ala found in the peptidoglycan precursor of the bacterial cell wall.[25] Encountering similar problems that the β-lactam family have encountered, *S. aureus* has an increasing number of strains that keep emerging that are resistant to vancomycin.[26]
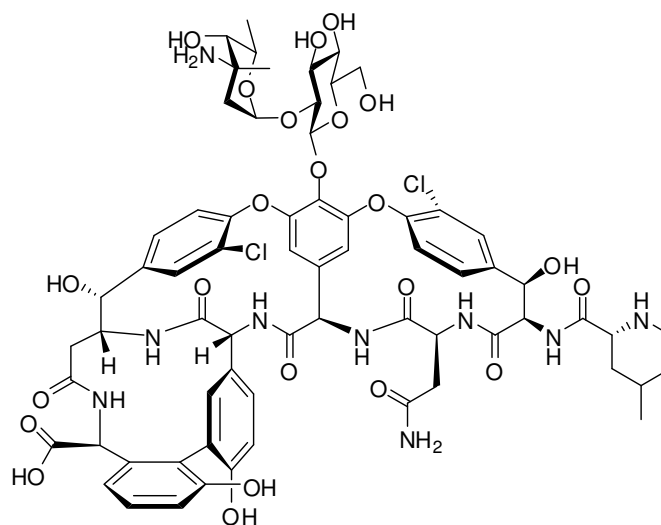
Figure 13: The structure of vancomycin.

With the emergence of vancomycin-resistant *Staphlycoccus aureus* (VRSA) strains, alternate forms of the antibiotic have to be developed to combat the resistance. The structure of vancomycin had to be deduced and was accomplished *via* X-ray crystallography so the compound could then be synthesized.[27] The next strategy would be to synthesize the natural product to enable transformations at any place in the compound. Several strategies have been employed ranging from typical reaction sequences to dealing with problems of atropisomerisms found in the aglycon portion of the compound.[25,28-30] A recent modification to the vancomycin aglycon was engineered so that it would overcome a change from the D-Ala-D-Ala moiety to the D-Ala-D-Lac moiety of the most common strains of enterococci resistant to vancomycin. The outcome

was the removal of one carbonyl in the pentapeptide chain which was replaced with a methlyene. This change was achievable through assembly of that peptide *via* reductive amination.[31]

Antibiotics have also been effective when used to disrupt ribosome function. The most common antibiotics that belong to this class include streptomycin, tetracyclines, macrolides, and erythromycin.[16] The bacterial components and secreted products that affect the pathogenesis of *S. aureus* infections are numerous and include surface-associated adhesions, a capsular polysaccharide, exoenzymes, and exotoxins, some of which cause diseases such as toxic shock syndrome and food poisoning.[12,32] The capsular polysaccharide (CP) has emerged as a novel target for possible vaccines and antibiotics.[34,35] The CP is also present in various bacteria so antibiotic activity has the possibility to have a broad spectrum. Most of the clinical isolates of *S. aureus* produce capsular polysaccharides and eleven serotypes have been identified.[35] Of the eleven serotypes, serotypes 5 and 8 account for ~25% and 50%, respectively, of isolates recovered from humans.[12]
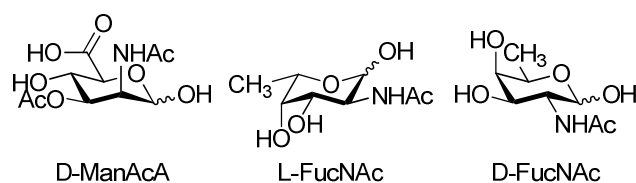
Figure 14: Structures of saccharide residues in *S. aureus* serotypes 5 and 8.

The monosaccharides (Figure 14) that construct the repeating trisaccharide serotypes 5 and 8 consist of 2-acetamido-D-mannosamineuronic acid (*N*-acetyl-D-mannosamineuronic acid or D-ManAcA), 2-acetamido-2,6-dideoxy-L-galactose (*N*-

acetyl-L-fucosamine or L-FucNAc), and 2-acetamido-2,6-dideoxy-D-galactose (*N*-acetyl-D-fucosamine or D-FucNAc) residues.
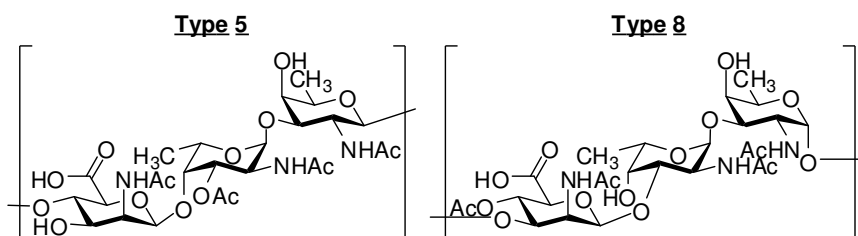
Figure 15: Structures of the repeating units of the capsular polysaccharide of serotypes 5 and 8 of *Staphylococcus aureus*.

The serotype 5 capsular polysaccharide manufactured by *S. aureus* has a trisaccharide repeating unit structure of (→4)-3-*O*-Ac-β-D-ManNAcA-(1→4)-α-L-FucNAc-(1→3)-β-D-FucNAc-(1→). The structure of serotype 5 is very similar to the structure of serotype 8, which is (→3)-4-*O*-Ac-β-D-ManNAcA-(1→3)-α-L-FucNAc-(1→3)-β-D-FucNAc-(1→).[36] The differences between serotype 5 and 8 include the linkages between the sugars and the position of *O*-acetylation of the mannosamineuronic acid residues (Figure 15).

The biosynthesis of the microcapsule serotype 5 (Figure 16) involves three main pathways for each of the sugars present in the microcapsule. All three pathways begin with the same starting material namely UDP-*N*-acetyl-D-glucosamine (UDP-D-GlcNAc). The genes that code for the enzymes that make the transformations are shown in parentheses with their respective gene products underneath them. The first pathway begins with a 4,6-dehydratase yielding UDP-2-acetamido-2,6-dideoxy-D-*xylo*-4-hexulose which is reduced *via* a 4-reductase to UDP-D-FucNAc. The final reaction that occurs utilizes a tranferase to attach the sugar residue to a carrier lipid. The second pathway

utilizes a 4,6-dehydratase and a 3,5-epimerase to give UDP-2-acetamido-2,6-dideoxy-L-*lyxo*-4-hexulose which is then reduced to UDP-L-6dTalNAc by a reductase. A reaction mediated by a 2-epimerase affords UDP-L-FucNAc which is attached to D-FucNAc by a transferase. The last pathway begins with a 2-epimerase to produce UDP-D-ManNAc which is then oxidized to UDP-D-ManNAcA *via* a dehydrogenase. Finally a transferase bonds D-ManNAcA to L-FucNAc to form the type 5 repeating trisaccharide unit (Figure 15) of *S. aureus*.[12]
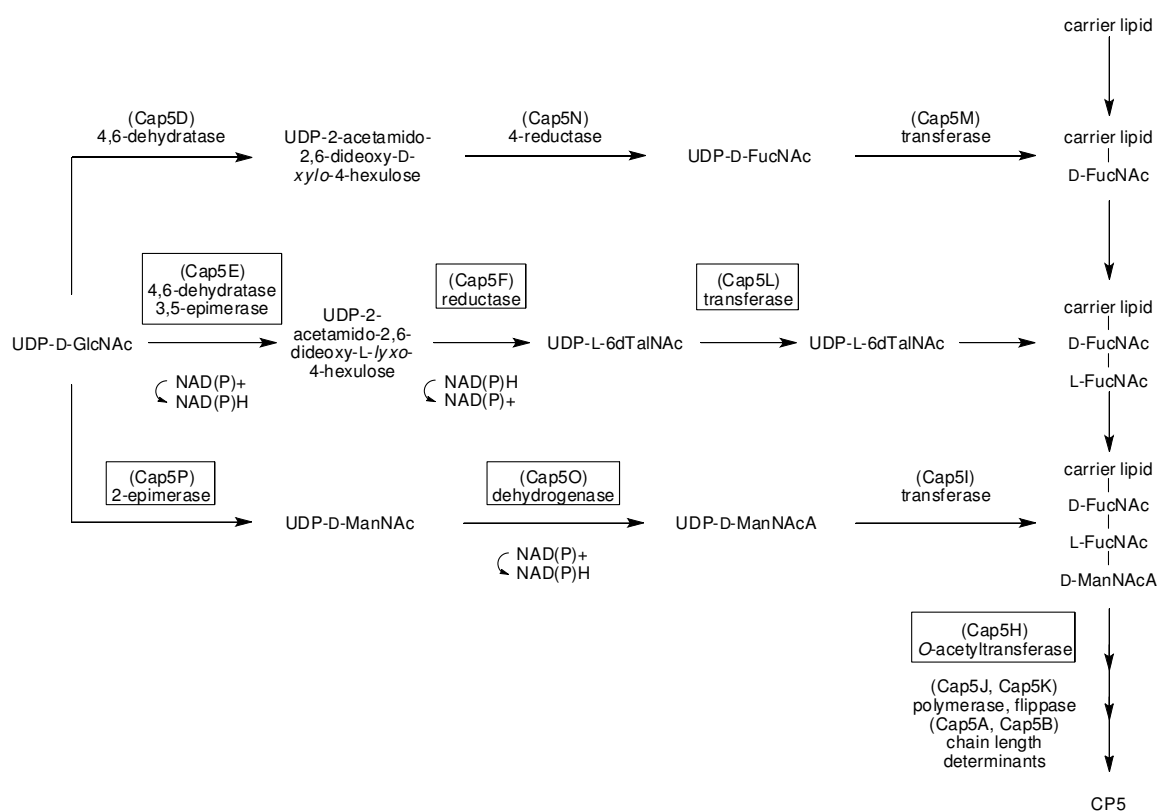
Figure 16: Biosynthesis of the microcapsule serotype 5 of *Staphylococcus aureus*.

Another representation showing the chemical structures associated with the capsular polysaccharide biosynthesis can prove to be useful for determining possible antibiotic targets (Scheme 1). This shows two enzymatic products in the transformation

of UDP-D-GlcNAc to UDP-D-FucNAc. Slight chemical alterations to any of these compounds could possibly inhibit the enzymes that carry out the next step of the biosynthesis.
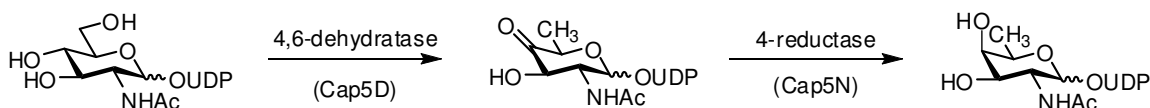
Scheme 1: Transformation of UDP-D-GlcNAc to UDP-D-FucNAc.

N-Acetyl-D-fucosamine is found in both serotypes 5 and 8. As previously shown, the activated form in the bacterium is uridine 5′-(2-acetamido-2,6-dideoxy-α-D-galactopyranosyl diphosphate) and acts as the monosaccharide initiating chain growth.[37] Previous studies enabled the introduction of a label into the acetyl group of *N*-acetyl-D-fucosamine. Illarionov *et al.* synthesized an *N*-acetyl-D-fucosamine derivative using 3,4-di-*O*-acetyl-1,5-anhydro-2,6-dideoxy-D-*lyxo*-hex-1-enitol (3,4-di-*O*-acetyl-D-fucal) as the initial compound. The capability of introducing a [^{14}C] radioactive label will enable further researchers the ability to do biosynthetic studies on *N*-acetyl-D-fucosamine.[37]
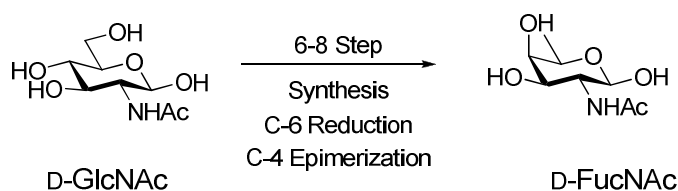
Equation 1: Synthesis of *N*-acetyl-D-fucosamine.

N-Acetyl-D-fucosamine is not available commercially and it is not logical to isolate this compound biologically because not enough material is available to support the high demand for antibiotic development. However it would be feasible to synthesize this

compound from a material that is readily available and relatively affordable. *N*-Acetyl-D-glucosamine would be a good choice because it is possible to synthesize *N*-acetyl-D-fucosamine in eight steps (Equation 1).
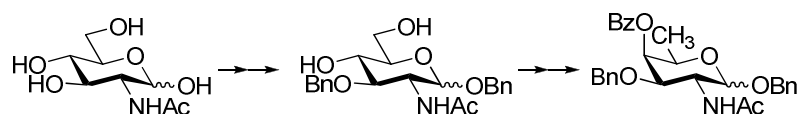
Scheme 2: Horton synthesis of *N*-acetyl-D-fucosamine.

Horton's work will serve as the model for the synthesis of *N*-acetyl-D-fucosamine derivatives.[38] This synthesis starts with *N*-acetyl-D-glucosamine and through a series of protection and deprotection steps and functional group interconversions, it affords the orthogonally protected product which can be subsequently deprotected producing the target molecule *N*-acetyl-D-fucosamine (Scheme 2).

The complete Horton synthesis is shown in Scheme 3. Through a series of protection and deprotection steps followed by a reduction and epimerization and finally two more deprotection steps, the target compound was made. It begins by protecting O-4 and O-6 with an isopropylidene acetal protecting group and then protection of O-1 and O-3 *via* the Williamson ether synthesis. Subsequent deprotection of the isopropylidene acetal affords a diol. Activation of C-4 and C-6 as sulfonates facilitates chemoselective reduction of the primary sulfonate at C-6 but not the secondary sulfonate. The next step is an S$_N$2 reaction that epimerizes C-4 followed by deprotection of the ester and hydrogenation affording *N*-acetyl-D-fucosamine.
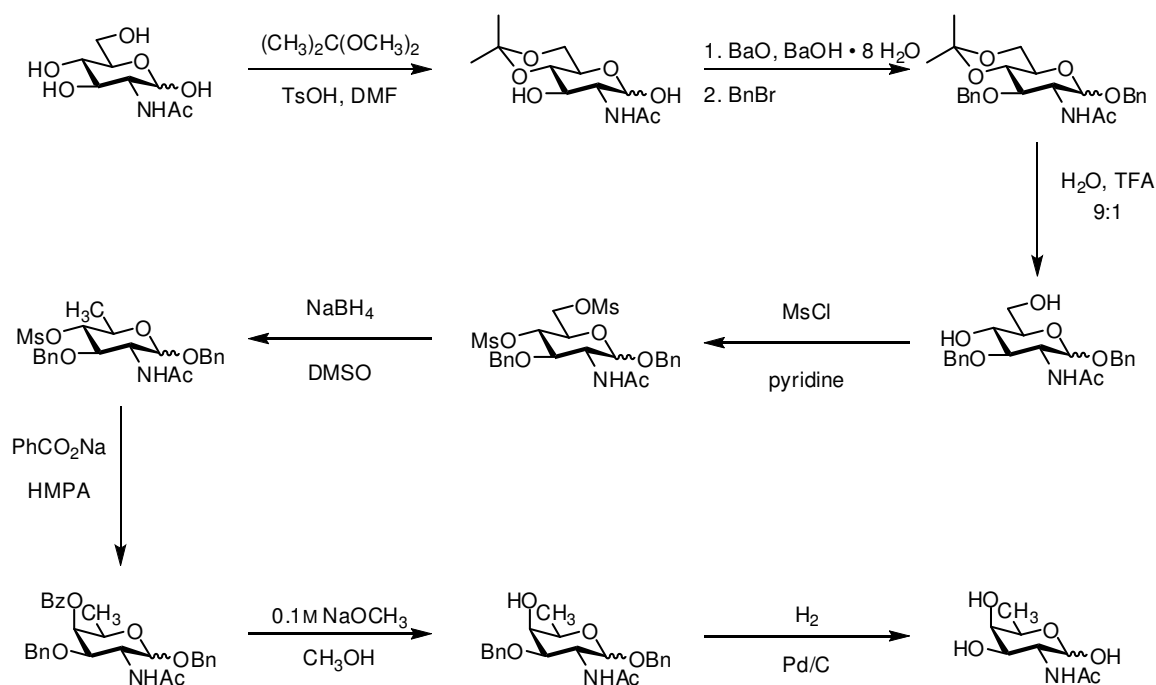
Scheme 3: Complete Horton synthesis of *N*-acetyl-D-fucosamine.

The main goal of this project is to synthesize analogues of *N*-acetyl-D-fucosamine and its biosynthetic intermediates. As described before, slight modifications of natural products allows the possibility of inhibiting enzymes thus serving as antibiotics. A modification to the Horton synthesis may produce biologically active compounds of interest. Fluorinated drugs represent 20-25% of drugs in the pharmaceutical pipeline and includes Fluoxetine also known as Prozac® (antidepressant), Faslodex (anticancer), Flurithromycin (antibacterial) and Efavirenz (antiviral), all of which illustrate the wide range of disease areas benefiting from fluorine chemistry and, from a molecular point of view, the structural diversity of the fluorinated component.[39] Linezolid is a fluorinated drug currently used to treat infections caused by Gram-positive bacteria and belongs to a class of antibacterial agents called oxazolidinones that specifically target early ribosomal protein synthesis.[40] Fluorinated carbohydrates, in particular, have proven to be useful in

studies both of binding interactions between carbohydrates and proteins, and in mechanisms of glycosyl transfer. The reason that fluorinated carbohydrates are useful is twofold. The substitution of a sugar hydroxyl by a fluorine is sterically conservative since it is smaller than the original hydroxyl and, secondly, the hydrogen bonding capabilities of these substituents vary considerably.[41] Because naturally occurring organofluorine compounds are rare, organofluorine compounds are accessible solely by organic synthesis.[42] These compounds will serve as likely candidates to be inhibitors of capsular polysaccharide formation in *S. aureus* or possible labels for enzymatic studies.

Statement of Problem

In the *Staphylococcus aureus* bacterium, carbohydrates comprise the protective microcapsule making it a logical target for antibiotics. The microcapsule acts as a defensive coating that protects against the human immune system. Slightly changing the functionality of these carbohydrates could inhibit the enzymes that produce the microcapsule and exposure to traditional antibiotics would then alleviate the symptoms caused by the bacterium. Of the three carbohydrates that make up the microcapsule, this research will focus on *N*-acetyl-D-fucosamine. Although not available commercially, *N*-acetyl-D-fucosamine can be synthesized from a commercially available starting material; *N*-acetyl-D-glucosamine. A synthesis based on Horton chemistry will afford the product *N*-acetyl-D-fucosamine, and this synthesis will be manipulated to provide compounds capable of serving as possible antibiotics against the *Staphylococcus aureus* bacterium or as labels in enzymatic studies.

Results and Discussion

The primary goal of this project is to synthesize the natural product *N*-acetyl-D-fucosamine from a compound that is relatively abundant and available commercially, namely *N*-acetyl-D-fucosamine. The Horton synthesis will serve as the model for this work (Scheme 3).[38] The secondary goal is to modify the synthesis which may produce small molecule mimetic compounds possibly capable of serving as antibiotic agents against the capsular polysaccharide of *S. aureus* or as labeled compounds in any future enzymatic studies on the bacterium. The small molecule mimetic compounds will be approached by performing nucleophilic substitution using fluorinating reagents as the nucleophiles. Organofluorine compounds have proved to be useful in the pharmaceutical industry by having a broad range of biomedical applications including as antimicrobials.[39-41]

1. *O*-Glycoside Synthesis

The first attempt in the synthesis of *N*-acetyl-D-fucosamine involved protecting the anomeric center of the commercially available starting material *N*-acetyl-D-glucosamine (**1**). This glycosylation was accomplished by bubbling HCl gas through methanol for several minutes, then adding a solution of GlcNAc dissolved in methanol and stirring the mixture. Once TLC (3:1 ethyl acetate:methanol) proved the starting material was consumed from the appearance of a new, less polar spot with an R_f of 0.26, the reaction mixture was evaporated under reduced pressure affording **2α/β** as a yellowish solid in a 94% yield (Scheme 4). The mechanism is thought to be S_N1 with the ^{1}H NMR spectrum shows two singlets at 3.22 and 3.31 ppm representing the methoxyl

protons of the equatorial (β) and axial (α) anomers respectively. The ratio of α and β anomers are 2:1 respectively which can be attributed to the anomeric effect. Electrospray ionization (ESI) mass spectrometry has also confirmed the presence of **2α/β** with a mass of 258.2 representing the calculated molecular ion (plus sodium).
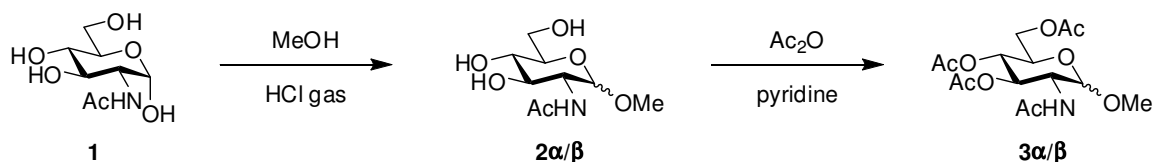
Scheme 4: GlcNAc to methyl glycoside mixture and subsequent acetylation.

^{1}H signals were able to be correlated with known signals by analyzing a ^{1}H-^{1}H-COSY spectrum of **2α/β**. The H-1α at 4.53 ppm (J = 3.4 Hz) is known because of the small coupling constant representing *gauche* orientation relative to H-2. From the ^{1}H-^{1}H-COSY spectrum, the signal for H-2α is a multiplet at 3.43 ppm and clearly correlates with H-1α (Figure 17). The N$\underline{H}$Acα signal at 7.78 ppm also correlates with H-2α as well, but the splitting pattern for H-2α was unable to be determined due to poor resolution. Any further correlations were unable to be determined for the α anomer. The proton H-1β at 4.17 ppm (J = 8.4 Hz) is known because of the large coupling constant representing *anti* orientation relative to H-2. The signal for H-2β is a multiplet at 3.63 ppm and clearly correlates with H-1β. The N$\underline{H}$Acβ signal at 7.84 ppm also correlates with H-2β as well, but the splitting pattern for H-2β was unable to be determined due to poor resolution. Any further correlations were unable to be determined for the β anomer. A ^{13}C NMR spectrum also indicated the presence of two methoxy groups around 55.0 ppm.

Figure 17: ^{1}H-^{1}H COSY spectrum of **2α/β**.

Subsequent acetylation using acetic anhydride and pyridine affords **3α/β** as a clear oil in 30% yield with the *O*-3, *O*-4, and *O*-6 positions blocked with acetate protecting groups. This was done previously[10] because the less polar protected compound is easier to separate *via* flash chromatography than **2α/β** and the ^{1}H NMR spectrum is much more resolved due to the electron-withdrawing acetate groups. The ^{1}H NMR spectrum was

very complex for **3α/β** and a ¹H-¹H COSY spectrum was required to solve the structure (Figure 18).
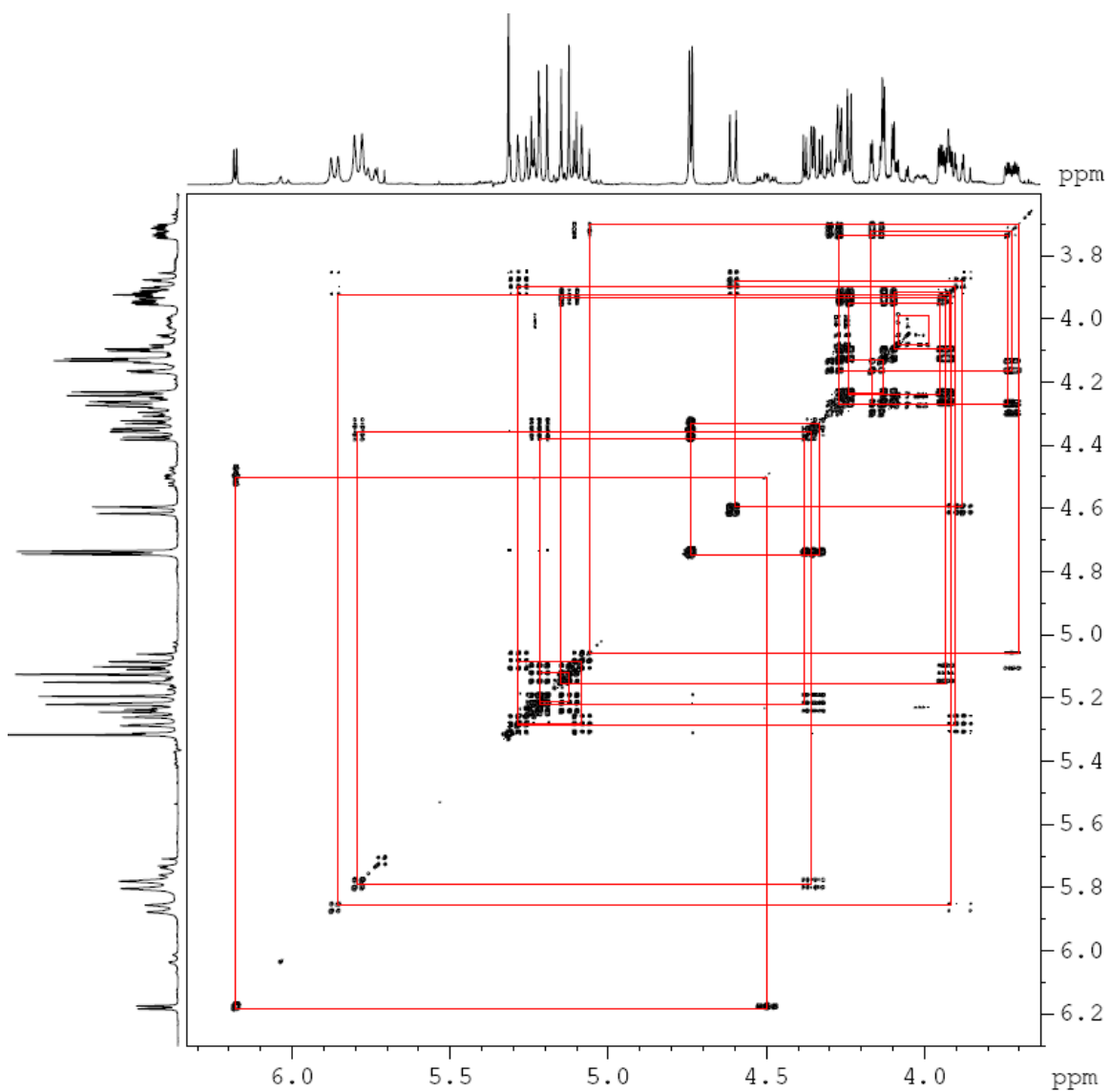
Figure 18: ¹H-¹H COSY spectrum of **3α/β**.

Structure elucidation will begin with the α-anomer. The anomeric H-1α at 4.74 ppm (*J* = 3.6 Hz) has a small coupling with H-2α making it *gauche* with respect to H-2α. Coupling between H-2α and N<u>H</u>Acα is larger at 9.6 Hz and coupling between H-2α to H-3α, H-3α to H-4α, and H-4α to H-5α are all large and are ~10.0 Hz which indicates *anti*

orientations around the ring. This indicates that the ring is likely in a chair conformation because the ring protons (H-2α to H-5α) would all have an axial conformation. The H-6α and H-6'α signals exhibit a large geminal coupling of ~12.5 Hz. Both have smaller vicinal couplings with H-5α giving them a *gauche* orientation with the –OAc *anti* with respect to H-5α. The β-anomer exhibits much of the same properties as the α-anomer. Relatively large couplings between ring protons (H-2β to H-5β) are indicative of a chair conformation. All other vicinal and geminal couplings are about the same except between H-1β and H-2β (*J* = 8.5 Hz). This coupling is large because the relationship between H-1β and H-2β is *anti*. The –OMeα and –OMeβ signals at 3.42 and 3.51 ppm reaffirm the synthesis of the *O*-glycoside. The ratio is seen to be 2:1 of α- and β-anomers respectively and can be attributed to the anomeric effect. The presence of four acetate signals for **3α/β** confirms three unprotected hydroxyls on the starting material **2α/β**. The ^{13}C NMR spectrum of **3α/β** also indicates product formation in an anomeric mixture by the appearance of eight acetate signals around 20.0 ppm. Electrospray ionization (ESI) mass spectrometry has also confirmed the presence of **3α/β** with a mass of 384.2 representing the calculated molecular ion (plus sodium). Because the next reaction proceeds with **2α/β**, the anomers were not separated for **3**.
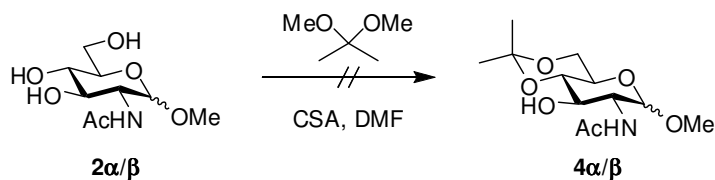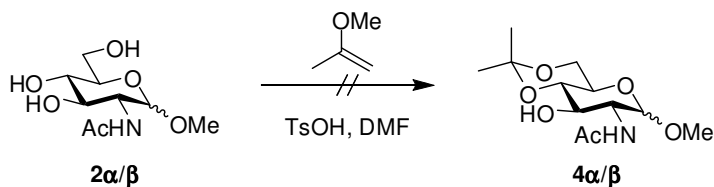

Equation 2. Attempted protection of **2α/β** using 2,2-dimethoxypropane and CSA.

The next step in the synthesis involves protection of *O*-4 and *O*-6 with an isopropylidene group. The first attempt utilized 2,2-dimethoxypropane with a catalytic

amount of camphor sulfonic acid (CSA) and *N,N*-dimethylformamide (DMF) as the solvent (Equation 2). The procedure[10] involves **2α/β** being dissolved in DMF and in a separate flask, 2,2-dimethoxypropane and CSA were also dissolved in DMF. The two solutions were combined and let stir while being monitored peridically by TLC (3:1 ethyl acetate:methanol). After four days TLC showed only starting material to be present.

Equation 3. Attempted protection of **2α/β** using 2-methoxypropene and TsOH.

The next attempt at protecting position *O*-4 and *O*-6 utilized a different acetalation reagent and organic acid (Equation 3). These reaction conditions were also previously attempted by others.[10] The sugar **2α/β** was dissolved in DMF and 2-methoxypropene was added and the reaction was allowed to let stir. The organic acid *p*-toluene sulfonic acid monohydrate (TsOH) was then added and the reaction was monitored by TLC (methanol). After 24 hours of stirring, TLC showed no signs of a reaction occurring.
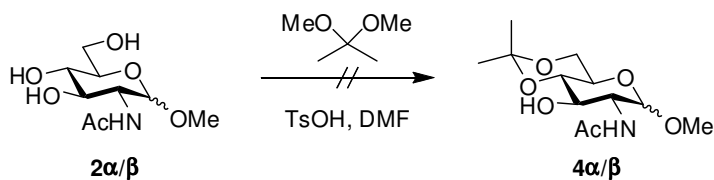
**Equation 4.** Attempted protection of **2α/β** using 2,2-dimethoxypropane and TsOH.

The last attempt utilized conditions[43] adapted from Hasegawa *et. al*. which uses 2,2-dimethoxypropane and TsOH (Equation 4). The starting material **2α/β** and TsOH

was dissolved in DMF and was let stir at 85 °C for 15 minutes. 2,2-Dimethoxypropane

was then added dropwise *via* syringe and the reaction was stirred for an additional 15

minutes at 85 °C. Like the two previous attempts, TLC (3:1 ethyl acetate:methanol)

showed no product formation.

The difficulties incurred may be a result from having a mixture of the anomers

2α/β as the starting materials. Previous studies[10] have successfully separated the

anomeric mixture and protected the *O*-glycoside with an isopropylidene group. Although

the next step in the synthesis attempted to protect *O*-3 with a benzyl group, it proved to

be unsuccessful. It was then decided to strictly adhere to the synthesis[38] outlined by

Horton and Saeki as they were successful at producing the target compound *N*-acetyl-D-

fucosamine.
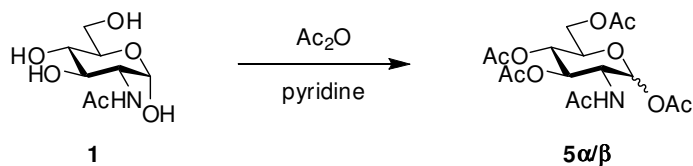
Equation 5. Protection of GlcNAc to afford pentaacetate **5α/β**.

To check the purity of the commercially available starting material **1**, an

acetylation reaction was performed by using acetic anhydride and pyridine which

afforded the pentaacetate **5** with the *O*-1, *O*-3, *O*-4, and *O*-6 positions protected with

acetate groups (Equation 5). GlcNAc was dissolved in pyridine under N_2 atmosphere and

acetic anhydride was added dropwise *via* syringe. The reaction was monitored by TLC

(3:1 ethyl acetate:methanol) and, after 24 hours, the appearance of a new less polar spot

with an R_f of 0.68 showed product formation. After performing an aqueous workup the

reaction was evaporated under reduced pressure to give crude **5α/β** in 63% yield.

Characterization utilizing ^{1}H, ^{13}C, and ^{1}H-^{1}H COSY NMR spectroscopy concluded that **5** was made in a 10:1 ratio of α:β anomers respectively. Five singlets around 1.8 ppm indicated that there are five acetate groups in the molecule. The ratio of α:β anomers were calculated by integrating the respective signals in the ^{1}H NMR spectrum. The α anomer would be expected to exhibit a relatively small coupling constant because the acetate at *C*-1 would be axial whereas H-1 would be equatorial. If in the equatorial configuration, the conformation between H-1 and H-2 would be *gauche* and based on the Karplus curve, the coupling constant should be small. Experimentally the H-1α was found to be a doublet at 6.18 ppm (J_{1-2} = 3.7 Hz). The β anomer would have H-1 and H-2 in the *anti* orientation and have a larger coupling relative to the α anomer. The β anomer was found to also be a doublet slightly more downfield at 6.25 ppm (J_{1-2} = 9.4 Hz). The signals for H-3α and H-4α were not resolved well enough to compute coupling constants between them. Both protons should have the same splitting pattern namely doublets of doublets. One coupling constant on each proton can be established based on the vicinal coupling constants of the neighboring protons. The doublet of doublet of doublets representing H-2α is at 4.49 ppm (J_{1-2} = 3.6, $J_{2\text{-N}\underline{\text{H}}\text{Ac}}$ = 9.1, J_{2-3} = 10.8 Hz) and the coupling constant between H-2α and H-3α can be deduced to have the value J = 10.8 Hz. The large coupling between the two protons corresponds well to the Karplus curve as the relationship between H-2α and H-3α is *anti*. This same approach applies to H-4α by examining the couplings with the H-5α doublet of doublet of doublets at 3.99 ppm (J_{5-6} = 2.6, $J_{5-6'}$ = 3.9, J_{4-5} = 9.6 Hz). The splitting pattern is first indicative of the magnetic difference between the two protons bonded to C-6α. The smaller couplings observed between H-5α to H-6α and H-5α to H-6'α are representative of both vicinal couplings

being in the *gauche* orientation (Figure 19). There is also geminal coupling between H-6α and H-6'α. Both protons exhibit a doublet of doublets splitting pattern meaning they are coupled with two magnetically different protons, namely, a smaller vicinal coupling and a larger geminal coupling. The smaller vicinal coupling was already discussed through being coupled to H-5α. The geminal couplings exhibited by H-6α at 4.07 ppm ($J_{6-6'}$ = 12.5 Hz) and H-6'α at 4.26 ppm ($J_{6-6'}$ = 12.5 Hz) conclude the orientation at H-5α.
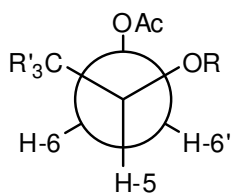

Figure 19: Orientation of **5α/β** at *C*-5 and *C*-6.

The coupling between H-3α and H-4α is still in question and was easily deduced by a ^{1}H-^{1}H-COSY (Figure 20). If examined closely, the 2H multiplet at 5.23 ppm exhibits two couplings with H-2α and H-5α along with being coupled within itself. This information leads to a conclusion that there are two overlapping signals whose splitting patterns are not able to be distinguished representing H-3α and H-4α. The five signals around 20.0 ppm in the ^{13}C NMR spectrum also indicate that five acetate groups are present. Electrospray ionization (ESI) mass spectrometry has also confirmed the presence of **5α/β** with a mass of 412.2 representing the calculated molecular ion (plus sodium).
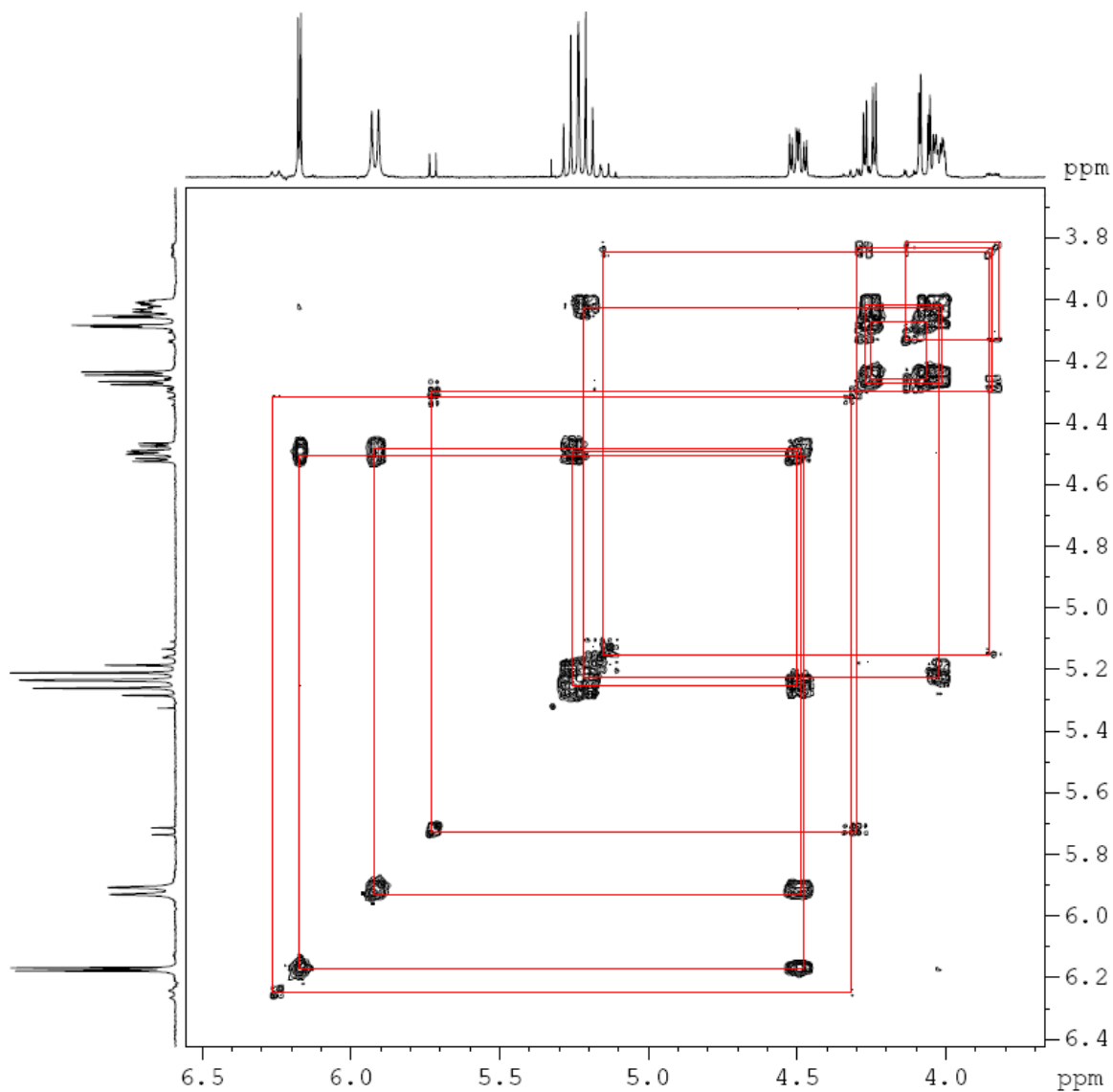
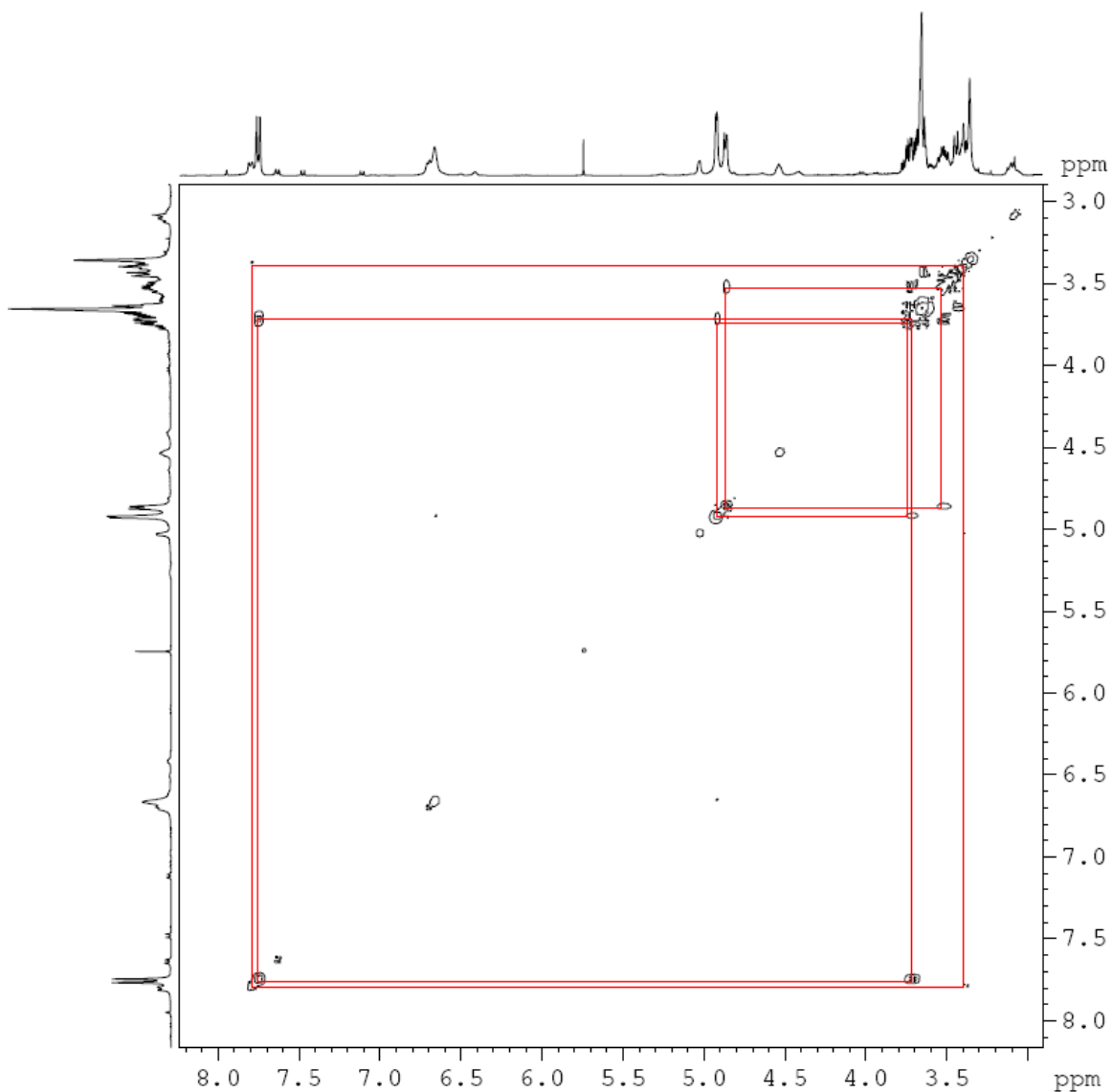**Figure 20:** ^{1}H-^{1}H COSY spectrum of **5α/β**.

An alternate route to *N*-acetyl-D-fucosamine begins with the protection of positions *O*-4 and *O*-6 simultaneously with an isopropylidene group (Scheme 5). Conditions[43] adapted from Hasegawa *et. al.* use 2,2-dimethoxypropane and TsOH. The starting material **1** and TsOH were dissolved in DMF and let stir at 85 °C for 15 minutes. 2,2-Dimethoxypropane was then added dropwise *via* syringe and the reaction was stirred for an additional 15 minutes at 85 °C. The reaction was let cool to room temperature and

analysis by TLC (3:1 ethyl acetate:methanol) showed product formation by a spot with an

R_f of 0.58 as compared to the polar starting material **1**. The reaction was neutralized by

the addition of sodium carbonate. The solvent was evaporated under reduced pressure

leaving a light brown solid, which was dissolved in ethyl acetate and precipitated with the

addition of methylene chloride, resulting in a 1.3:1 ratio of **6α/β** anomers as a white solid

in 69% yield.
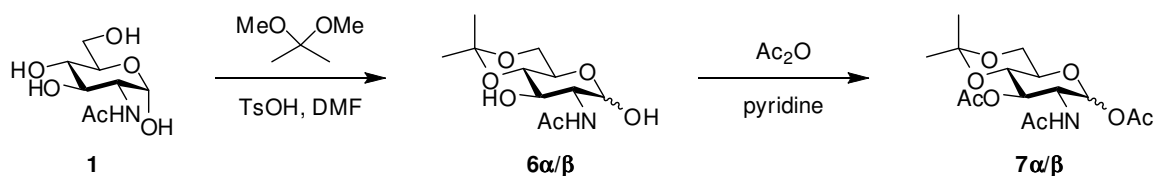
Scheme 5: 4,6-*O*-Isopropylidene protected **6α/β** and subsequent triacetate **7α/β**.

Two 3H singlets in the ^{1}H NMR spectrum, whose chemical shifts are 1.31 and

1.43 ppm, represent each methyl group on the isopropylidene group. One of the signals

is more downfield relative to the other signal because each has different magnetic

environments. The isopropylidene group is locked in a chair conformation thus having

one axial and one equatorial methyl group. The four signals around 20.0 ppm in the ^{13}C

spectrum indicate the two methyl groups of each anomer are present Electrospray

ionization (ESI) mass spectrometry has also confirmed the presence of **6α/β** with a mass

of 284.1 representing the calculated molecular ion (plus sodium).

Figure 21: ^{1}H-^{1}H COSY spectrum of **6α/β**.

Acetylation of **6α/β** was carried out to better resolve the ring proton signals so the data could be interpreted (Scheme 5). To a solution of **6α/β** in pyridine, acetic anhydride was added dropwise *via* syringe. After 24 hours of stirring, TLC (ethyl acetate) showed the formation of a new spot with an R_f of 0.28 indicating product formation. The reaction was poured over ice water and extracted with CH_2Cl_2. The organics were washed with 5% v/v H_2SO_4 and de-ionized water. Drying over $MgSO_4$ and reducing resulted in a

crude 4:1 **7α/β** mixture as a clear oil in 70% yield. Purification *via* flash column chromatography afforded **7α** as a clear oil in 31% yield. The appearance of two acetate signals around 2.0 ppm in the ^{1}H NMR spectrum signifies two free hydroxyls in the starting material were consumed. Electrospray ionization (ESI) mass spectrometry has also confirmed the presence of **7α** with a mass of 368.2 representing the calculated molecular ion (plus sodium).
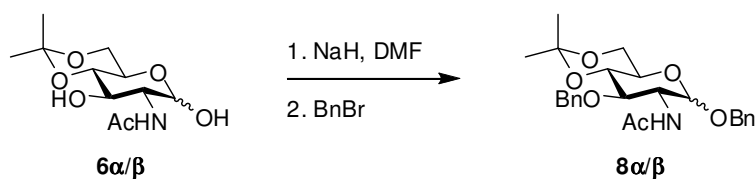
**Equation 6.** 1,3-*O*-Benzyl and 4,6-*O*-isopropylidene protected glycoside **8α/β**.

Since the *O*-4 and *O*-6 positions were now protected, the *O*-glycoside was then synthesized by benzylating positions *O*-1 and *O*-3. Standard Williamson ether synthesis conditions were employed (Equation 6). To a solution of **6α/β** in DMF was added sodium hydride. Benzyl bromide was then added dropwise *via* syringe with stirring, stirring was continued overnight at ~25 °C. Analysis by TLC (ethyl acetate) showed the formation of a new, less polar UV-active spot (R_f = 0.40) indicating product formation. The reaction was then extracted and dried. The solvent was then evaporated under reduced pressure and flash column chromatography was then performed (ethyl acetate) that afforded **8α/β** as a yellow syrup in 6 % yield. Four different spots were separated three of which suggested a ring opening effect by showing a signal of an aldehydic proton around 9-10 ppm. The remaining fraction indicated a 3:2 ratio of α to β anomers respectively. The 10H multiplet at 7.30 ppm signifies the addition of two mono-substituted phenyl rings onto the molecule. Electrospray ionization (ESI) mass

spectrometry has also confirmed the presence of **8α/β** with a mass of 464.3 representing the calculated molecular ion (plus sodium). Overall the classical Williamson ether synthesis was not clean and extensive purification was required to obtain a relatively clean sample.
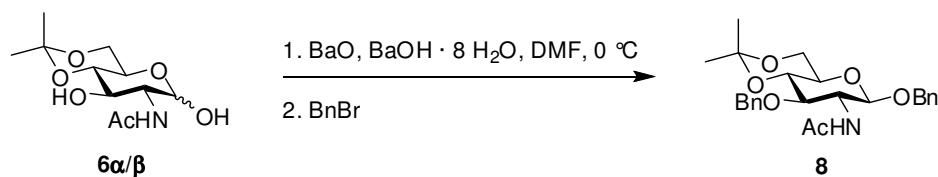
**Equation 7.** Alternative conditions for protected glycoside **8β**.

Another procedure[38] borrowed from Horton *et. al.* involves the Williamson ether synthesis but using a different base. The base chosen was a mixture of barium hydroxide octahydrate with barium oxide. Thus, an ice-cold solution of **6α/β** in DMF were added barium oxide and barium hydroxide octahydrate. Benzyl bromide was then added dropwise *via* syringe with stirring and stirring was continued for 2 hours at 0 °C and overnight at ~25 °C. Analysis by TLC (1:6 hexanes:ethyl acetate) showed the formation of a new spot with an R_f of 0.58 indicating product formation. The mixture was then diluted with methylene chloride, filtered to remove inorganic material, and the inorganic residue washed with methylene chloride. The combined methylene chloride solutions were evaporated under reduced pressure to an oil. The oil was stirred with 1:1 water:hexanes overnight resulting in a solid mass that upon isolation was dissolved in ethanol and precipitated with water to afford **8β** as a white solid in 34% yield. Electrospray ionization (ESI) mass spectrometry has also confirmed the presence of **8β** with a mass of 464.2 representing the calculated molecular ion (plus sodium).
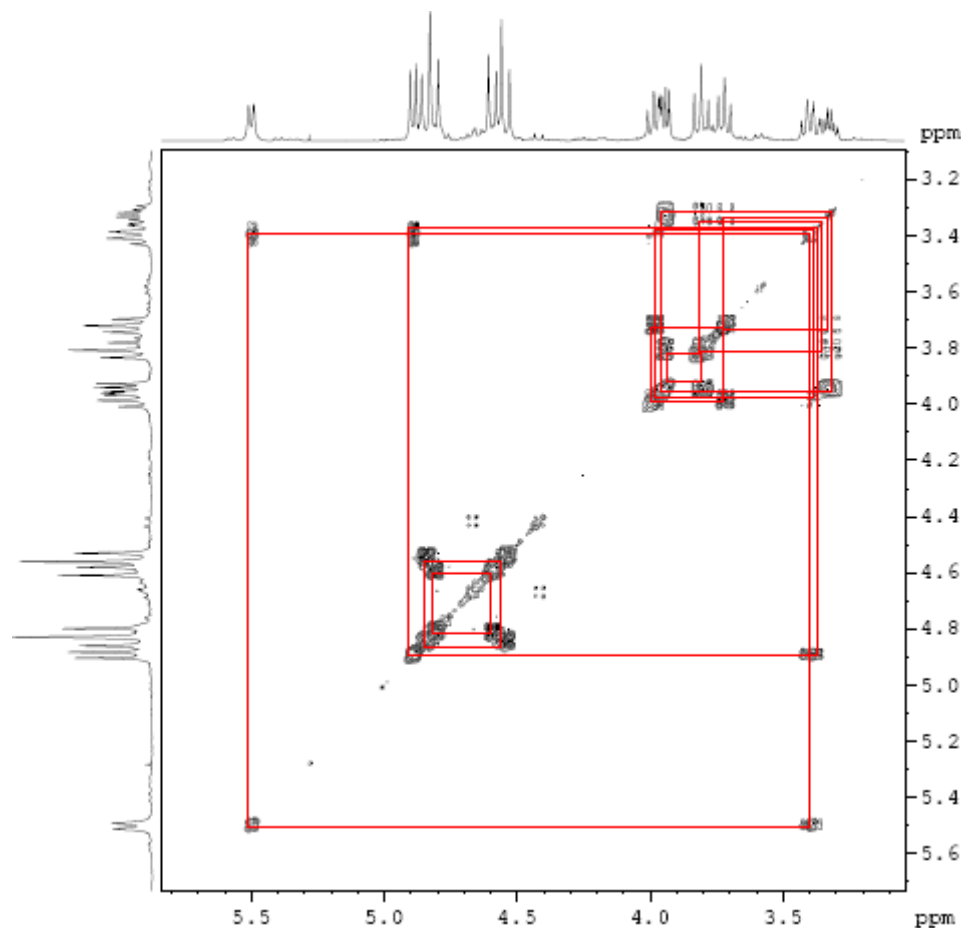
Figure 22: ^{1}H-^{1}H COSY spectrum of **8β**.

Complete characterization was carried out by utilizing ^{1}H, ^{13}C, and ^{1}H-^{1}H COSY NMR spectra. The ^{1}H-^{1}H COSY spectrum proved to be pivotal in the characterization of **8β** (Figure 22). Beginning with the proton bonded to the anomeric center, the H-1 doublet at 4.89 ppm ($J_{1\text{-}2}$ = 8.4 Hz) is representative of isolating the β anomer because the relationship between H-1 and H-2 would be *anti* for the β anomer thus exhibiting a larger coupling between the two. This is due to H-2 being axial as well as H-1 having the axial conformation. The H-2 doublet of doublet of doublets at 3.40 ppm ($J_{1\text{-}2}$ = 8.2, $J_{2\text{-NHAc}}$ = 8.2, $J_{2\text{-}3}$ = 10.0 Hz) shows large coupling between H-2 to NHAc and H-2 to H-3. The

large coupling between H-2 and H-3 is indicative of the two protons being *anti* with relation to each other because both are axial. The doublet of doublets for H-3 at 3.98 ppm (J_{2-3} = 9.9, J_{3-4} = 8.9 Hz) with a large coupling is also indicative of an *anti* orientation between H-3 and H-4. The triplet for H-4 at 3.98 ppm (J_{2-3} = 9.2, J_{3-4} = 9.2 Hz) also has large couplings representing an *anti* orientation between H-4 and H-5. The doublets of triplets of H-5 at 3.72 ppm (J_{4-5} = 10.0, J_{5-6} = 10.0, $J_{5-6'}$ = 5.3 Hz) exhibits an *anti* orientation between H-4 to H-5 and also between H-5 and H-6. This means H-6 is in the axial position and H-6' is in the equatorial position. H-6' is known to be in the equatorial conformation because of the small coupling between H-5 and H-6' is representative of a *gauche* relationship (Figure 23).
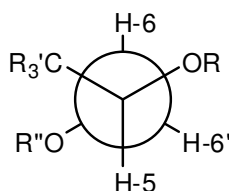
Figure 23: Conformation of **8β** at *C*-5 and *C*-6.

As seen previously geminal coupling is exhibited between H-6 and H-6'. Both protons have separate shifts and they also are doublet of doublets representing two distinct magnetic environments with separate respective coupling constants. As expected with geminal coupling the constants are larger being ~10.8 Hz. The ^{1}H-^{1}H-COSY spectrum proved to be important for structure elucidation of **8β**. All four benzylic protons exhibit geminal coupling and appeared to be two sets of doublets of doublets on the ^{1}H spectrum but when analyzed with the ^{1}H-^{1}H-COSY spectrum, they were found to be four separate doublets all exhibiting large coupling constants of ~12.0 Hz. A 10H

multiplet at 7.29 ppm signifies the addition of two mono-substituted phenyl rings. To ensure that the NHAc doublet at 5.50 ppm ($J_{\text{NHAc-2}}$ = 7.8 Hz) is the amide proton and not the anomeric proton, a simple experiment was performed where the NMR sample was doped with D_2O and a spectrum was taken the next day. Since the amide proton is somewhat acidic, a proton exchange will occur between D_2O and NHAc which will turn into NDAc and will not be observed in the ^{1}H NMR spectrum. The spectrum in the blue is the original sample and the spectrum in the red is the D_2O doped sample of **8β** (Figure 24). The disappearance of the doublet at 5.50 ppm confirms that the doublet belongs to the amide proton.
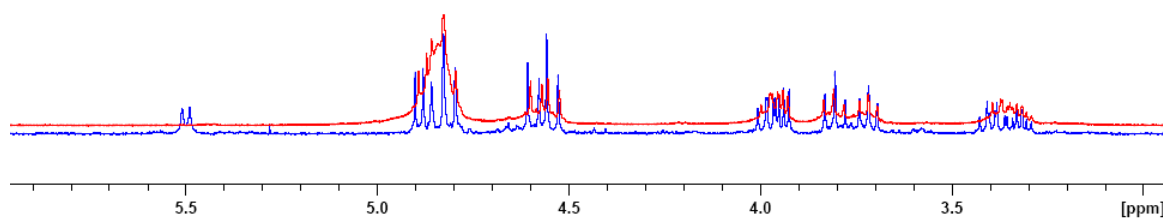
Figure 24: D_2O proton exchange experiment with **8β**.

In comparison, the alternative reaction conditions of the Williamson ether synthesis are preferred to the classical method. Based on difficulty alone, purification after the classical conditions is quite laborious when compared to the alternative. Purity is also better with the alternative conditions even without performing flash column chromatography. Percent yield is also better with the alternative conditions as opposed to the classical conditions (34% to 6 % respectively). The next step in the synthesis is the deprotection of an **8α/β** mixture to afford the 4,6-deprotected diol **9α/β** (Scheme 6). To a solution of **8α/β** in dioxane, a 9:1 H_2O:TFA mixture was added to the reaction. After 24 hours of stirring, TLC (ethyl acetate) showed the formation of product with an R_f of 0.23.

The organics were extracted, dried, and reduced resulting in an oil that was triturated with methylene chloride affording a 1:1 mixture of **9α/β** as a white solid in 89% yield. The disappearance of two singlets at 1.43 and 1.50 ppm indicates the removal of the isopropylidene protecting group. The ^{13}C NMR spectrum confirms the loss of the two signals of the isopropylidene group that were around 20.0 ppm. Electrospray ionization (ESI) mass spectrometry also confirms the presence of **9α/β** with a mass of 424.2 representing the calculated molecular ion (plus sodium).
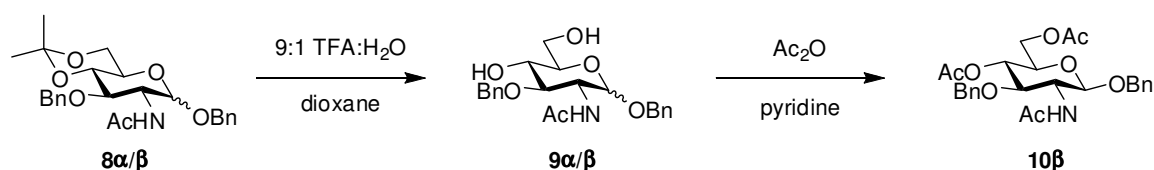
Scheme 6: Deprotected glycoside **9α/β** and subsequent triacetate **10β**.

Acetylation was carried out on **9α/β** to afford the triacetate **10β** to resolve the ring proton signals (Scheme 6). To a solution of **9α/β** in pyridine, acetic anhydride was added dropwise *via* syringe. After 24 hours of stirring, TLC (ethyl acetate) showed the formation of a spot with an R_f of 0.63 indicating product formation. The reaction was poured over ice water and then the organics were extracted with CH_2Cl_2. The organics were washed with 5% v/v H_2SO_4 and de-ionized water. Drying over $MgSO_4$ and reducing resulted in **10β** as a white solid in 20% yield. Electrospray ionization (ESI) mass spectrometry has also confirmed the presence of **10β** with a mass of 508.3 representing the calculated molecular ion (plus sodium). The ring protons exhibit similar findings as previous compounds in that the relationships between each vicinal proton are *anti* because the coupling constants are large. This does correlate with the ring preferring a chair conformation. The appearance of two singlets around 2.0 ppm indicates two

acetates were added to the starting material **9α/β** which must have been a diol. The doublet representing H-1 at 5.09 ppm (J = 8.1 Hz) is indicative of the β configuration with the proton having an axial conformation. Geminal coupling is observed with both H-6 and H-6' and H_{A-1} and H_{A-2} but not with the second set of benzylic protons. The other set of benzylic protons show as a 2H multiplet at 4.58 ppm. The ^{1}H-^{1}H-COSY spectrum confirms the structural assignments (Figure 25).
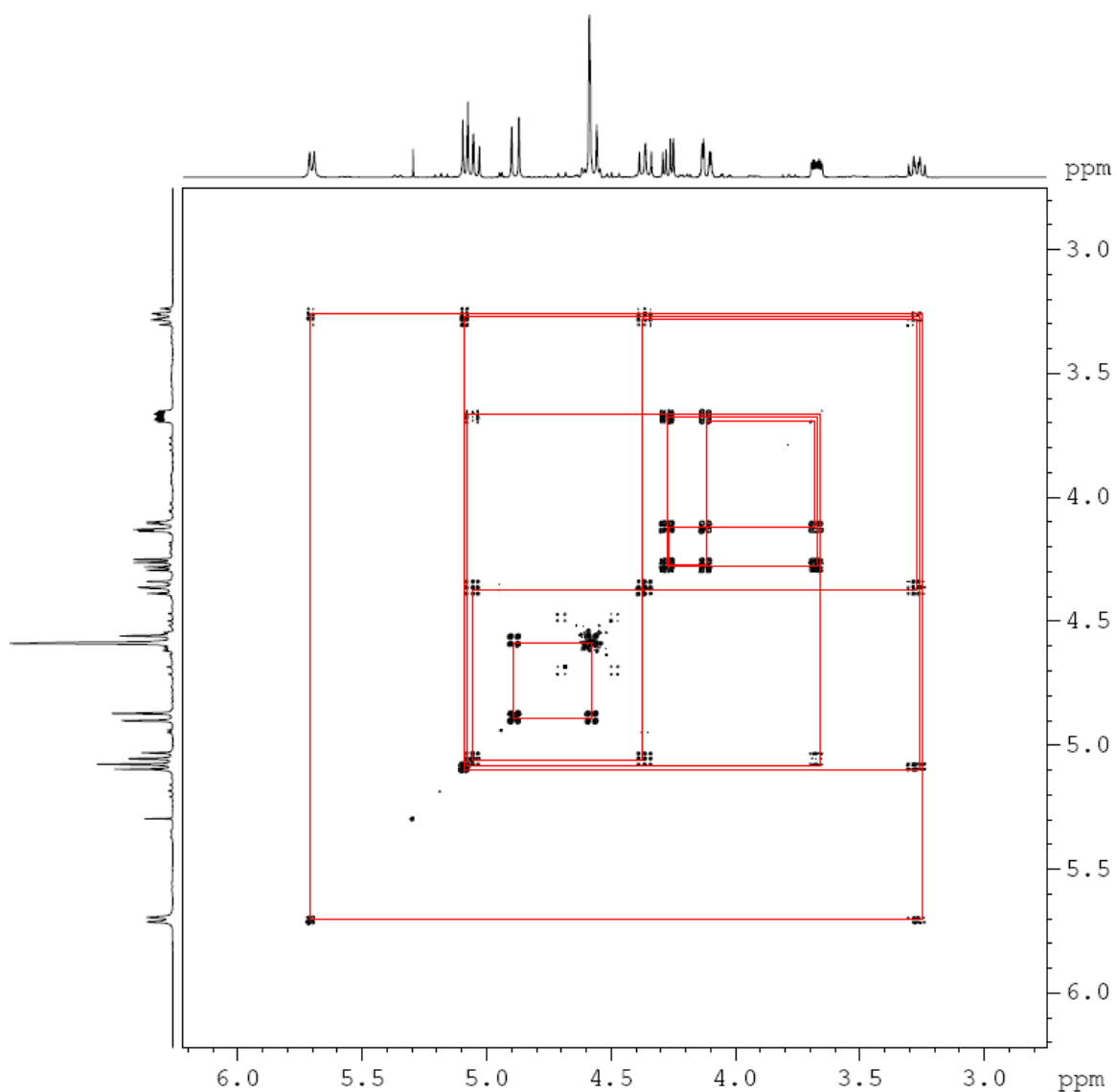
Figure 25: ^{1}H-^{1}H COSY spectrum of **10β**.

Activation of the diol **9α/β** affords the more electrophilic 4,6-di-*O*-methylsulfonyl glycoside **11β** (Equation 8). To a solution of **9α/β** in pyridine was added methanesulfonyl chloride dropwise *via* syringe. The mixture was stirred at 0 °C for 2-3 hours and then overnight at ~25 °C. TLC (ethyl acetate) showed the formation of a spot with an R_f of 0.51 indicating product formation. Ice was added to the reaction mixture with stirring and cooling, the organics were extracted, and reducing resulted in a yellow solid. The solid was then dissolved in ethanol/methanol and precipitated with de-ionized water to afford **11β** as a white solid in 55% yield. Electrospray ionization (ESI) mass spectrometry has also confirmed the presence of **11β** with a mass of 580.2 representing the calculated molecular ion (plus sodium).
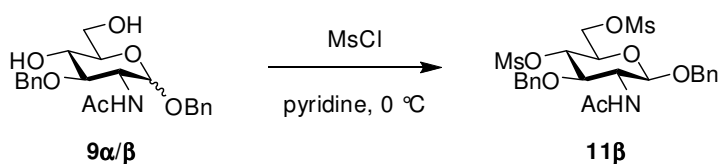
Equation 8. Formation of the bis-mesylate **11β**.

The ^{1}H NMR spectrum **11β** shows two indicative 3H singlets at 2.91 and 3.04 ppm representative of the methyl substituent belonging to each mesyl group. The conformation of **11β** is similar to previous compounds where the ring protons all have an *anti* orientation meaning the ring is in a chair conformation. The β anomer is exclusively present with H-1 at 5.04 ppm ($J = 7.9$ Hz) with an *anti* orientation with respect to H-2. The H-6 protons exhibit large geminal coupling, but both have relatively small vicinal coupling making them *gauche* with H-5. The primary substituent off of *C*-6 exhibits similar orientations as **5α/β** where it is *anti* with respect to H-5. The ^{1}H-^{1}H-COSY spectrum was used to elucidate the structure of **11β** (Figure 26).
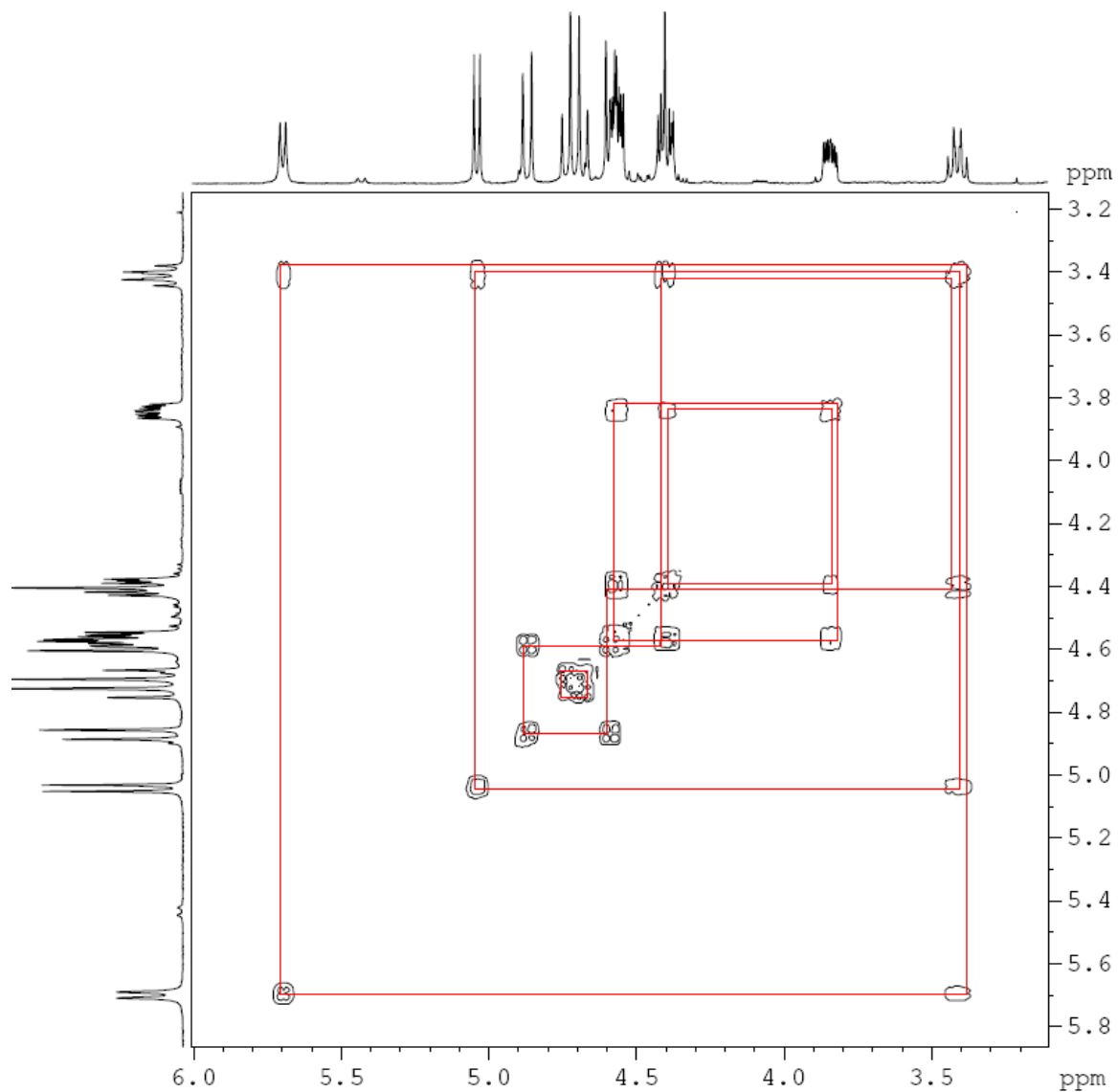
Figure 26: ^{1}H-^{1}H COSY spectrum of **11β.**

The glycoside **11α/β** was chemoselectively reduced to form the pyranoside **12α/β** (Equation 9) by dissolving the glycoside **11α/β** in dimethylsulfoxide and adding sodium borohydride to the reaction mixture. The mixture was stirred at 85 °C (oil bath) overnight until TLC (1:6 hexanes:ethyl acetate) showed the formation of product with an R_f of 0.28. The reaction mixture was then poured into a solution of 2% aqueous acetic acid and diluted with ice-water. The resultant suspension was allowed to let stir

overnight at ~25 °C. The white precipitate was filtered off, washed with water, and recrystallized from ethanol to afford **12α/β** as needles in 41% yield.
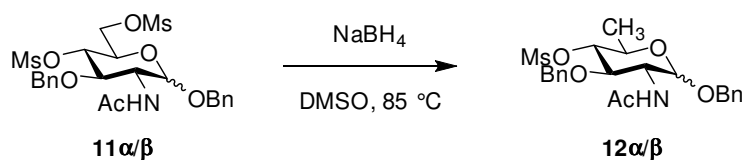
Equation 9. Chemoselective reduction of the primary sulfonate affording **12α/β**.

The ^{1}H NMR spectrum showed the disappearance of a singlet at 3.04 ppm but the other singlet at 2.88 ppm remained. This data correlates with the loss of a mesyl protecting group. The primary mesylate would act as a leaving group before the secondary mesyl group based on steric hindrance at their relative carbon reactive centers. Electrospray ionization (ESI) mass spectrometry has also confirmed the presence of **12α/β** with a mass of 486.2 representing the calculated molecular ion (plus sodium). The ^{1}H NMR spectrum was complicated with the anomeric mixture of the product but was resolved with the ^{1}H-^{1}H-COSY spectrum (Figure 27). Most of the signals are relatively similar as those previously described with the exception of the protons bonded to the reduced C-6. Newly formed doublets for the C-6 CH_3 groups that shifted upfield from previous locations represent the α and β anomers at 1.35 ppm ($J_{5\alpha-6\alpha}$ = 6.3 Hz) and 1.43 ppm ($J_{5\beta-6\beta}$ = 6.2 Hz) respectively. The other change in the spectrum is the splitting pattern of H-5. This proton previously showed as a doublet of doublet of doublets because of the coupling between H-4, H-6, and H-6'. Now that the C-6 has three equivalent H atoms, H-5 observes the protons on C-6 as the same and has one coupling constant with them. Still coupled separately to H-4, H-5 is now split into a doublet of

doublets at 3.63 and 3.93 ppm for the β and α anomers respectively. There is also a loss of a 3H singlet around 3.04 ppm signifying the loss of a mesyl group.
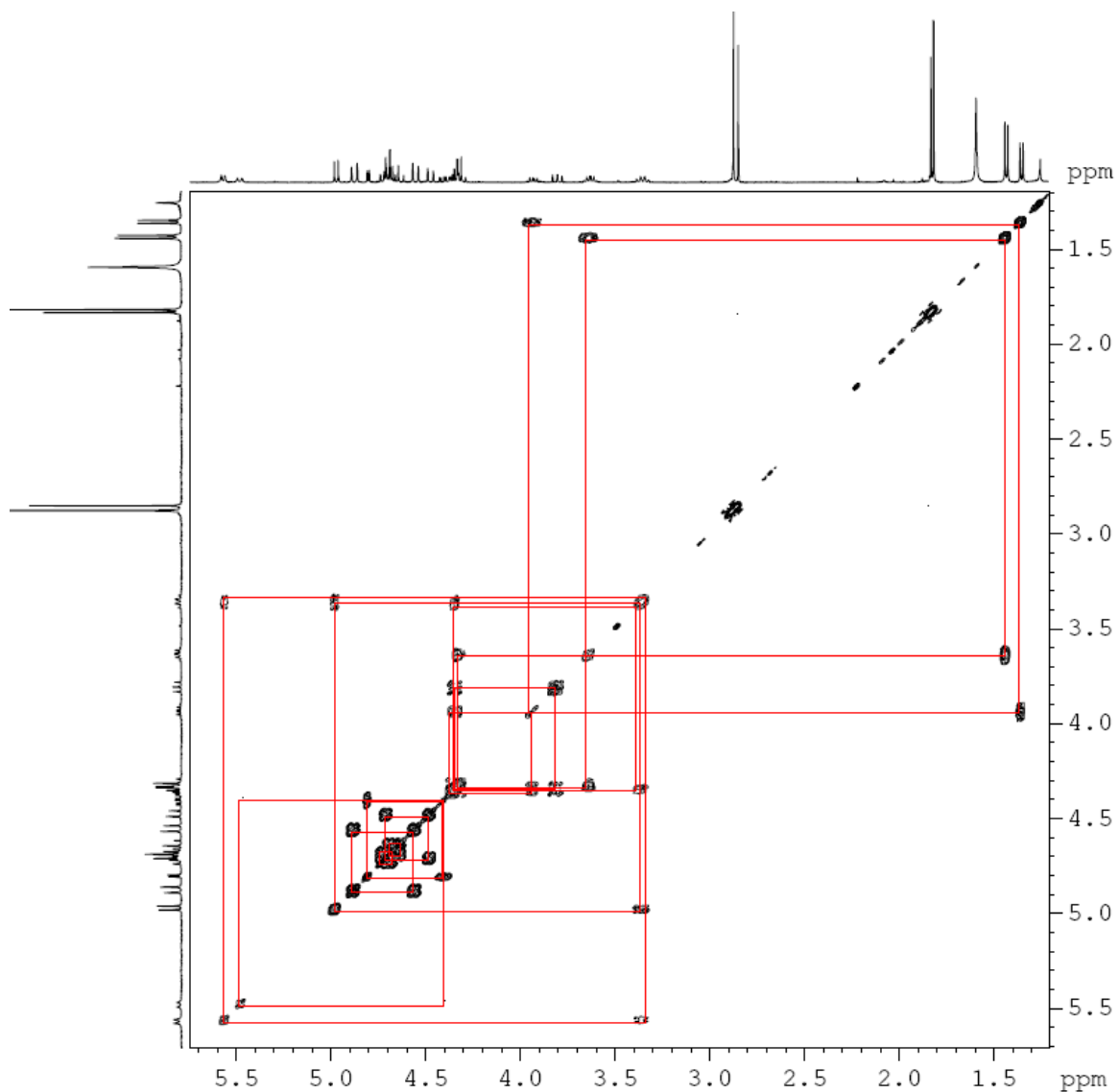
Figure 27: ^1H-^1H COSY spectrum of **12α/β**.

The last step performed toward the synthesis D-FucNAc was the epimerization of the glucoside **12α/β** and the formation of the galactoside **13α/β**. The pyranoside **12α/β** was dissolved in hexamethylphosphoric triamide (HMPA) and then sodium benzoate was added to the mixture which was stirred at 140-145 °C (oil bath) overnight. TLC (1:6

hexanes:ethyl acetate) indicated product with an R_f of 0.59. The reaction mixture was cooled and poured into ice-water and the resultant suspension was refrigerated overnight. The white precipitate was collected, washed with de-ionized water and dissolved in ethyl acetate. The solution was dried with $MgSO_4$ and treated with carbon powder. After removal of $MgSO_4$ and carbon powder, the filtrate was concentrated and was purified *via* flash column chromatography (1:1 hexanes:ethyl acetate) to afford a light brown powder. The powder was then dissolved in ethanol and triturated with water to afford **13α/β** as a white powder in 50% yield.
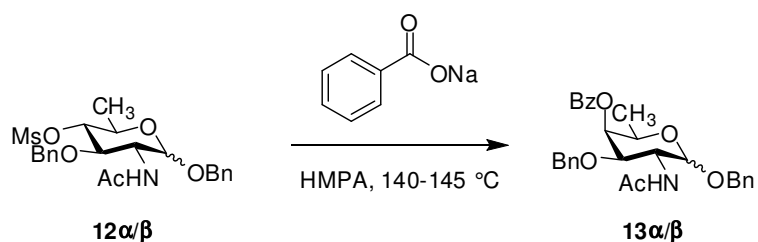
Equation 10. Attempted epimerization of **12α/β** to afford fucopyranoside **13α/β**.

Electrospray ionization (ESI) mass spectrometry confirmed the presence of **12α/β** and **13α/β** with a mass of 512.3 representing the calculated molecular ion of **13α/β** and also 486.2 representing the calculated molecular ion of **12α/β** (both plus sodium). The ^{1}H NMR spectrum was not resolved well enough to accurately interpret any of the data. This is due to the combination of both anomers of starting material and the product. Flash chromatography (1:1 hexanes:ethyl acetate) was carried out but the sample remained impure due to similar R_f values of both compounds resulting in no separation between them. It was decided at this point to focus attention away from the synthesis of *N*-acetyl-D-fucosamine and more towards synthesizing fluorine-containing mimics of the natural product.

2. Attempted Fluorination of *O*-Glycosides

Many diverse reaction conditions[44] exist that can introduce one or several fluorine atoms into sugars using various leaving groups and reagents. Typical leaving groups include, but are not limited to, alcohols, triflates, epoxides, and mesyl groups. Reagents that may be used include DAST, TASF, TBAF, KHF_2, KF, CsF and more. Work done[45] by Kim *et. al.* proposed a new class of S_N2 reactions, using metal fluorides, that are catalyzed by protic solvents (Equation 11).
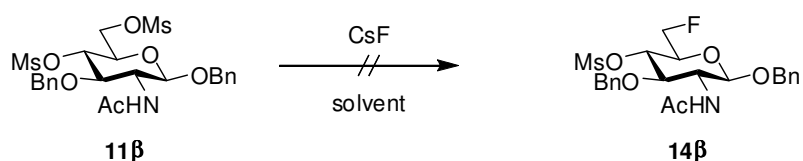
Equation 11. Attempted fluorination of sulfonate **11β** using CsF and solvent.

The first attempt at fluorinating *C*-6 involved using CsF in *t*-amyl alcohol. The reaction was refluxed at 90 °C for one hour but the sugar **11β** was mostly insoluble in *t*-amyl alcohol and when analyzed by TLC (ethyl acetate) only starting material was found present with an R_f of 0.51 (Table 2). Based on work[45] done by Kim *et. al.*, this solvent was found to produce the best yield when compared to the other solvents used. To aid solubility, DMF was then added to the reaction mixture *via* syringe. Kim *et. al.* proved CsF in DMF does work, but with lower yields than in the former solvent. This solved the solubility problem but after stirring for 24 hours at ~25 °C, TLC (ethyl acetate) indicated the solution contained exclusively **11β**. Two more equivalents of CsF were then added to the reaction mixture which was stirred for another 24 hours at ~25 °C but the results were the same. An aqueous workup was performed and analysis with ^{1}H NMR confirmed **11β**

was the only compound present by the two signature singlets around 3.0 ppm representing two mesyl groups.

Table 2: Attempted fluorination of sulfonate **11β** using CsF and various conditions.

Equivalents	Solvent	Temperature (°C)	Time (h)	R_f value*
1.1	*t*-amyl alcohol	90	1	0.51
1.1	*t*-amyl alcohol/DMF	25	24	0.55
3.1	*t*-amyl alcohol/DMF	25	48	0.53

*R_f value of **11β** is 0.53 (all use ethyl acetate as the solvent system)

Because DMF has been reported to facilitate fluorination of primary mesylates with the metal fluoride CsF, the starting material **11β** was dissolved solely in DMF. It was decided to use 3.0 equivalents of CsF instead of 1.1 because increasing the amount of reagent used should make the reaction kinetically faster since **11β** would have a higher probability of finding CsF in solution (Equation 12).
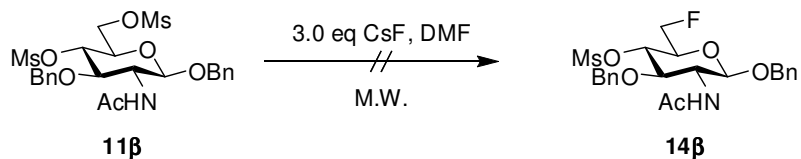
Equation 12. Attempted microwave-assisted fluorination of sulfonate **11β**.

In addition to increasing the number of equivalents, this reaction was performed using a CEM Discover Benchmate microwave (M.W.) at 100 °C. Microwave-assisted reactions have been shown to reduce reaction times, for example from 720 minutes using conventional methods to 4 minutes using microwave-assisted methods.[46] Hence, if it

were possible to "force" a reaction to occur, the conditions employed here would be expected to accomplish the task.

Table 3: Attempted microwave-assisted fluorination of sulfonate **11β**.

Temperature (°C)	Time (h)	R_f value*
100	0.5	0.50
100	1.5	0.53
100	2.5	0.52

*R_f value of **11β** is 0.53 (all use ethyl acetate as the solvent system)

The reaction was heated for 30 minutes and analysis by TLC (ethyl acetate) confirmed no product formation (Table 3). The mixture was then heated for an additional 60 minutes but TLC still indicated no product formation. Heating for another 60 minutes still did not show product formation by analysis with TLC. These conditions were unsuccessful at producing the target compounds. After an aqueous workup, ^{1}H and ^{19}F NMR spectroscopy confirmed **11β** was present exclusively. Metal fluoride reactions under these conditions were not attempted any further and attention was focused on more conventional methods.
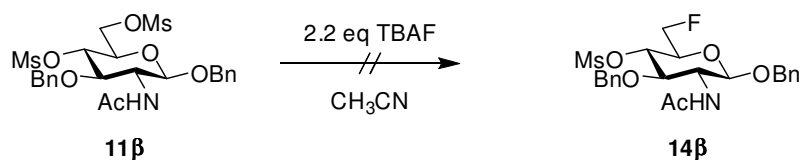
Equation 13. Attempted fluorination of sulfonate **11β** using TBAF in CH$_3$CN.

The next attempt at fluorinating the bis-mesyl glycoside **11β** employed tetra-*n*-butyl ammonium fluoride (TBAF) as a possible fluorinating reagent. Standard

conditions[47] were employed using 2.2 equivalents of TBAF in acetonitrile (Equation 13). The reaction was stirred at ~25 °C for 24 hours when analysis by TLC (ethyl acetate) showed no product formation with a spot having an R_f of 0.52. The reaction was then heated at 70 °C for 72 hours. TLC (ethyl acetate) of the reaction mixture confirmed the starting material was still present. An aqueous workup was still performed and when analyzed with ^{1}H and ^{19}F NMR spectroscopy, **11β** was confirmed to be present exclusively.

Table 4: Attempted fluorination of sulfonate **11β** using TBAF and various conditions.

Temperature (°C)	Time (h)	R_f value*
25	24	0.52
70	72	0.50

*R_f value of **11β** is 0.53 (all use ethyl acetate as the solvent system)

At this point in the attempted fluorination of **11β**, it is known that the primary mesylate could be reduced with NaBH$_4$, but was it possible with larger nucleophiles? Out of the vast array of nucleophiles, sodium azide (NaN$_3$) was chosen because it is one of the strongest nucleophiles and was also readily available. If the azide could not carry out an S$_N$2 reaction on the primary mesylate, than it is likely that other nucleophiles would not have the ability to perform this reaction as well.
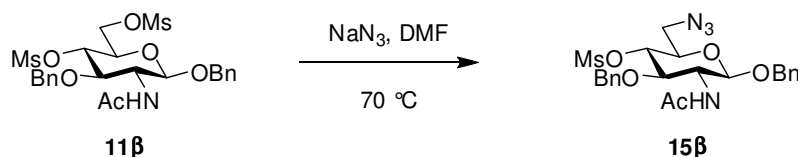
Equation 14. Chemoselective nucleophilic substitution of sulfonate **11β**.

The standard reaction conditions include dissolving **11β** in DMF, the addition of NaN$_3$, and heating the mixture at 70 °C (Equation 14). At first, 1.1 equivalents of NaN$_3$ were added to the mixture and after 24 hours of heating TLC (ethyl acetate) indicated that no reaction occurred because the spot had an R$_f$ of 0.50 (Table 5). The next reaction that was performed increased the amount of NaN$_3$ to 10 equivalents and after stirring for 24 hours at 70 °C, a spot with an R$_f$ of 0.59 appeared indicating that product had formed.

Table 5: Chemoselective nucleophilic substitution of sulfonate **11β** using NaN$_3$ and various conditions.

Equivalents	Time (h)	R$_f$ value*
1.1	24	0.50
10	24	0.59

*R$_f$ value of **11β** is 0.53 (all use ethyl acetate as the solvent system)

Characterization by ^{1}H NMR showed the loss of a singlet at 3.04 ppm that represents the primary mesyl group. Unlike **12α/β**, the product **15β** was not expected to show a doublet around 1.5 ppm, but should be more downfield because of the electronegative azide substituent. This did prove to be the case for **15β** where a 2H doublet appeared at 3.55 ppm representing the H-6 protons. An assumption must be made to explain why there is one doublet as opposed to two doublets of doublets. The only explanation that could be made is the bond between *C*-5 and *C*-6 rotates enabling both protons on *C*-6 to be magnetically equivalent or that $J_{5\text{-}6'} \equiv J_{5\text{-}6}$. A ^{1}H-^{1}H-COSY spectrum confirms that the doublet belongs to the protons on *C*-6 and that the signal correlates with the multiplet at 4.45 ppm belonging to H-5. Electrospray ionization (ESI)

mass spectrometry has also confirmed the presence of **15β** with a mass of 527.2 representing the calculated molecular ion (plus sodium).
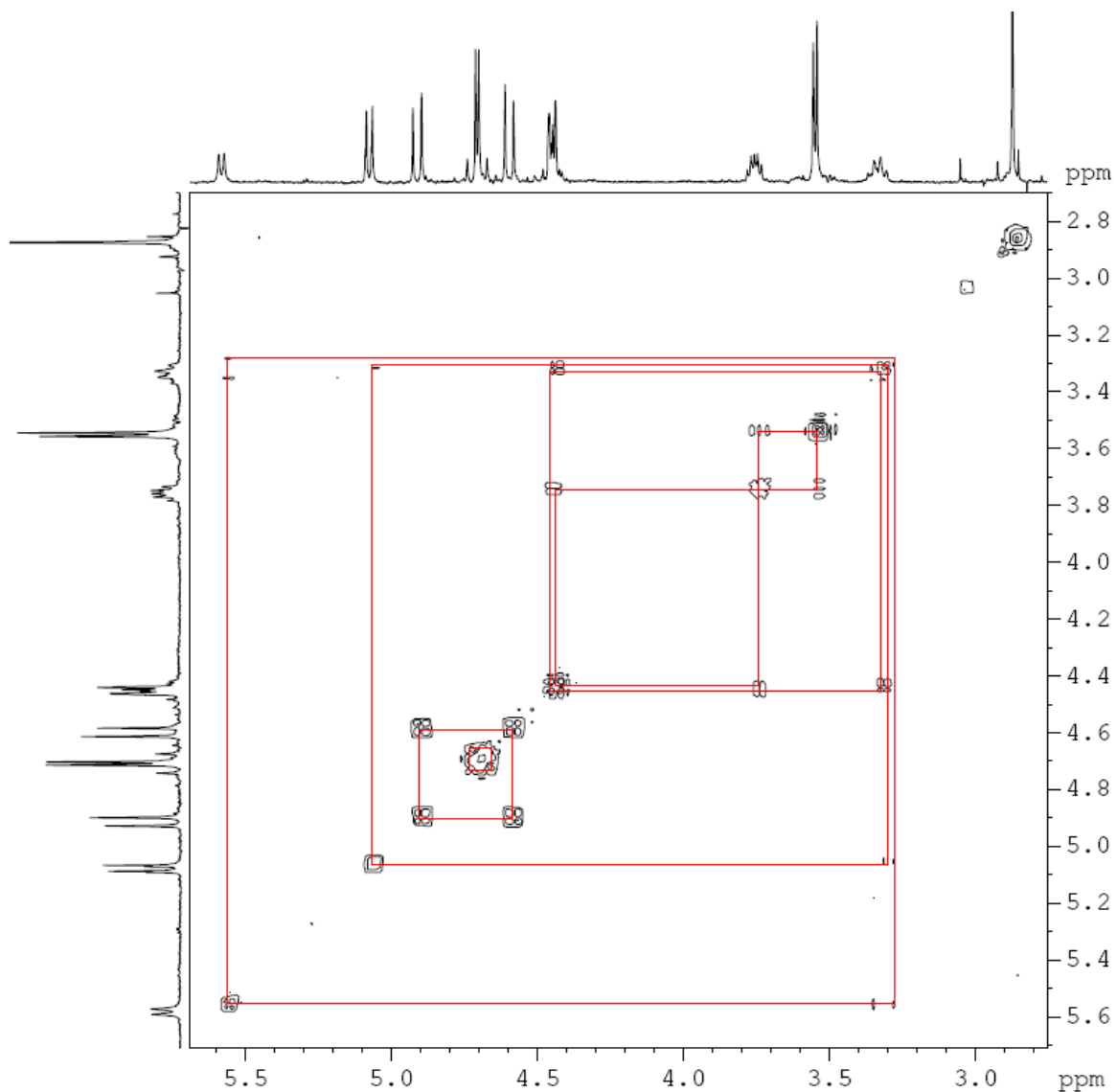
Figure 28: ^{1}H-^{1}H COSY spectrum of **15β**.

A common fluorinating reagent in the literature that is readily used to fluorinate carbohydrates and other molecules is (diethylamino)sulfur trufluoride (DAST).[48-50] Even though DAST is thermally unstable[51] and is usually reacted with hydroxyls, an experiment was performed to test if the reagent would react with mesylates (Equation 15)

since the displacement of the primary mesylate was proved with NaN$_3$. Thermal stability was regulated by reacting at -42 °C in a dry ice/acetonitrile bath.
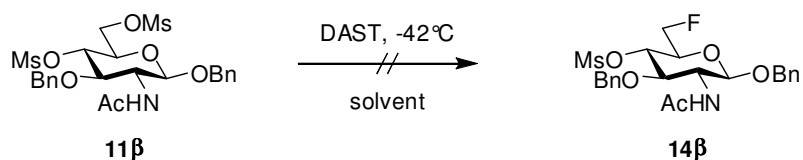
Equation 15. Attempted fluorination of sulfonate **11β** with DAST.

The first reaction conditions used included adding DAST dropwise *via* syringe to **11β** without any solvent (Table 6). The mixture was stirred neat for 0.5 hours and just as with a previous set of conditions, **11β** did not dissolve. Methylene chloride was added to aid solvation and this reaction mixture was stirred for 24 hours. Analysis with TLC (ethyl acetate) indicated no reaction had occured. Methanol (10 mL) was added to the reaction mixture to quench remaining DAST and after evaporating, purification *via* flash column chromatography (3:1 ethyl acetate:methanol) gave 0.04 g of **11β** as a white solid. Characterization by ^{1}H and ^{19}F NMR spectroscopy confirmed that the starting material **11β** was recovered exclusively.

Table 6: Attempted fluorination of sulfonate **11β** using DAST and various conditions.

Equivalents	Solvent	Time (h)	R_f value*
6	neat	0.5	0.50
40	CH$_2$Cl$_2$	24	0.52

*R_f value of **11β** is 0.53 (all use ethyl acetate as the solvent system)

Conclusion

Development of a synthetic route to *N*-acetyl-D-fucosamine was unsuccessful based on time requirements. The first pathway of the *O*-glycoside synthesis halted with the protection of *O*-4 and *O*-6. This was alleviated by protecting those centers first and then synthesizing the *O*-glycoside. The pathway continued successfully until the sixth step with the attempted epimerization of *C*-4. There is evidence that this reaction occured, but not enough to convinsingly characterize the compound. If a pure starting material is used for this step the reaction should give the expected product.

The attempts at synthesizing mimics of *N*-acetyl-D-fucosamine were also unsuccessful but a great deal of information was gathered from the various experiments that were performed. From the data collected, the direction that this project should take is with the DAST reagent and not with the others.

Future work should include attempting the epimerization of **12** again but the anomers should be separated to avoid unresolved spectra. A separate pathway should be attempted by protecting the primary hydroxyl of the 4,6-diol then attempting the Mitsunobu reaction on *C*-4. The Mitsunobu is a classical reaction that has been adapted to many different systems and avoids the use of toxic solvents such as HMPA. The DAST fluorinating reagent is used more frequently than any other reagent used herein and has been shown in the literature to work almost exclusively with free hydroxyls. The first thing that should be done with this process is to react the 4,6-diol with DAST as it should give mono and di-fluorinated sugars. It has been shown that DAST can even epimerize stereocenters of sugars and the difluoro compound would be a good possibility as it would epimerize and fluorinate *C*-6 all within five steps.

Experimental

General Procedures

A Varian Gemini 2000 NMR, Bruker Avance III, and Bruker Avance II spectrometers were used to obtain 400 MHz ^{1}H, 400 MHz ^{1}H-^{1}H-COSY, and 100 MHz ^{13}C spectra using CDCl$_3$ (0.1% w/v TMS) and DMSO (d_6, 99.9 atom % D) as the solvents. Chemical shifts (δ) are recorded in parts per million (ppm). Multiplicities for NMR spectra are listed as follows: s (singlet), d (doublet), dd (doublet of doublets), ddd (doublet of doublet of doublets), dt (doublet of triplets), m (multiplet), and all coupling constants (J) are labeled in Hertz. A Bruker Esquire-HP 1100 LC/MS was used to obtain mass spectra. A CEM Discover Benchmate microwave was used to perform microwave-assisted reactions. Whatman aluminum-backed plates were used for thin layer chromatography. Flash column chromatography was performed with 32-60 mesh 60-Å silica gel.

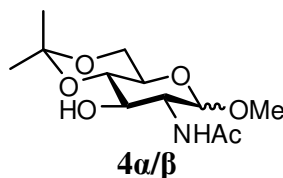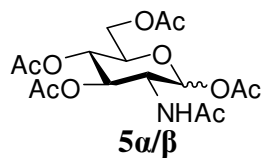**Formation of Methyl 2-acetamido-2-deoxy-α,β-D-glucopyranoside (2α/β) from 2-acetamido-2-deoxy-α-D-glucopyranose (1).**

2α/β
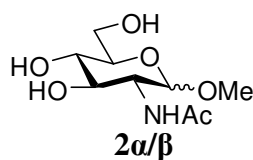
In a 500 mL round-bottom flask equipped with a rubber septum and magnetic stir bar, 2-acetamido-2-deoxy-α-D-glucopyranose (**1**, 10.000 g, 45.2 mmol) was dissolved in methanol (120 mL). In a separate 1000 mL round-bottomed flask, HCl gas was bubbled through methanol (120 mL) for 15 minutes. The 2-acetamido-2-deoxy-α-D-glucopyranose/methanol solution was then added to the HCl-saturated methanol solution

with the aid of another aliquot of methanol (120 mL). After 24 hours of stirring, TLC (3:1 ethyl acetate:methanol) showed the formation of a new, less polar UV-active spot (R_f = 0.26) indicating product formation. The reaction mixture was evaporated resulting in **2α/β** as a yellowish solid in 94% yield.

^{1}H NMR (d_6-DMSO): δ 1.79 (s, 3H, NH<u>Ac</u>β), 1.82 (s, 3H, NH<u>Ac</u>α), 3.22 (s, 3H, -OMeα), 3.31 (s, 3H, -OMeβ), 3.43 (m, H-2α), 3.63 (m, H-2β), 4.08 (m, H-3α, H-3β, H-4α, H-4β, H-5α, H-5β, H-6α, H-6'α, H-6β, H-6'β), 4.17 (d, 1H, H-1β, J = 8.4 Hz), 4.53 (d, 1H, H-1α, J = 3.4 Hz), 7.78 (d, 1H, N<u>H</u>Acα, J = 8.8 Hz), 7.84 (d, 1H, N<u>H</u>Acβ, J = 7.7 Hz).

^{13}C NMR (d_6-DMSO): δ 22.62, 23.12, 53.88, 54.23, 55.03, 55.60, 60.78, 60.97, 70.52, 70.62, 70.70, 72.68, 74.35, 76.97, 97.85, 101.89, 169.09, 169.45.

m/z calculated: 235.11   *m/z* found: 258.2 (M + Na)

Melting Point: 114-116 °C

Formation of Methyl 2-acetamido-3,4,6-tri-*O*-acetyl-2-deoxy-α,β-D-gluco pyranoside (3α/β) from Methyl 2-acetamido-2-deoxy-α,β-D-glucopyranoside (2α/β).
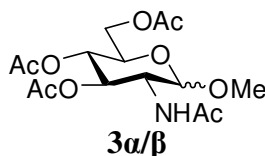
3α/β

In an oven-dried 25 mL round-bottom flask equipped with a rubber septum and magnetic stir bar and under N$_2$ atmosphere, methyl 2-acetamido-2-deoxy-α,β-D-

glucopyranoside (**2α/β**, 0.099 g, 0.421 mmol) was dissolved in pyridine (3 mL). Acetic anhydride (0.80 mL, 8.42 mmol) was added dropwise *via* syringe. After 24 hours, TLC (3:1 ethyl acetate:methanol) showed the formation of a new, less polar UV-active spot (R_f = 0.42) indicating product formation. The reaction was poured over ice water (15 mL) and then the organics were extracted with CH_2Cl_2 (2 x 10 mL). The organics were washed with 5% v/v H_2SO_4 (3 x 10 mL) and de-ionized water (1 x 10 mL). Drying over $MgSO_4$ and reducing resulted in **3α/β** as a clear oil in 30% yield.

^{1}H NMR (CDCl$_3$): δ 1.96 (s, 3H, -NH<u>Ac</u>β), 1.97 (s, 3H, -NH<u>Ac</u>α), 2.02 (s, 3H, -Acβ), 2.03 (s, 3H, -Acα), 2.10 (s, 3H, -Acβ), 2.11 (s, 3H, -Acα), 3.42 (s, 3H, -OMeα), 3.51 (s, 3H, -OMeβ), 3.72 (ddd, 1H, H-5β, *J* = 2.4, 4.7, 10.0 Hz), 3.89 (dt, 1H, H-2β, *J* = 8.6, 8.6, 10.5 Hz), 3.93 (ddd, 1H, H-5α, *J* = 2.3, 4.6, 10.0 Hz), 4.11 (dd, 1H, H-6'α, *J* = 2.4, 12.3 Hz), 4.15 (dd, 1H, H-6β *J* = 2.6, 12.4 Hz), 4.25 (dd, 1H, H-6α, *J* = 4.5, 12.7 Hz), 4.28 (dd, 1H, H-6'β, *J* = 4.6, 13.1 Hz), 4.35 (ddd, 1H, H-2α, *J* = 3.6, 9.6, 10.6 Hz), 4.61 (d, 1H, H-1β, *J* = 8.4 Hz), 4.74 (d, 1H, H-1α, *J* = 3.6 Hz), 5.08 (t, 1H, H-4β, *J* = 9.6, 9.6 Hz), 5.12 (t, 1H, H-4α, *J* = 9.7, 9.7 Hz), 5.22 (t, 1H, H-3α, *J* = 10.0, 10.0 Hz) 5.29 (dd, 1H, H-3β, *J* = 9.4, 10.6 Hz), 5.79 (d, 1H, N<u>H</u>Acα, *J* = 9.6 Hz) 5.87 (d, 1H, N<u>H</u>Acβ, *J* = 8.8 Hz).

^{13}C NMR (CDCl$_3$): δ 20.61, 20.64, 20.69, 20.73, 20.94, 23.01, 23.19, 23.33, 51.78, 53.46, 54.47, 55.41, 56.78, 61.98, 67.59, 68.06, 68.58, 71.26, 71.74, 72.40, 98.25, 101.56, 169.33, 169.43, 170.00, 170.05, 170.37, 170.74, 170.90, 171.35.

m/z calculated: 361.14   *m/z* found: 384.2 (M + Na)

Melting Point: oil

Attempted formation of Methyl 2-acetamido-2-deoxy-4,6-*O*-isopropylidene-α,β-D-glucopyranose (4α/β) from Methyl 2-acetamido-2-deoxy-α,β-D-glucopyranose (2α/β).

4α/β
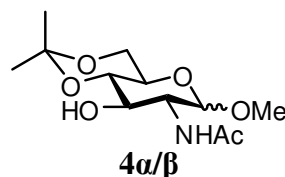
In a 100 mL round-bottom flask equipped with a rubber septum and magnetic stir bar, methyl 2-acetamido-2-deoxy-α,β-D-glucopyranose (**2α/β**, 0.66 g, 2.81 mmol) was dissolved in *N,N*-dimethylformamide (5 mL). D(+)-10-Camphorsulfonic acid (0.135 g, 0.581 mmol) and 2,2-dimethoxypropane (10 mL, 81.3 mmol) were added and the mixture was stirred. After 24 hours, TLC (3:1 ethyl acetate:methanol) indicated that only starting material was present.

Attempted formation of Methyl 2-acetamido-2-deoxy-4,6-*O*-isopropylidene-α,β-D-glucopyranose (4α/β) from Methyl 2-acetamido-2-deoxy-α,β-D-glucopyranose (2α/β).

4α/β
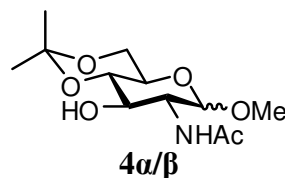
In a 25 mL round-bottom flask equipped with a rubber septum and magnetic stir bar, methyl 2-acetamido-2-deoxy-α,β-D-glucopyranose (**2α/β**, 0.154 g, 0.655 mmol), DMF (1.5 mL), and 2-methoxypropene (0.45 mL, 4.70 mmol) were mixed and then *p*-toluene sulfonic acid monohydrate (0.025 g, 0.145 mmol) was added. After 24 hours, TLC (methanol) indicated that only starting material was present.

Attempted formation of Methyl 2-acetamido-2-deoxy-4,6-*O*-isopropylidene-α,β-D-glucopyranose (4α/β) from Methyl 2-acetamido-2-deoxy-α,β-D-glucopyranose (2α/β).

HO—
NHAc
OMe
4α/β

In a 100 mL three neck round-bottom flask equipped with a rubber septum and magnetic stir bar, methyl 2-acetamido-2-deoxy-α,β-D-glucopyranose (**2α/β**, 0.838 g, 4.32 mmol) and *p*-toluene sulfonic acid monohydrate (0.013 g, 0.075 mmol) were dissolved in *N,N*-dimethylformamide (13 mL) and stirred for 15 minutes at 80-85 °C. Next, 2,2-dimethoxypropane (2.0 mL, 20.9 mmol) was added dropwise *via* syringe. The reaction mixture was stirred at 80-85 °C for another 15 minutes and was let cool to room temperature. After 24 hours of stirring, TLC (3:1 ethyl acetate:methanol) indicated that only starting material was present.

Formation of 2-acetamido-1,3,4,6-tetra-*O*-acetyl-2-deoxy-α,β-D-glucopyranose (5α/β) from 2-acetamido-2-deoxy-α-D-glucopyranose (1).

OAc
AcO—
AcO—
NHAc
OAc
5α/β

In an oven-dried 25 mL round-bottom flask equipped with a rubber septum and magnetic stir bar and under N$_2$ atmosphere, 2-acetamido-2-deoxy-α-D-glucopyranose (**1**, 0.100 g, 0.452 mmol) was dissolved in pyridine (3 mL). Acetic anhydride (0.94 mL, 9.94 mmol) was added dropwise *via* syringe.   After 24 hours, TLC (3:1 ethyl

acetate:methanol) showed the formation of a new, less polar UV-active spot ($R_f = 0.68$) indicating product formation. The reaction was poured over ice water (20 mL) and then the organics were extracted with CH_2Cl_2 (2 x 5 mL). The organics were washed with 5% v/v H_2SO_4 (3 x 5 mL) and de-ionized water (1 x 10 mL). Drying over $MgSO_4$ and reducing resulted in **5α/β** as a white solid in 63% yield.

^{1}H NMR (CDCl$_3$): δ 1.95 (s, 3H, CH$_3$α), 2.05 (s, 3H, CH$_3$α), 2.06 (s, 3H, CH$_3$α), 2.09 (s, 3H, CH$_3$α), 2.20 (s, 3H, CH$_3$α), 3.84 (ddd, 1H, H-5β, J = 2.2, 4.5, 9.6 Hz), 3.99 (ddd, 1H, H-5α, J = 2.6, 3.9, 9.6 Hz), 4.07 (1H, dd, H-6α, J = 2.3, 12.5 Hz), 4.12 (1H, dd, H-6β, J = 2.2, 12.5 Hz), 4.26 (dd, 1H, H-6'α, J = 4.1, 12.5 Hz), 4.30 (m, 1H, H-2β), 4.49 (ddd, 1H, H-2α, J = 3.6, 9.1, 10.8 Hz), 5.15 (m, 2H, H-3β, H-4β), 5.23 (m, 2H, H-3α, H-4α), 5.72 (d, 1H, NHAcβ, J = 8.8 Hz), 5.91 (d, 1H, NHAcα, J = 9.1 Hz), 6.18 (d, 1H, H-1α, J = 3.7 Hz), 6.25 (d, 1H, H-1β, J = 9.4 Hz).

^{13}C NMR (CDCl$_3$): δ 20.58, 20.72, 20.74, 20.93, 22.98, 50.95, 61.55, 67.55, 69.68, 70.59, 90.65, 168.77, 169.17, 170.16, 170.73, 171.58.

m/z calculated: 389.13   *m/z* found: 412.2 (M + Na)

Melting Point: 70-74 °C

Formation of 2-acetamido-2-deoxy-4,6-*O*-isopropylidene-α,β-D-glucopyranose (6α/β) from 2-acetamido-2-deoxy-α-D-glucopyranose (1).

6α/β
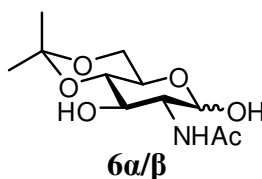
In a 250 mL three neck round-bottom flask equipped with a rubber septum and magnetic stir bar, 2-acetamido-2-deoxy-α-D-glucopyranose (**1**, 10.000 g, 45.21 mmol) and *p*-toluene sulfonic acid monohydrate (0.105 g, 0.610 mmol) were dissolved in *N,N*-dimethylformamide (60 mL) and stirred for 15 minutes at 80-85 °C. Next, 2,2-dimethoxypropane (22 mL, 229.7 mmol) was added dropwise *via* syringe. The reaction mixture was stirred at 80-85 °C for another 15 minutes and was let cool to room temperature. After 24 hours, TLC (3:1 ethyl acetate:methanol) showed the formation of a new, less polar UV-active spot (R_f = 0.58) indicating product formation. The resulting mixture was neutralized with sodium carbonate and filtered into a 100 mL round-bottom flask. The solvent was evaporated and the remaining light brownish solid was dissolved in ethyl acetate. Methylene chloride was then added which turned the solution a milky color. Filtering resulted in **6α/β** as a white solid in 69% yield.

^{1}H NMR (DMSO): δ 1.31 (s, 3H, CH$_3$), 1.43 (s, 3H, CH$_3$), 1.83 (s, 3H, NH<u>Ac</u>), 3.52 (dt, 1-H, H-2β, *J* = 5.3, 9.5, 9.5 Hz), 3.72 (ddd, 1-H, H-2α, *J* = 3.6, 8.6, 10.0 Hz), 4.87 (1H, H-1β, *J* = 5.8 Hz), 4.92 (1H, H-1α, *J* = 3.1 Hz), 7.75 (1H, N<u>H</u>Acα, *J* = 8.5 Hz), 7.80 (1H, N<u>H</u>Acβ, *J* = 7.8 Hz).

^{13}C NMR (DMSO): δ 19.01, 19.11, 22.58, 23.02, 29.05, 29.16, 54.75, 58.00, 61.47, 61.84, 62.88, 66.67, 67.46, 70.89, 74.14, 75.02, 91.40, 95.90, 98.69, 98.82, 169.34, 169.45.

m/z calculated: 261.12   *m/z* found: 284.1 (M + Na)

Melting Point: 166-172 °C (decomposed)

Formation of 2-acetamido-1,3,-di-*O*-acetyl-2-deoxy-4,6-*O*-isopropylidene-α,β-D-glucopyranose (7α/β) from 2-acetamido-2-deoxy-4,6-*O*-isopropylidene-α,β-D-glucopyranose (6α/β).

7α/β
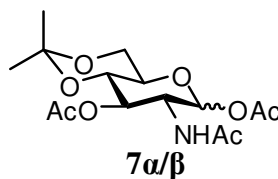
In an oven-dried 25 mL round-bottom flask equipped with a rubber septum and magnetic stir bar and under N_2 atmosphere, 2-acetamido-2-deoxy-4,6-*O*-isopropylidene-α,β-D-glucopyranose (**6α/β**, 1.28 g, 4.90 mmol) was dissolved in pyridine (20 mL). Acetic anhydride (16 mL, 169.3 mmol) was added dropwise *via* syringe. After 24 hours, TLC (ethyl acetate) showed the formation of a new, less polar UV-active spot ($R_f = 0.28$) indicating product formation. The reaction was poured over ice water (100 mL) and then the organics were extracted with CH_2Cl_2 (2 x 20 mL). The organics were washed with 5% v/v H_2SO_4 (3 x 20 mL) and de-ionized water (1 x 20 mL). Drying over $MgSO_4$ and reducing afforded crude 4:1 **7α/β** respectively as a clear oil in 70% yield. Flash column chromatography was then performed (ethyl acetate) to afford **7α** as a clear oil in 31 % yield

^{1}H NMR (CDCl$_3$): δ 1.40 (s, 3H, CH$_3$), 1.50 (s, 3H, CH$_3$), 1.94 (s, 3H, O<u>Ac</u>), 2.10 (s, 3H, O<u>Ac</u>), 2.19 (s, 3H, O<u>Ac</u>), 3.74 (m, 2H, H-6, H-6'), 3.83 (t, H-4, J = 9.3, 9.3 Hz), 3.89 (m, 1H,), 4.43 (ddd, 1H, H-2, J = 3.6, 9.2, 10.6 Hz), 5.16 (dd, 1H, H-3, J = 9.3, 10.6 Hz), 5.75 (d, 1H, N<u>H</u>Ac, J = 9.2 Hz), 6.09 (d, 1H, H-1, J = 3.8 Hz).

^{13}C NMR (CDCl$_3$): δ 19.00, 20.57, 20.70, 20.73, 20.96, 21.00, 22.94, 22.96, 28.94, 29.69, 51.32, 51.79, 61.21, 62.05, 65.87, 67.60, 70.20, 71.32, 73.16, 73.86, 90.59, 91.00, 91.22, 100.05, 169.26, 169.63, 170.57, 170.94, 172.02, 172.36.

m/z calculated: 345.14   *m/z* found: 368.2 (M + Na)

Melting Point: oil

Formation of benzyl 2-acetamido-3-*O*-benzyl-2-deoxy-4,6-*O*-isopropylidene-α,β-D-glucopyranoside (8α/β) from 2-acetamido-2-deoxy-4,6-*O*-isopropylidene-α,β-D-glucopyranose (7α/β).

8α/β
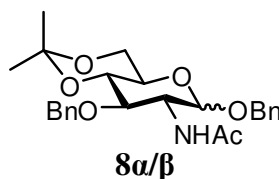
To a solution of 2-acetamido-2-deoxy-4,6-*O*-isopropylidene-α,β-D-glucopyranose (**7α/β**, 4.37 g, 16.73 mmol) in *N,N*-dimethylformamide (140 mL) was added sodium hydride (0.883 g, 36.81 mmol). Benzyl bromide (4.37 mL, 36.81 mmol) was then added dropwise *via* syringe with stirring. Stirring was continued overnight at ~25 °C. Analysis by TLC (ethyl acetate) showed the formation of a new, less polar UV-active spot (R$_f$ =

0.40) indicating product formation. The reaction was then poured into 100 mL of H_2O/ice mixture. The product was extracted with CH_2Cl_2 (1 x 50 mL), washed with ammonium chloride (1 x 60 mL), and washed with $NaHCO_3$ (1 x 60 mL). The organic layer was finally washed with de-ionized H_2O (1 x 100 mL), dried with anhydrous $MgSO_4$ and the solvent was then evaporated off. Flash column chromatography was then performed (ethyl acetate) to afford a 3:2 ratio of **8α/β** as a yellow syrup in 6 % yield.

^{1}H NMR (d_6-DMSO): δ 1.31 (s, 3H, CH$_3$), 1.45 (s, 3H, CH$_3$), 1.84 (s, 3H, NHAc), 3.50 (m, H-3, H-4, H-5, H-6, benzylic-H), 3.82 (dt, 1H, H-2α, J = 3.2, 9.1, 9.1 Hz), 4.45 (d, 1H, benzylic-H$_{A-1}$, J = 12.6 Hz), 4.66 (d, 1H, benzylic-H$_{A-2}$, J = 12.6 Hz), 4.75 (d, 1H, H-1α, J = 3.8 Hz), 4.95 (d, 1H, H-1β, J = 6.0 Hz), 7.33 (m, 10H, Ar-H), 7.65 (d, 1H, NHAcα, J = 9.2 Hz), 7.90 (d, 1H, NHAcβ, J = 8.3 Hz).

m/z calculated: 441.22   *m/z* found: 464.3 (M + Na)

Melting Point: syrup

Alternative formation of benzyl 2-acetamido-3-*O*-benzyl-2-deoxy-4,6-*O*-isopropylidene-β-D-glucopyranoside (8β) from 2-acetamido-2-deoxy-4,6-*O*-isopropylidene-α,β-D-glucopyranose (7α/β).

8β
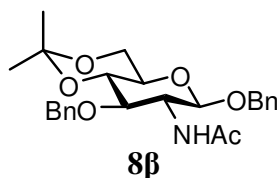
To an ice-cold solution of 2-acetamido-2-deoxy-4,6-*O*-isopropylidene-α,β-D-glucopyranose (**7α/β**, 4.44 g, 16.99 mmol) in *N,N*-dimethylformamide (30 mL) were

added barium oxide (26.06 g, 169.9 mmol) and barium hydroxide octahydrate (10.72 g, 33.98 mmol). Benzyl bromide (12.0 mL, 101.03 mmol) was then added dropwise *via* syringe with stirring. Stirring was continued for 2 hours at 0 °C and overnight at ~25 °C. Analysis by TLC (1:6 hexanes:ethyl acetate) showed the formation of a new, less polar UV-active spot (R_f = 0.58) indicating product formation. The mixture was then diluted with methylene chloride (250 mL), filtered to remove inorganic material, and the inorganic residue washed with methylene chloride (150 mL). The combined methylene chloride solutions were evaporated under reduced pressure to an oil. The oil was stirred with 1:1 water:hexanes (150 mL) overnight resulting in a solid mass that, upon isolation, was dissolved in ethanol and precipitated with water to afford **8β** as a white solid in 34% yield.

^{1}H NMR (CDCl$_3$): δ 1.43 (s, 3H, CH$_3$), 1.50 (s, 3H, CH$_3$), 1.82 (s, 3H, CH$_3$), 3.32 (dt, 1H, H-5, J = 5.3, 10.0, 10.0 Hz), 3.40 (dt, 1H, H-2, J = 8.2, 8.2, 10.0 Hz), 3.72 (t, 1H, H-4, J = 9.2, 9.2 Hz), 3.81 (t, 1H, H-6, J = 10.5, 10.5 Hz), 3.95 (dd, 1H, H-6', J = 5.4, 10.8 Hz), 3.98 (dd, 1H, H-3, J = 8.9, 9.9 Hz), 4.54 (d, 1H, benzylic-H$_{A-1}$, J = 12.0 Hz), 4.59 (d, 1H, benzylic-H$_{B-1}$, J = 11.9 Hz), 4.81 (d, 1H, benzylic-H$_{B-2}$, J = 12.3 Hz), 4.84 (d, 1H, benzylic-H$_{A-2}$, J = 12.3 Hz), 4.89 (d, 1H, H-1 , J = 8.4 Hz), 5.50 (d, 1H, NHAc , J = 7.8 Hz), 7.29 (m, 10H, Ar-H).

^{13}C NMR (CDCl$_3$): δ 19.11, 23.51, 29.18, 57.35, 62.27, 66.87, 71.12, 73.99, 75.35, 77.25, 99.29, 99.77, 127.65, 127.91, 127.99 (double), 128.09 (double), 128.31 (double), 128.41 (double), 137.27, 138.74, 170.23.

m/z calculated: 441.22   *m/z* found: 464.2 (M + Na)

Melting Point: 116-122 °C

Formation of benzyl 2-acetamido-3-*O*-benzyl-2-deoxy-α,β-D-glucopyranoside (9α/β) from benzyl 2-acetamido-3-*O*-benzyl-2-deoxy-4,6-*O*-isopropylidene-α,β-D-glucopyranoside (8α/β).

9α/β
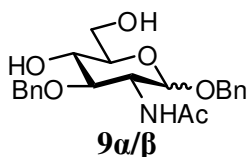
In a 100 mL round-bottom flask equipped with a rubber septum, N$_2$ balloon, and magnetic stir bar, benzyl 2-acetamido-3-*O*-benzyl-2-deoxy-4,6-*O*-isopropylidene-β-D-glucopyranoside (**8α/β**, 0.870 g, 1.97 mmol) was dissolved in dioxane (20 mL). A mixture of 9:1 H$_2$O:TFA (30 mL) was then added to the reaction mixture. After 24 hours, TLC (ethyl acetate) showed the formation of a new, more polar UV-active spot (R$_f$ = 0.23) indicating product formation. The organics were extracted with CH$_2$Cl$_2$ (3 x 15 mL). The organics were washed with saturated sodium bicarbonate (3 x 15 mL) and de-ionized water (1 x 15 mL). Drying over MgSO$_4$ and reducing resulted in an oil that was triturated with methylene chloride affording a 1:1 ratio of **9α/β** as a white solid in 89% yield.

^{1}H NMR (*d$_6$*-DMSO): δ 1.79 (s, 3H, NH<u>Ac</u>), 3.17 (m, 1H, H-2), 3.35 (m, 1H, H-4), 3.45 (t, 1H, H-3, *J* = 9.5, 9.5 Hz), 3.54 (dt, 1H, H-5, *J* = 5.9, 5.9, 11.8 Hz), 3.67 (m, 1H, H-6'), 3.74 (dd, 1H, H-6, *J* = 6.0, 11.9 Hz), 4.43 (d, 1H, H-1β, *J* = 8.4 Hz), 4.55 (d, 1H,

benzylic-H_{A-1}, J = 12.4 Hz), 4.57 (d, 1H, benzylic-H_{B-1}, J = 11.4 Hz), 4.59 (d, 1H, H-1α,

J = 3.8 Hz), 4.78 (d, 1H, benzylic-H_{B-2}, J = 11.5 Hz), 4.80 (d, 1H, benzylic-H_{A-2}, J = 12.4

Hz), 5.25 (d, 1H, N$\underline{H}$Acβ, J = 6.4 Hz), 7.29 (m, 10H, Ar-H), 7.88 (d, 1H, N$\underline{H}$Acα, J = 9.2

Hz).

^{13}C NMR (d_6-DMSO): δ 22.96, 54.10, 60.88, 69.46, 70.12, 73.44, 77.05, 82.76, 100.48,

127.16, 127.26 (double), 127.39 (double), 128.00 (double), 128.21 (double), 128.26,

138.06, 139.27, 169.01.

m/z calculated: 401.18 m/z found: 424.2 (M + Na)

Melting Point: 176-178 °C

Formation of benzyl 2-acetamido-4,6-di-O-acetyl-3-O-benzyl-2-deoxy-β-D-glucopyranoside (10β) from benzyl 2-acetamido-3-O-benzyl-2-deoxy-β-D-glucopyranoside (9β).
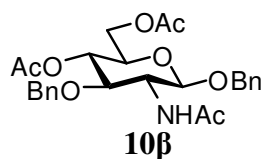
10β

In an oven-dried 25 mL round-bottom flask equipped with a rubber septum and

magnetic stir bar and under N_2 atmosphere, benzyl 2-acetamido-3-O-benzyl-2-deoxy-β-

D-glucopyranoside (**9β**, 0.020 g, 0.050 mmol) was dissolved in pyridine (1 mL). Acetic

anhydride (0.20 mL, 2.1 mmol) was added dropwise *via* syringe. After 24 hours, TLC

(ethyl acetate) showed the formation of a new, less polar UV-active spot (R_f = 0.63)

indicating product formation. The reaction was poured over ice water (10 mL) and then

the organics were extracted with CH_2Cl_2 (2 x 5 mL). The organics were washed with 5% v/v H_2SO_4 (3 x 5 mL) and de-ionized water (1 x 5 mL). Drying over $MgSO_4$ and reducing resulted in **10β** as a white solid in 20% yield.

^{1}H NMR (CDCl$_3$): δ 1.84 (s, 3H, CH$_3$), 1.96 (s, 3H, CH$_3$), 2.09 (s, 3H, CH$_3$), 3.27 (ddd, 1H, H-2, J = 7.5, 8.1, 10.2 Hz), 3.67 (ddd, 1H, H-5, J = 2.5, 5.1, 9.9 Hz), 4.12 (dd, 1H, H-6, J = 2.5, 12.2 Hz), 4.27 (dd, 1H, H-6', J = 5.1, 12.2 Hz), 4.36 (dd, 1H, H-3, J = 9.1, 10.2 Hz), 4.57 (d, 1H, benzylic H$_{A-1}$, J = 11.8 Hz), 4.58 (s, 2H, PhCH$_2$OR), 4.89 (d, 1H, benzylic H$_{A-2}$, J = 11.8 Hz), 5.05 (dd, 1H, H-4, J = 8.8, 9.6 Hz), 5.09 (d, 1H, H-1, J = 8.1 Hz), 5.70 (d, 1H, NHAc, J = 7.4 Hz), 7.29 (m, 10H, Ar-H).

^{13}C NMR (CDCl$_3$): δ 20.85 (double), 23.52, 57.98, 62.46, 70.69, 71.35, 71.85, 74.13, 77.58, 98.62, 127.85, 127.90 (double), 128.04 (double), 128.14 (double), 128.46 (double), 128.49, 137.01, 138.00, 169.67, 170.69, 170.88.

m/z calculated: 485.20   *m/z* found: 508.3 (M + Na)

Melting Point: 166-172 °C

Formation of benzyl 2-acetamido-3-*O*-benzyl-2-deoxy-4,6-di-*O*-methylsulfonyl-β-D-glucopyranoside (11β) from benzyl 2-acetamido-3-*O*-benzyl-2-deoxy-β-D-glucopyranoside (9β).
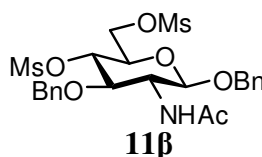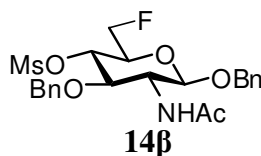

11β

In an oven-dried 50 mL round-bottom flask equipped with a rubber septum and magnetic stir bar and under N_2 atmosphere, benzyl 2-acetamido-3-O-benzyl-2-deoxy-β-D-glucopyranoside (**9β**, 0.41 g, 1.02 mmol) was dissolved in pyridine (10 mL). Methanesulfonyl chloride (0.24 mL, 3.06 mmol) was added dropwise *via* syringe. The mixture was stirred at 0 °C for 2-3 hours and then overnight at ~25 °C. TLC (ethyl acetate) showed the formation of a new, less polar UV-active spot (R_f = 0.51) indicating product formation. Several pieces of ice were added to the reaction mixture with stirring and cooling. The organics were extracted with CH_2Cl_2 (3 x 20 mL). The organics were washed with 5% v/v H_2SO_4 (3 x 20 mL) and de-ionized water (1 x 20 mL). Drying over $MgSO_4$ and reducing resulted in a yellow solid. The solid was then dissolved in ethanol/methanol and precipitated with de-ionized water to afford **11β** as a white solid in 55% yield.

^{1}H NMR (CDCl$_3$): δ 1.83 (s, 3H, O<u>Ac</u>), 2.91 (s, 3H, SO$_2$<u>CH$_3$</u>), 3.04 (s, 3H, SO$_2$<u>CH$_3$</u>), 3.41 (dt, 1H, H-2, J = 7.8, 7.8, 9.6 Hz), 3.84 (ddd, 1H, H-5, J = 2.9, 5.4, 9.5 Hz), 4.39 (dd, 1H, H-6, J = 5.3, 11.3 Hz), 4.40 (t, 1H, H-3, J = 9.3, 9.3 Hz), 4.56 (t, 1H, H-4, J = 9.1, 9.1 Hz), 4.57 (dd, 1H, H-6', J = 2.8, 11.4 Hz), 4.59 (d, 1H, benzylic-H$_{A-1}$, J = 11.8 Hz), 4.68 (d, 1H, benzylic-H$_{B-1}$, J = 11.4 Hz), 4.74 (d, 1H, benzylic-H$_{B-2}$, J = 11.3 Hz), 4.87 (d, 1H, benzylic-H$_{A-2}$, J = 11.8 Hz), 5.04 (d, 1H, H-1, J = 7.9 Hz) 5.70 (d, 1H, N<u>H</u>Ac, J = 7.6 Hz), 7.32 (m, 10H, Ar-H).

^{13}C NMR (CDCl$_3$): δ 23.44, 37.63, 38.69, 57.80, 67.76, 71.44, 71.46, 74.53, 77.66, 77.80, 98.41, 127.76 (double), 128.12, 128.17 (double), 128.55 (double), 128.63 (double), 128.72, 136.80, 137.45, 170.87.

m/z calculated: 557.14   *m/z* found: 580.2 (M + Na)

Melting Point: 152-154 °C

Formation of benzyl 2-acetamido-3-*O*-benzyl-2,6-dideoxy-4-*O*-methylsulfonyl-α,β-D-glucopyranoside (12α/β) from benzyl 2-acetamido-3-*O*-benzyl-2-deoxy-4,6-di-*O*-methylsulfonyl-α,β-D-glucopyranoside (11α/β).

12α/β
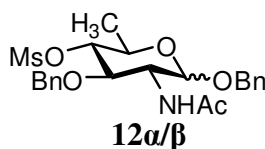
In an oven-dried 50 mL round-bottom flask equipped with a rubber septum and magnetic stir bar and under N$_2$ atmosphere, benzyl 2-acetamido-3-*O*-benzyl-2-deoxy-4,6-di-*O*-(methylsulfonyl)-α,β-D-glucopyranoside (**11α/β**, 0.500 g, 0.897 mmol) was dissolved in dimethylsulfoxide (25 mL). Sodium borohydride (0.136 g, 3.59 mmol) was added and N$_2$ atmosphere was reestablished. The mixture was stirred at 85 °C (oil bath) overnight. TLC (1:6 hexanes:ethyl acetate) showed the formation of a new, more polar UV-active spot (R$_f$ = 0.28) indicating product formation. The reaction mixture was then poured into a solution of 2% aqueous acetic acid (25 mL) and diluted with ice-water (100 mL). The resultant suspension was let stir overnight at ~25 °C. The white precipitate was filtered off, washed with water, and recrystallized with ethanol to afford 0.17g of **12α/β** as needles in 41% yield.

^{1}H NMR (CDCl$_3$): δ 1.35 (d, 3H, H-6α, *J* = 6.3), 1.43 (d, 3H, H-6β, *J* = 6.2), 1.82 (s, 3H, OAc), 1.83 (s, 3H, OAc), 2.85 (s, 3H, SO$_2$CH$_3$), 2.88 (s, 3H, SO$_2$CH$_3$), 3.36 (dt, 1H, H-2β, *J* = 8.0, 8.0, 9.7 Hz), 3.63 (dd, 1H, H-5β, *J* = 6.3, 9.0 Hz), 3.81 (dd, 1H, H-3α, *J* = 9.4, 10.5 Hz), 3.93 (dd, 1H, H-5α, *J* = 6.2, 9.5 Hz), 4.31 (t, 1H, H-4β, *J* = 9.2, 9.2 Hz), 4.34 (t, 1H, H-4α, *J* = 9.5, 9.5 Hz), 4.35 (t, 1H, H-3β, *J* = 9.4, 9.4 Hz), 4.40 (dt, 1H, H-2α, *J* = 3.8, 10.0, 10.0 Hz), 4.47 (d, 1H, benzylic-H$_{B-1}$, *J* = 11.8 Hz), 4.55 (d, 1H, benzylic-H$_{A-1}$, *J* = 11.8 Hz), 4.63 (d, 1H, benzylic-H$_{C-1}$, *J* = 10.9 Hz), 4.67 (d, 1H, benzylic-H$_{D-1}$, *J* = 11.6 Hz), 4.69 (d, 1H, benzylic-H$_{C-2}$, *J* = 10.9 Hz), 4.70 (d, 1H, benzylic-H$_{B-2}$, *J* = 12.2 Hz), 4.72 (d, 1H, benzylic-H$_{D-2}$, *J* = 11.4 Hz). 4.80 (d, 1H, H-1α, *J* = 3.8 Hz), 4.88 (d, 1H, benzylic-H$_{A-2}$, *J* = 11.8 Hz), 4.97 (d, 1H, H-1β, *J* = 8.2 Hz), 5.48 (d, 1H, NHAcα, *J* = 9.6 Hz) 5.57 (d, 1H, NHAcβ, *J* = 7.6 Hz), 7.34 (m, 20H, Ar-Hα/β).

^{13}C NMR (CDCl$_3$): δ 17.61, 17.88, 23.38, 23.52, 29.71, 38.64, 38.77, 52.75, 58.61, 66.43, 69.97, 70.00, 71.24, 74.30, 74.47, 77.22, 78.10, 83.22, 83.47, 96.78, 98.29, 127.64 (double), 128.02, 128.06, 128.13 (double), 128.18 (triple), 128.21, 128.39, 128.49 (double), 128.60 (double), 128.66 (double), 128.73 (double), 136.79, 137.16 (double), 137.67, 169.70, 170.78.

m/z calculated: 463.17   *m/z* found: 486.2 (M + Na)

Melting Point: 170-172 °C (decomposed)

Attempted formation of benzyl 2-acetamido-4-*O*-benzoyl-3-*O*-benzyl-2,6-dideoxy-α,β-D-glucopyranoside (13α/β) from benzyl 2-acetamido-3-*O*-benzyl-2,6-dideoxy-4-*O*-methylsulfonyl-α,β-D-glucopyranoside (12α/β).

13α/β
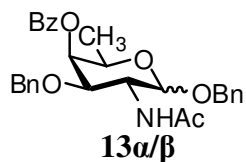
In a 50 mL round-bottom flask equipped with a rubber septum, a magnetic stir bar, and equipped with a reflux condenser, benzyl 2-acetamido-3-*O*-benzyl-2,6-dideoxy-4-*O*-(methylsulfonyl)-α,β-D-glucopyranoside (**12α/β**, 0.170 g, 0.367 mmol) was dissolved in hexamethylphosphoric triamide (5 mL). Sodium benzoate (0.182 g, 1.27 mmol) was added and the mixture was stirred at 140-145 °C (oil bath) overnight. TLC (1:6 hexanes:ethyl acetate) showed the formation of a new, less polar UV-active spot (R_f = 0.59) indicating product formation. The reaction mixture was cooled and poured into ice-water (20 mL). The resultant suspension was refrigerated overnight. The white precipitate was collected, washed with de-ionized water and dissolved in ethyl acetate. The solution was dried with $MgSO_4$ and treated with carbon powder. After removal of $MgSO_4$ and carbon powder, the filtrate was concentrated to afford a light brown powder. The powder was then dissolved in ethanol and triturated with water to afford a mixture of **12α/β** and **13α/β** as a white powder in 50% yield. The ^{1}H NMR spectrum of the crude was complex, however the mass spectrum suggested that some of **12α/β** had been formed.

m/z calculated: 489.22   *m/z* found: 512.3 (M + Na)

Melting Point: 168-169 °C

General procedure for the attempted formation of benzyl 2-acetamido-6-fluoro-3-*O*-benzyl-2,6-dideoxy-4-*O*-methylsulfonyl-β-D-glucopyranoside (14β) from benzyl 2-acetamido-3-*O*-benzyl-2-deoxy-4,6-di-*O*-methylsulfonyl-β-D-glucopyranoside using CsF reagent (11β).
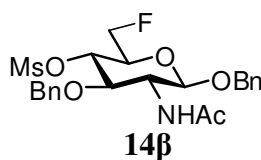
14β

In an oven-dried 25 mL round-bottom flask equipped with a rubber septum and magnetic stir bar and under N_2 atmosphere, benzyl 2-acetamido-3-*O*-benzyl-2-deoxy-4,6-di-*O*-(methylsulfonyl)-β-D-glucopyranoside (**11β**, 0.055 g, 0.099 mmol) was dissolved in a solvent (See Table 2). Cesium fluoride was added and N_2 atmosphere was reestablished. The mixture was stirred at different temperatures for varying amounts of time. TLC (ethyl acetate) showed no product formation. The reaction mixture was then extracted with methylene chloride (1 x 20 mL) then the organics were washed with de-ionized water (3 x 10 mL). The organics were then dried over anhydrous $MgSO_4$ and evaporated. The resulting oil was dissolved in ethanol, triturated with de-ionized water, and then purified *via* flash column chromatography to afford 0.05g of starting material **11** as a white solid.

Attempted formation of benzyl 2-acetamido-6-fluoro-3-*O*-benzyl-2,6-dideoxy-4-*O*-methylsulfonyl-β-D-glucopyranoside (14β) from benzyl 2-acetamido-3-*O*-benzyl-2-deoxy-4,6-di-*O*-methylsulfonyl-β-D-glucopyranoside *via* microwave assisted heating using CsF reagent (11β).

14β
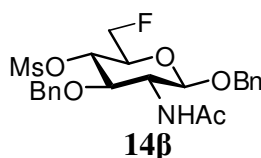
In a 10 mL pressurized vial equipped with a magnetic stirring bar, benzyl 2-acetamido-3-*O*-benzyl-2-deoxy-4,6-di-*O*-(methylsulfonyl)-β-D-glucopyranoside   (**11β**, 0.050 g, 0.090 mmol) was dissolved in *N,N*-dimethylformamide (4 mL). Cesium fluoride (0.041 g, 0.269 mmol) was added and the reaction mixture was heated (100 °C) in a microwave for varying amounts of time.   TLC (ethyl acetate) showed no product formation. The reaction mixture was then extracted with methylene chloride (1 x 10 mL) then the organics were washed with de-ionized water (3 x 10 mL). The organics were then dried over anhydrous MgSO₄ and evaporated. The resulting oil was dissolved in ethanol, triturated with de-ionized water, and then purified *via* flash column chromatography to afford 0.05g of starting material **11β** as a white solid.

Attempted formation of benzyl 2-acetamido-6-fluoro-3-*O*-benzyl-2,6-dideoxy-4-*O*-methylsulfonyl-β-D-glucopyranoside (14β) from benzyl 2-acetamido-3-*O*-benzyl-2-deoxy-4,6-di-*O*-methylsulfonyl-β-D-glucopyranoside (11β) using TBAF reagent

14β

In an oven-dried 25 mL round-bottom flask equipped with a rubber septum and magnetic stir bar and under N_2 atmosphere, benzyl 2-acetamido-3-*O*-benzyl-2-deoxy-4,6-di-*O*-(methylsulfonyl)-β-D-glucopyranoside (**11β**, 0.030 g, 0.054 mmol) was dissolved in acetonitrile (3 mL) and tetra-*n*-butylammonium fluoride (0.12 mL, 0.12 mmol) was added dropwise *via* syringe. The mixture was stirred at different temperatures for varying amounts of time. Analysis with TLC (ethyl acetate) indicated only starting material. De-ionized water (5 mL) was added to the reaction mixture and the resulting white precipitate was isolated, dissolved in methylene chloride, and washed with de-ionized water (2 x 10 mL). The organics were dried over anhydrous $MgSO_4$ and evaporated to give 0.019 g of **11β** as a white solid.

General procedure for the formation of benzyl 2-acetamido-6-azido-3-*O*-benzyl-2,6-dideoxy-4-*O*-methylsulfonyl-β-D-glucopyranoside (15β) from benzyl 2-acetamido-3-*O*-benzyl-2-deoxy-4,6-di-*O*-methylsulfonyl-β-D-glucopyranoside (11β).
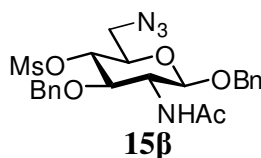
15β

In an oven-dried 25 mL round-bottom flask equipped with a rubber septum and magnetic stir bar and under N_2 atmosphere, benzyl 2-acetamido-3-*O*-benzyl-2-deoxy-4,6-di-*O*-(methylsulfonyl)-β-D-glucopyranoside (**11β**, 0.029 g, 0.052 mmol) was dissolved in *N*,*N*-dimethylformamide (6 mL). Sodium azide was added and N_2 atmosphere was reestablished. The mixture was stirred at 70 °C (oil bath) overnight. TLC (ethyl acetate) showed the formation of a new, less polar UV-active spot (R_f = 0.59) indicating product formation. The reaction mixture was then extracted with methylene chloride (1 x 20 mL)

then washed with de-ionized water (3 x 20 mL). The organics were then dried over anhydrous MgSO₄, evaporated, and purified *via* flash column chromatography (ethyl acetate) to afford 0.014g of **15β** as a white solid in 53% yield.

^{1}H NMR (CDCl₃): δ 1.84 (s, 3H, O$\underline{Ac}$), 2.87 (s, 3H, SO₂$\underline{CH_3}$), 3.34 (m, 1H, H-2), 3.55 (d, 2H, H-6, *J* = 5.0 Hz), 3.76 (m, 1H, H-5), 4.45 (m, 2H, H-3, H-4), 4.60 (d, 1H, benzylic-H$_{A-1}$, *J* = 11.6 Hz), 4.69 (d, 1H, benzylic-H$_{B-1}$, *J* = 11.4 Hz), 4.73 (d, 1H, benzylic-H$_{B-2}$, *J* = 11.5 Hz), 4.91 (d, 1H, benzylic-H$_{A-2}$, *J* = 11.7 Hz), 5.08 (d, 1H, H-1, *J* = 8.2 Hz), 5.58 (d, 1H, N$\underline{H}$Ac, *J* = 7.5 Hz).

m/z calculated: 504.17   *m/z* found: 527.2 (M + Na)

Melting Point: 172-176 °C

Attempted formation of benzyl 2-acetamido-6-fluoro-3-*O*-benzyl-2,6-dideoxy-4-*O*-methylsulfonyl-β-D-glucopyranoside (14β) from benzyl 2-acetamido-3-*O*-benzyl-2-deoxy-4,6-di-*O*-methylsulfonyl-β-D-glucopyranoside (11β) using DAST reagent
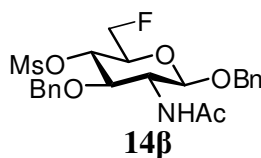
14β

In an oven-dried 25 mL round-bottom flask equipped with a rubber septum and magnetic stir bar and under N₂ atmosphere, benzyl 2-acetamido-3-*O*-benzyl-2-deoxy-4,6-di-*O*-(methylsulfonyl)-β-D-glucopyranoside (**11β**, 0.031 g, 0.056 mmol) was added diethylaminosulfur trifluoride (0.14 mL, 1.09 mmol) dropwise *via* syringe. The mixture was stirred neat or with methylene chloride (5 mL) for varying amounts of time.

Analysis with TLC (ethyl acetate) indicated no reaction had occured. Methanol (10 mL) was added to the reaction mixture and after evaporating, purification *via* flash column chromatography (3:1 ethyl acetate:methanol) gave 0.04 g of **11β** as a white solid.

References:

1. Guthrie, R. D.; Honeyman, J. *An Introduction to the Chemistry of Carbohydrates*; Oxford University: London, 1968; p 1.

2. El Khadem, H. S. *Carbohydrate Chemistry: Monosaccharides and Their Oligomers*; Academic: San Diego, 1988; pp. 1-5, 54, 191.

3. Stick, Robert V. *Carbohydrates: The Sweet Molecules of Life*; Academic: San Diego, 2001; pp 1, 3.

4. *The Carbohydrates: Chemistry and Biochemistry*; Pigman, W.; Horton, D., Eds.; Academic: New York, 1972; pp 2, 3, 7.

5. *Carbohydrate Chemistry*; Boons, G.-J., Ed.; Blackie Academic and Professional: London, 1998; pp 1, 10.

6. Collins, P. M.; Ferrier, R. J. *Monosaccharides: Their Chemistry and Their Roles in Natural Products*; John Wiley & Sons: New York, 1995; pp 1-27.

7. Bols, M. *Carbohydrate Building Blocks*; John Wiley & Sons: New York, 1996; p 1.

8. *Carbohydrate Chemistry*; Kennedy, J. F., Ed.; Oxford University: New York, 1988; pp 3-4, 33, 40.

9. Allavudeen, S. S.; Kuberan, B.; Loganathan, D. *Carbohydr. Res.* **2002**, *337*, 965-968.

10. Duncan, S. J. *Towards glycomimetic derivatives of N-acetyl-D-fucosamine*. M.S. Thesis, Youngstown State University, Youngstown, OH, August **2006**.

11. Osborn, H. M. I.; Khan, T. H. *Oligosaccharides: Their Synthesis and Biological Roles*; Oxford University: New York, 2000; pp 2, 9, 12-14.

12. O'Riordan, K.; Lee, J. C. *J. Clin. Microbiol. Rev.* **2004**, *17*, 218-234.

13. De Kerpel, W.; Roelandt, P.; Depoorter, M. *Eur. J. Plast. Surg.* **2004**, *27*, 182-184.

14. Chambers, H. F. *Emerging Infect. Dis.* **2001**, *7*, 178-182.

15. Hochkeppel, H. K.; Braun, D. G.; Vischer, W.; Imm, A.; Sutter, S.; Staeubli, U.; Guggenheim, R.; Kaplan, E. L.; Boutonnier, A.; Fournier, J. M. *J. Clin. Microbiol.* **1987**, *25*, 526-530.

16. Gale, E. F.; Cundliffe, E.; Reynolds, P. E.; Richmond, M. H.; Waring, M. J. *The Molecular Basis of Antibiotic Action*; John Wiley & Sons, 1981; pp 51-52, 121, 431, 448, 477.

17. *Biosynthesis of Antibiotics*; Snell, J. F., Ed.; Academic: New York, 1966; Vol. 1, pp 30, 42.

18. Cunha, B. A. *Seminars in Respiratory and Critical Care Medicine.* **2000**, *21*, 3-8.

19. Baquero, F.; Baquero-Artigao, G.; Cantón R.; García-Rey, C. *J. Antimicrob. Chemother*. **2002**, *Suppl*. *S2*, 27-37.

20. Aminov, R. I.; Mackie, R. I. *FEMS Microbiol. Lett.* **2007**, *27*, 147-161.

21. Andersson, D. I.; Levin, B. R. *Curr. Opin. Microbiol*. **1999**, *2*, 489-493.

22. Majiduddin, F. K.; Materon, I. C.; Palzkill, T. G. *Int. J. Med. Microbiol*. **2002**, *292*, 127-137.

23. Therrien, C.; Levesque, R. C. *FEMS Microbiol. Rev*. **2000**, *24*, 251-262.

24. Tenover, T. C.; Biddle, J. W.; Lancaster, M. V. *Emerging Infect. Dis.* **2001**, *7*, 327-332.

25. Boger, D. L. *Med. Res. Rev*. **2001**, *21*, 356-381.

26. Howe, R. A.; Monk, A.; Wootton, M; Walsh, T. R.; Enright, M. C. *Emerging Infect. Dis.* **2004**, *10*, 855-857.

27. Schäfer, M; Schneider, T. R.; Sheldrick, G. M. *Structure* **1996**, *4*, 1509-1515.

28. Evans, D. A.; Wood, M. R.; Trotter, B. W.; Richardson, T. I.; Barrow, J. C.; Katz, J. L. *Angew. Chem. Int. Ed.* **1998**, *37*, 2700-2704.

29. Evans, D. A.; Dinsmore, C. J.; Watson, P. S.; Wood, M. R.; Richardson, T. I.; Trotter, B. W.; Katz, J. L. *Angew. Chem. Int. Ed.* **1998**. *37*, 2704-2708.

30. Nicolaou, K. C.; Cho, S. Y.; Hughes, R.; Winssinger, N.; Smethurst, C.; Labischinski, H.; Endermann, R. *Chem. Eur. J.* **2001**. *7*. 3798-3823.

31. Crowley, B. M.; Boger, D. L. *J. Am. Chem. Soc.* **2006**. *128*. 2885-2892.

32. Kneidinger, B.; O'Riordan, K.; Li, J.; Brison, J.-R.; Lee, J. C.; Lam, J. S. *J. Biol. Chem.* **2003**, *278*, 3615-3627.

33. Götz, F. *Curr. Opin. Microbiol.* **2004**, *7*, 477-487.

34. García-Lara, J.; Masalha, M.; Foster, S. J. *Drug Discovery Today*. **2005**, *10*, 643-651.

35. *Staphylococcus aureus: Infection and Disease*; Honeyman, A., Friedman, H., Bendinelli, M., Eds.; Plenum: New York, 2001.

36. Jones, C. *Carbohydr. Res.* **2005**, *340*, 1097-1106.

37. Illarionov, P.; Torgov, V.; Hancock, I.; Shibaev, V. *Russ. Chem. Bull.* **2001**, *181*, 1303-1308.

38. Horton, D.; Saeki, H. *Carbohydr. Res.* **1978**, *63*, 270-276.

39. Purser, S.; Moore, P. R.; Swallow, S.; Gouverneur, V. *Chem. Soc. Rev.* **2008**, *37*, 320-330.

40. Ismail, F. M. D. *J. Fluorine Chem.* **2002**, *118*, 27-33.

41. *Fluorinated Carbohydrates: Chemical and Biochemical Aspects*; Taylor, N. F., Ed.; Developed from a symposium sponsored by the Division of Carbohydrate Chemistry

at the 194th Meeting of the American Chemical Society, New Orleans, LA, 1987, pp 59-60.

42. Shimizu, M.; Hiyama, T. *Angew. Chem. Int. Ed.* **2005**, *44*, 214-231.

43. Hasegawa, A.; Kiso, M. *Carbohydr. Res*. **1978**, *63*, 91-98.

44. Dax, K.; Albert, M.; Ortner, J.; Paul, B. J. *Carbohydr. Res*. **2000**, *327*, 47-86.

45. Kim, D. W.; Ahn, D. S.; Oh, Y. H.; Lee, S.; Kil, H. S.; Oh, S. J.; Lee, S. J.; Kim, J. S.; Ryu, J. S.; Moon, D. H.; Chi, D. Y. *J. Am. Chem. Soc.* **2006**, *128*, 16394-16397.

46. Seibel, J.; Hillringhaus, L.; Moraru, R. *Carbohydr. Res.* **2005**, *340*, 507-511.

47. Song, Z.; Hsung, R. P. *Org. Lett*. **2007**, *9*, 2199-2202.

48. Card, P. J. *J. Org. Chem*. **1983**, *48*, 393-395.

49. Card, P. J.; Reddy, G. S. *J. Org. Chem*. **1983**, *48*, 4734-4743.

50. Biedermann, D.; Sarek, J.; Klinot, J.; Hajduch, M.; Dzubak, P. *Synthesis*. **2005**, *7*, 1157-1163.

51. Pilcher, A. S.; Ammon, H. L.; DeShong, P. *J. Am. Chem. Soc*. **1995**, *117*, 5166-5167.

Appendix A
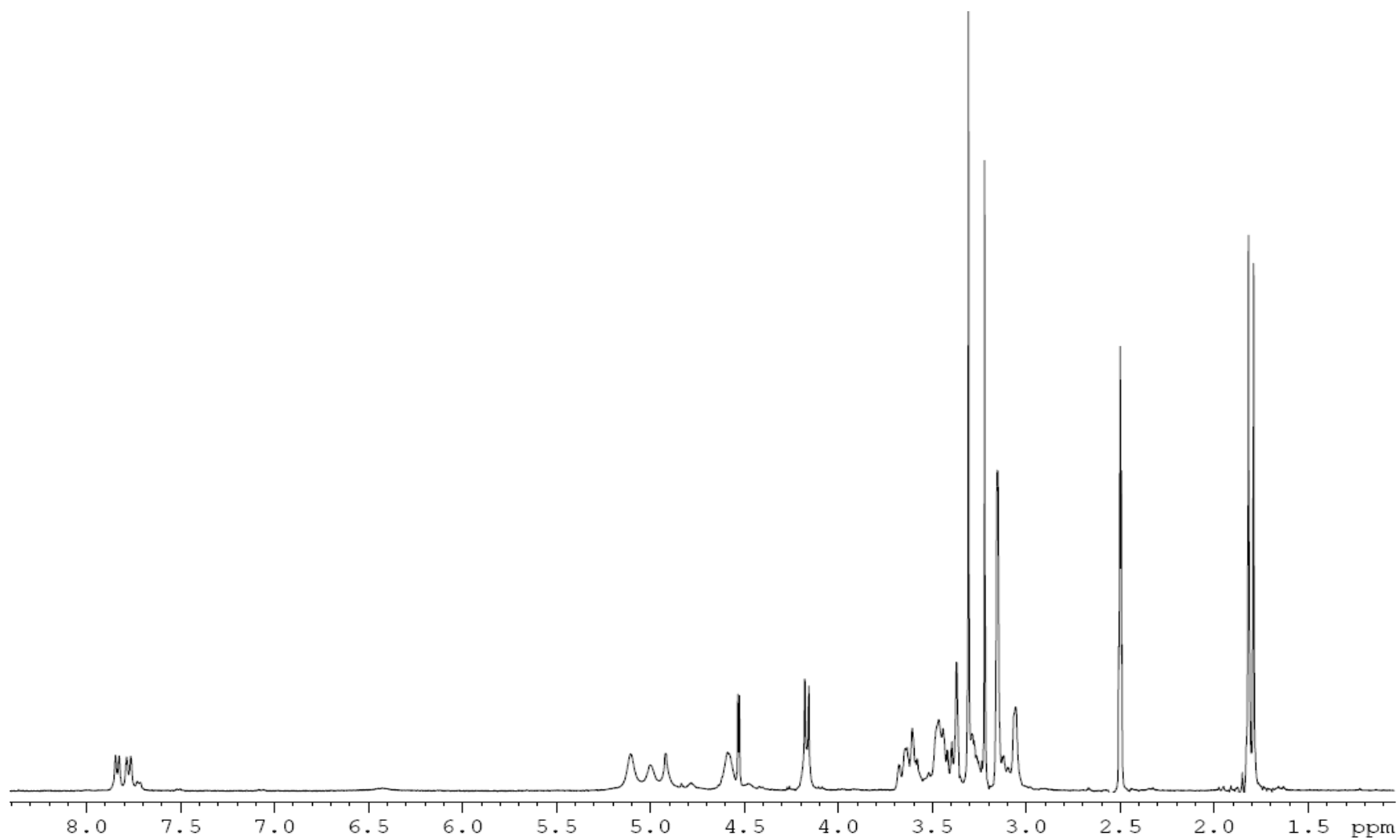
Figure 29: 400 MHz ^{1}H spectrum of **2α/β**.
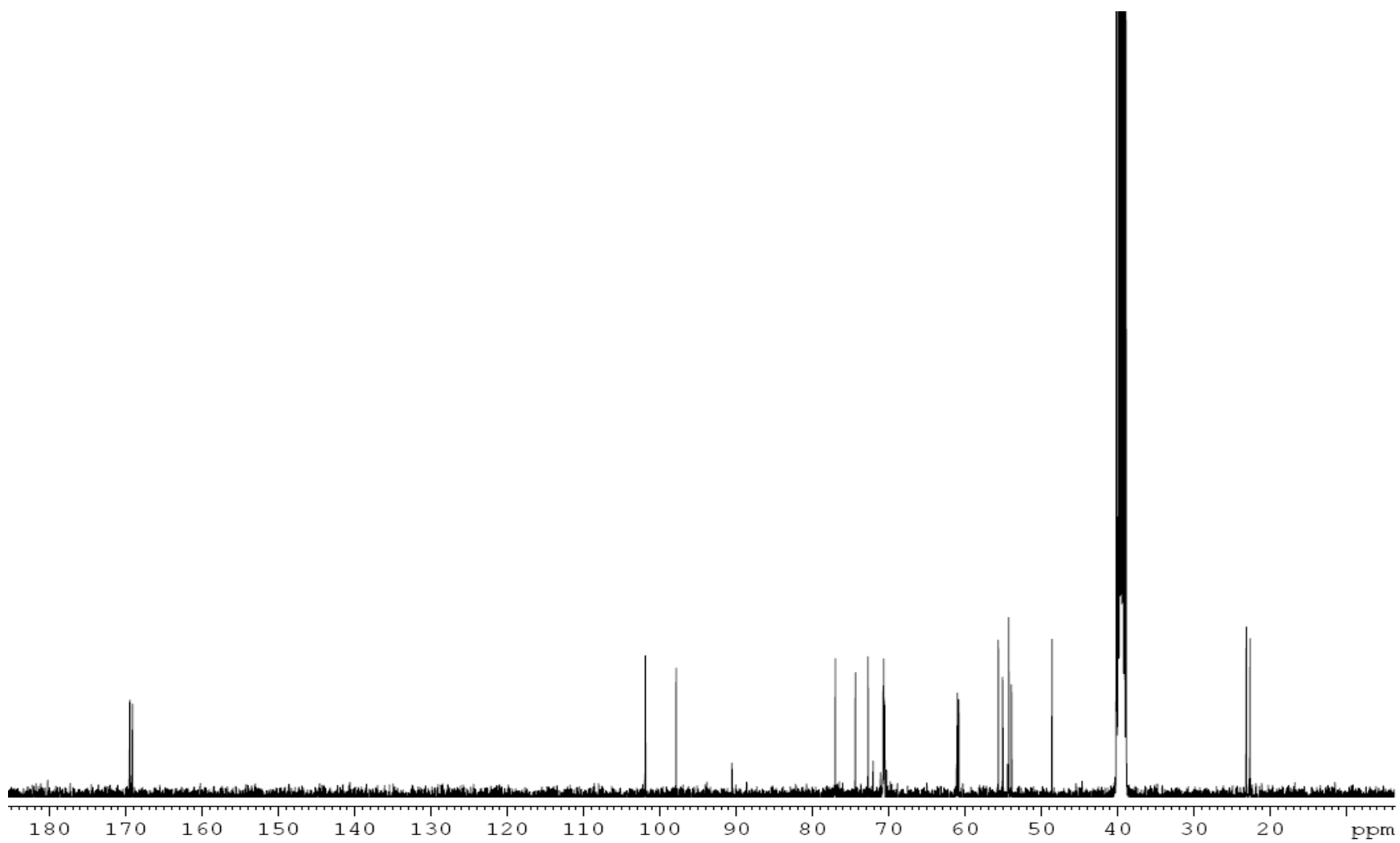
Figure 30: 100 MHz ^{13}C spectrum of **2α/β**.
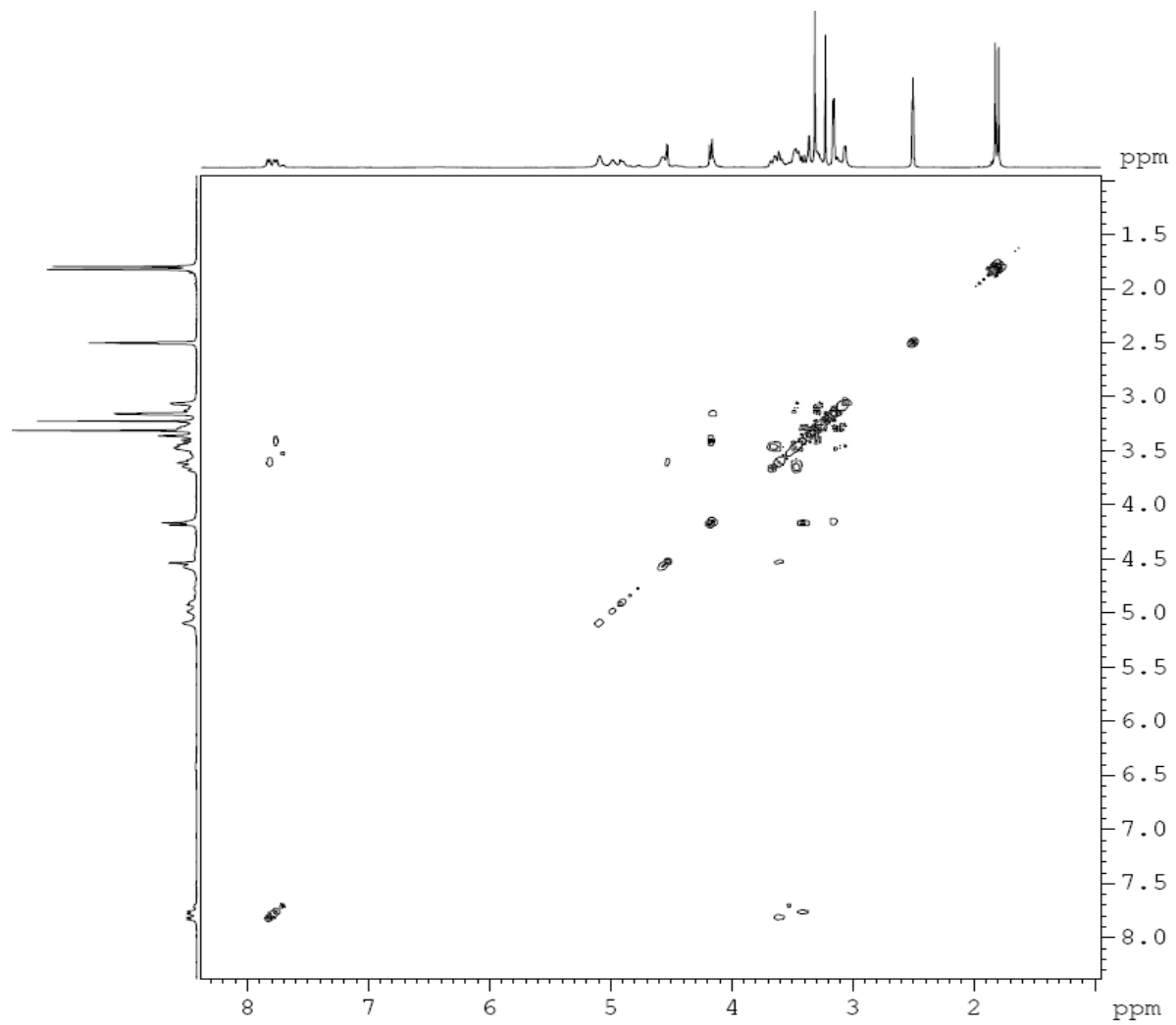
Figure 31: 400 MHz ^{1}H-^{1}H COSY spectrum of **2α/β**.

Display Report

Analysis Info

Analysis Name	ME2-1050.d	Acquisition Date	04/24/08 17:25:54	Operator	Administrator
Sample Name	ME-2-105	Method	XQ Default.ms	Instrument	Esquire-LC_00135
Comment	ME-2-105				

Acquisition Parameter

Ion Source Type	ESI	Mass Range Mode	Std/Normal	Ion Polarity	Positive	Alternating Ion Polarity	n/a
Scan Begin	15.00 m/z	Scan End	400.00 m/z	Averages	10 Spectra	Accumulation Time	1818 µs
Capillary Exit	99.3 Volt	Skim 1	28.5 Volt	Trap Drive	43.9	Auto MS/MS	Off

Bruker Daltonics DataAnalysis 3.0   printed: 04/24/08   17:38:28   Page 1 of 1
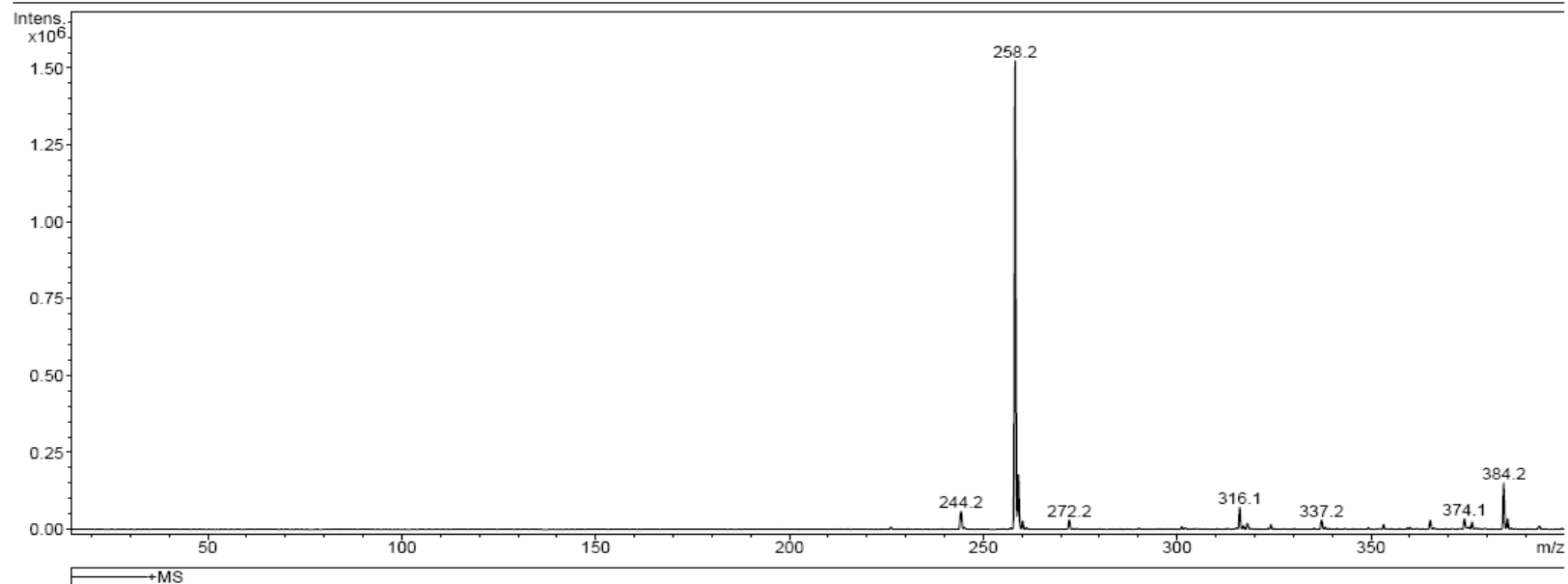
Figure 32: Mass spectrum of **2α/β**.
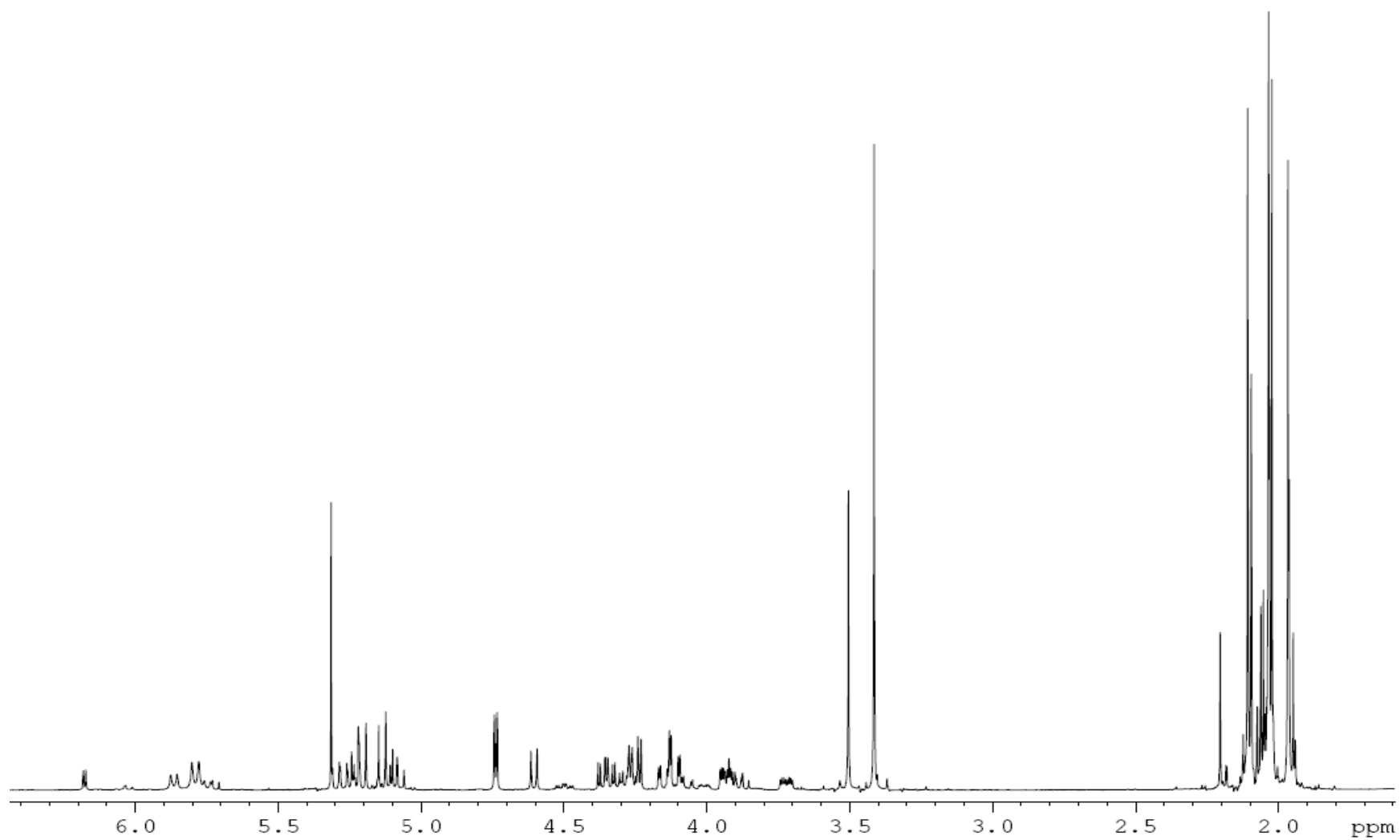
Figure 33: 400 MHz ^{1}H spectrum of **3α/β**.
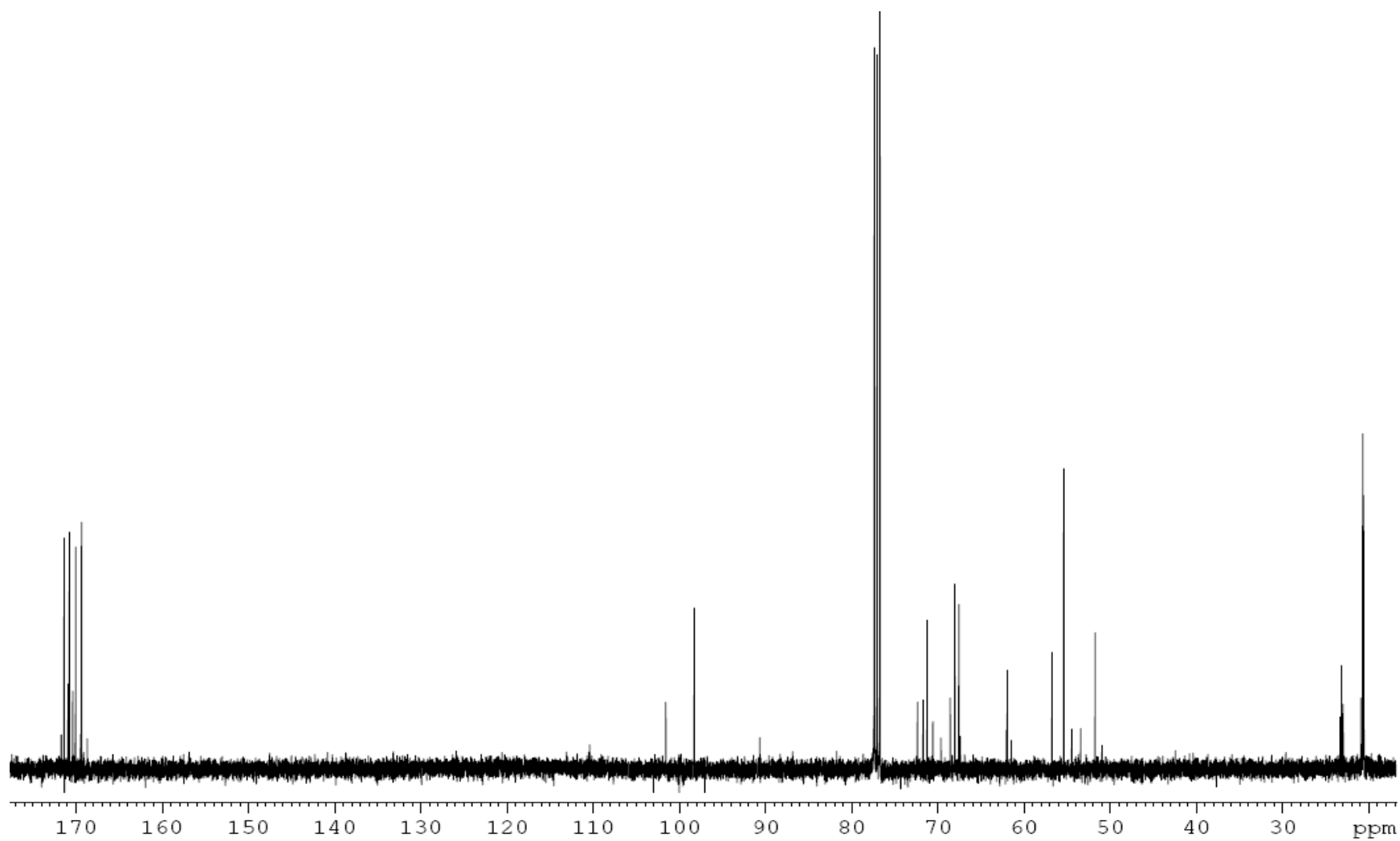
Figure 34: 100 MHz ^{13}C spectrum of **3α/β**.
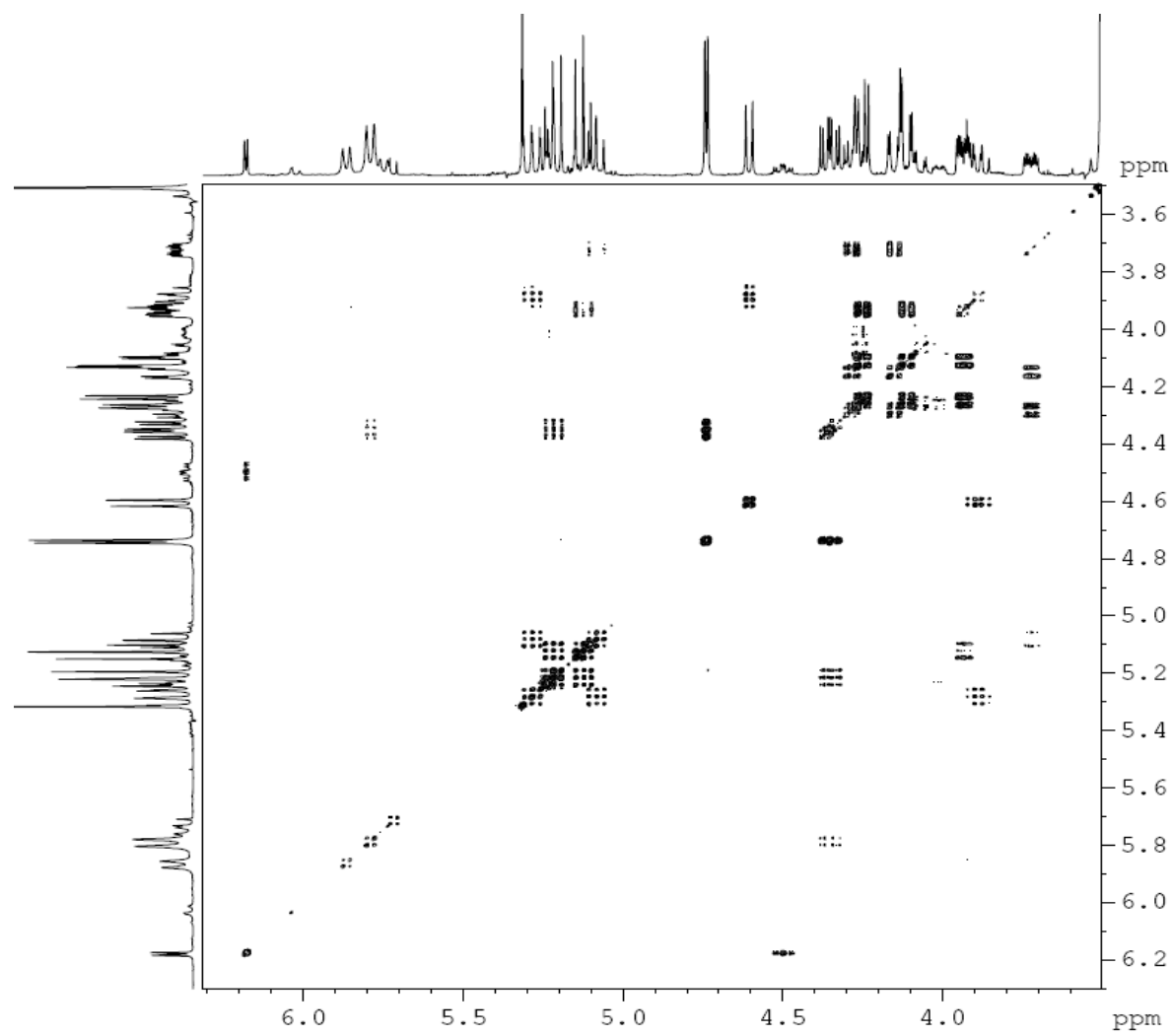
Figure 35: 400 MHz ¹H-¹H COSY spectrum of **3α/β**.

Display Report

Figure 36: Mass spectrum of **3α/β**.
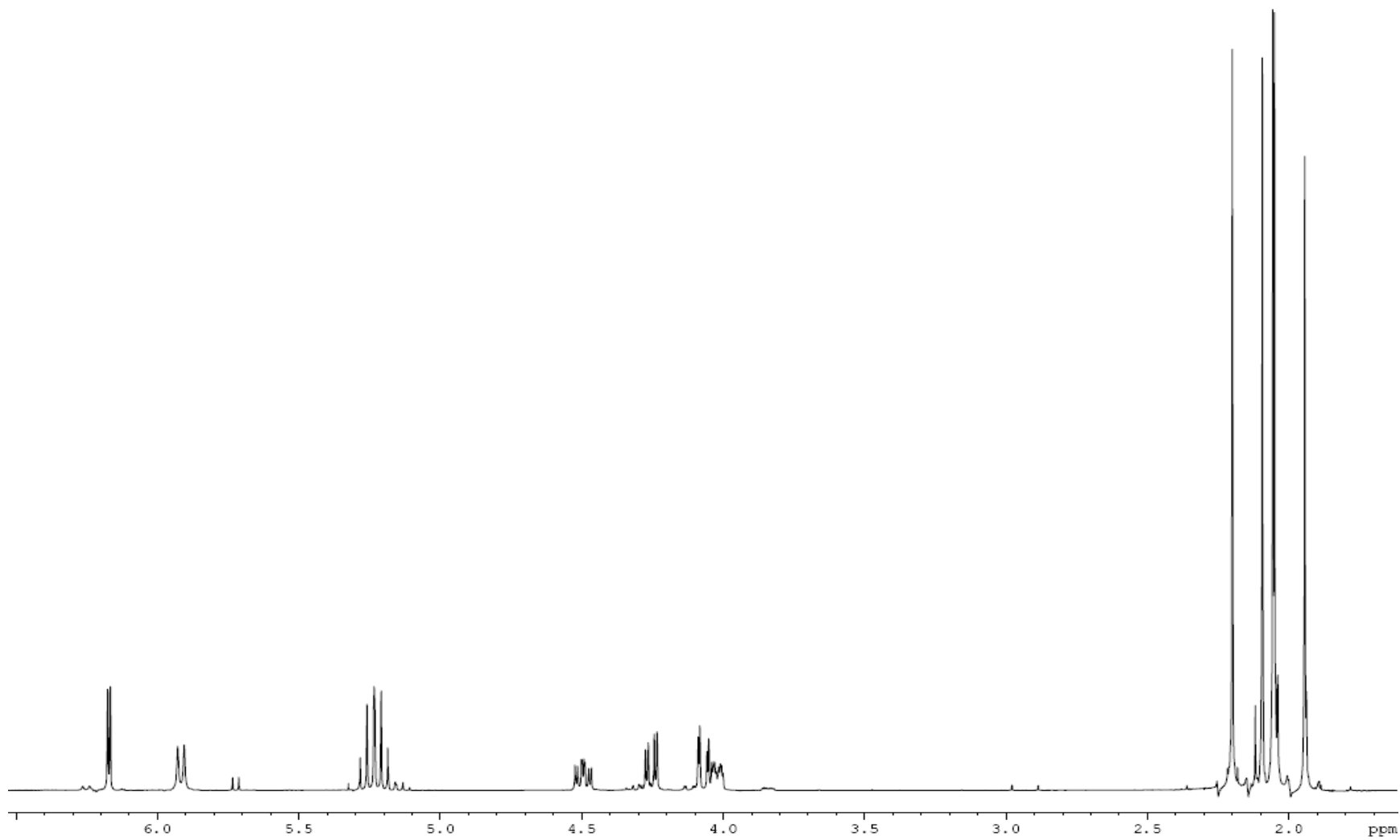
Figure 37: 400 MHz ^{1}H spectrum of **5α/β**.
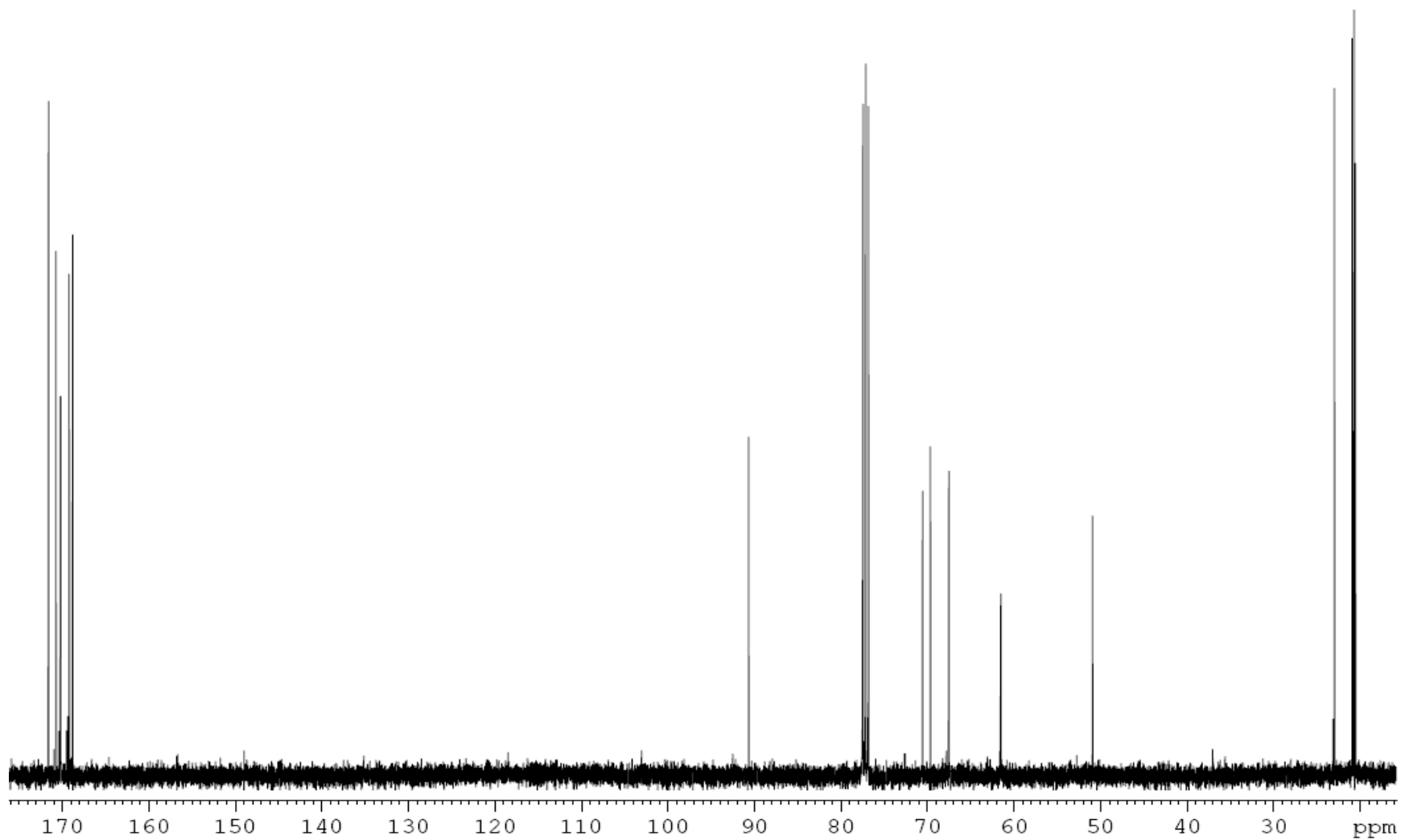
Figure 38: 100 MHz ^{13}C spectrum of **5α/β**.
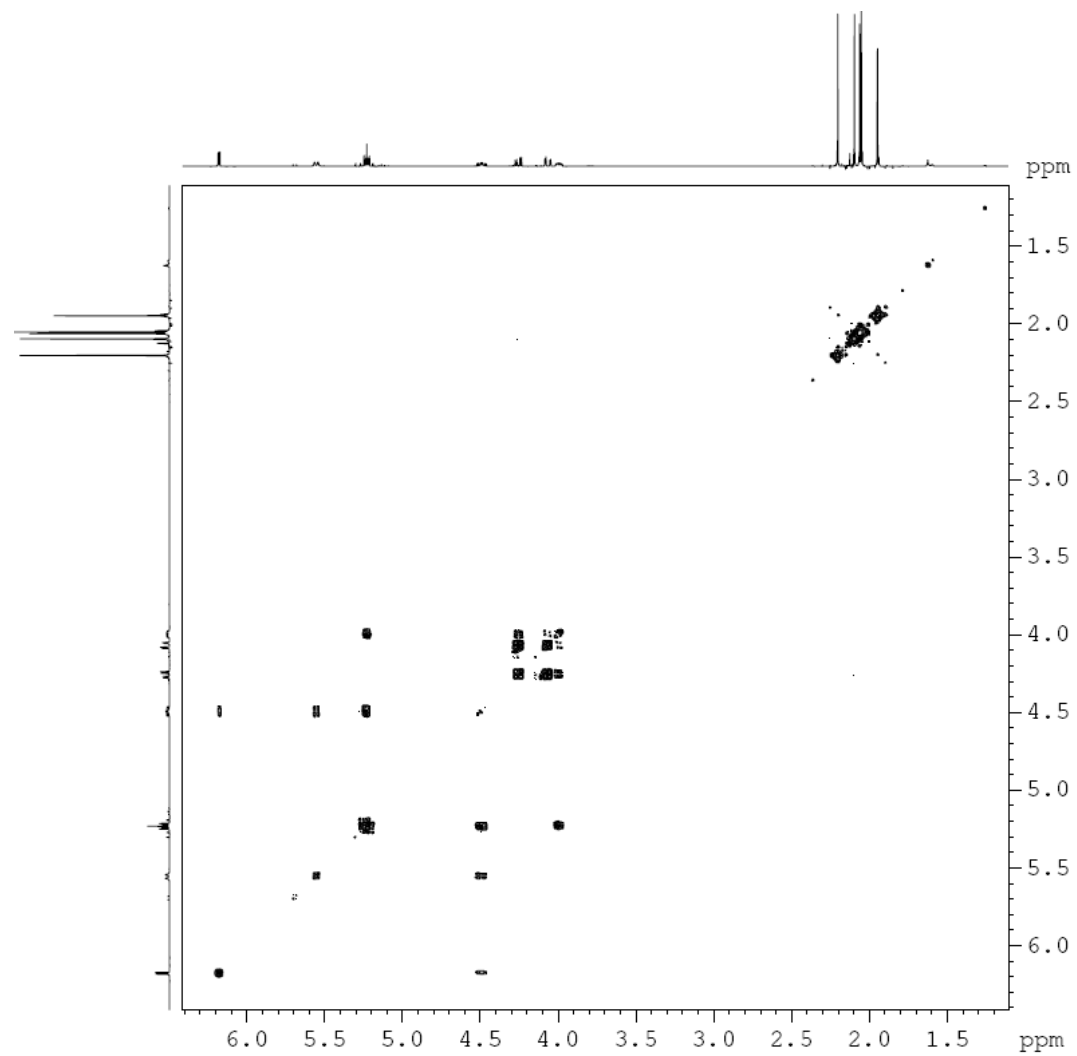
Figure 39: 400 MHz ^{1}H-^{1}H COSY spectrum of **5α/β**.

Figure 40: Mass spectrum of **5α/β**.
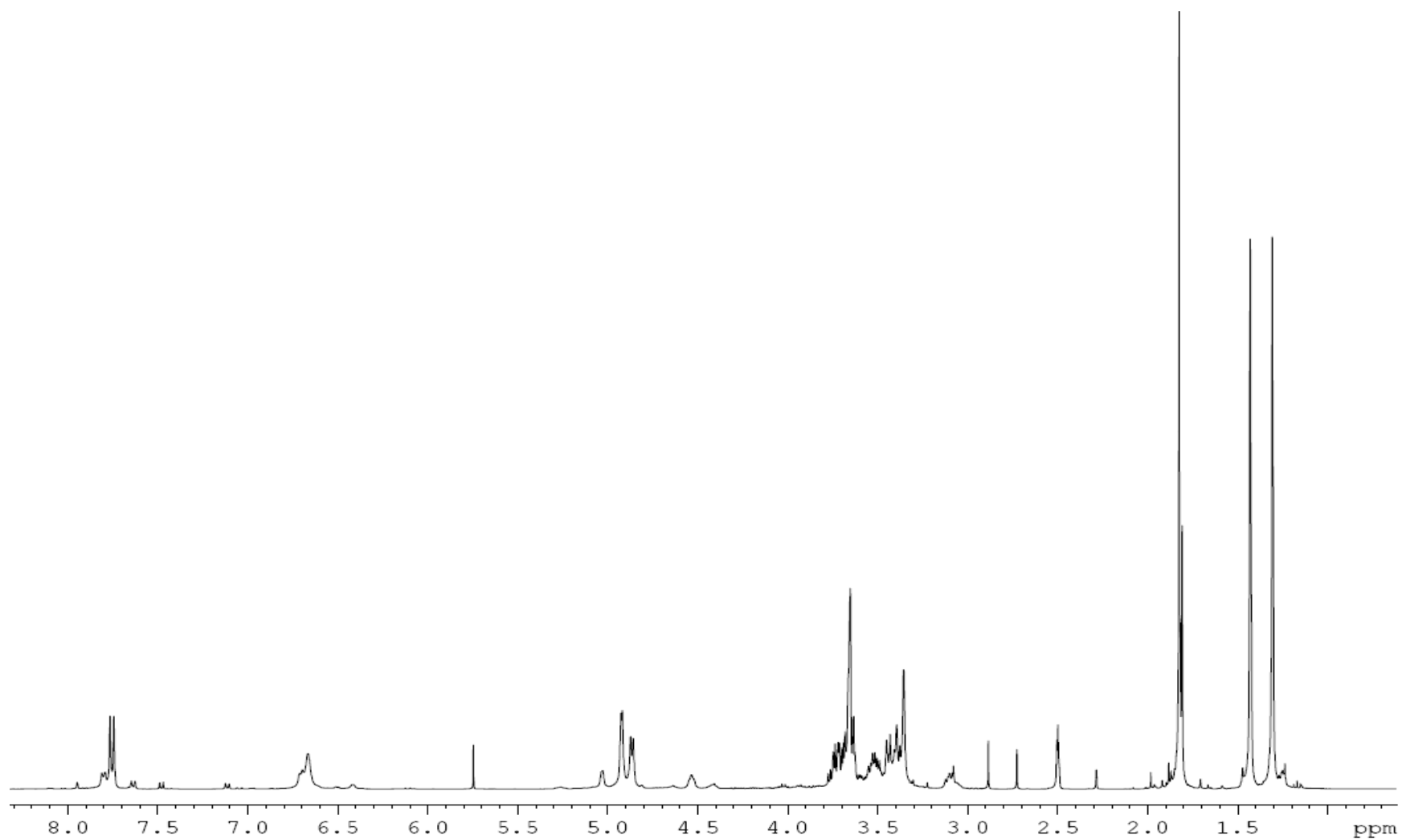
Figure 41: 400 MHz ^{1}H spectrum of **6α/β**.
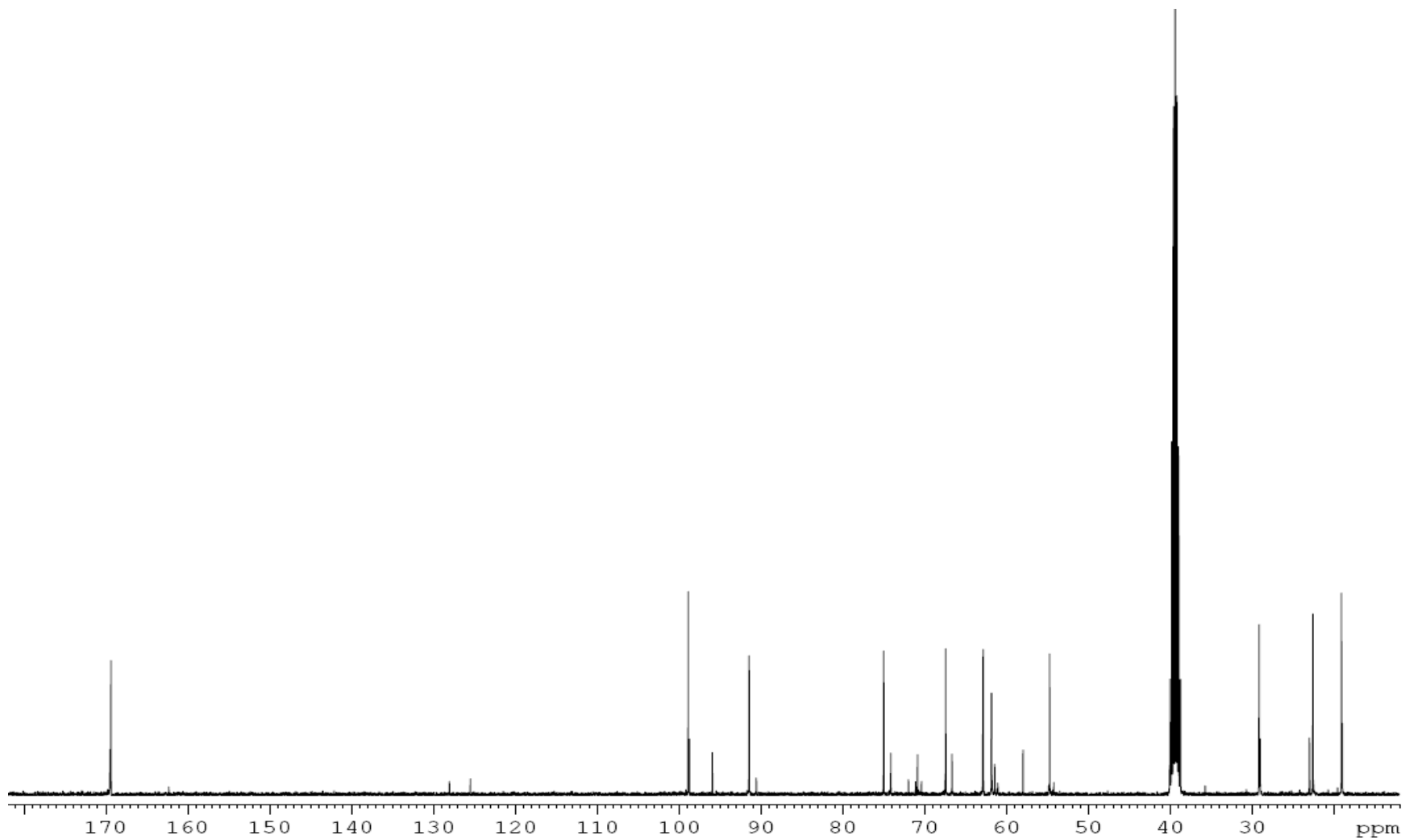
Figure 42: 100 MHz ^{13}C spectrum of **6α/β**.
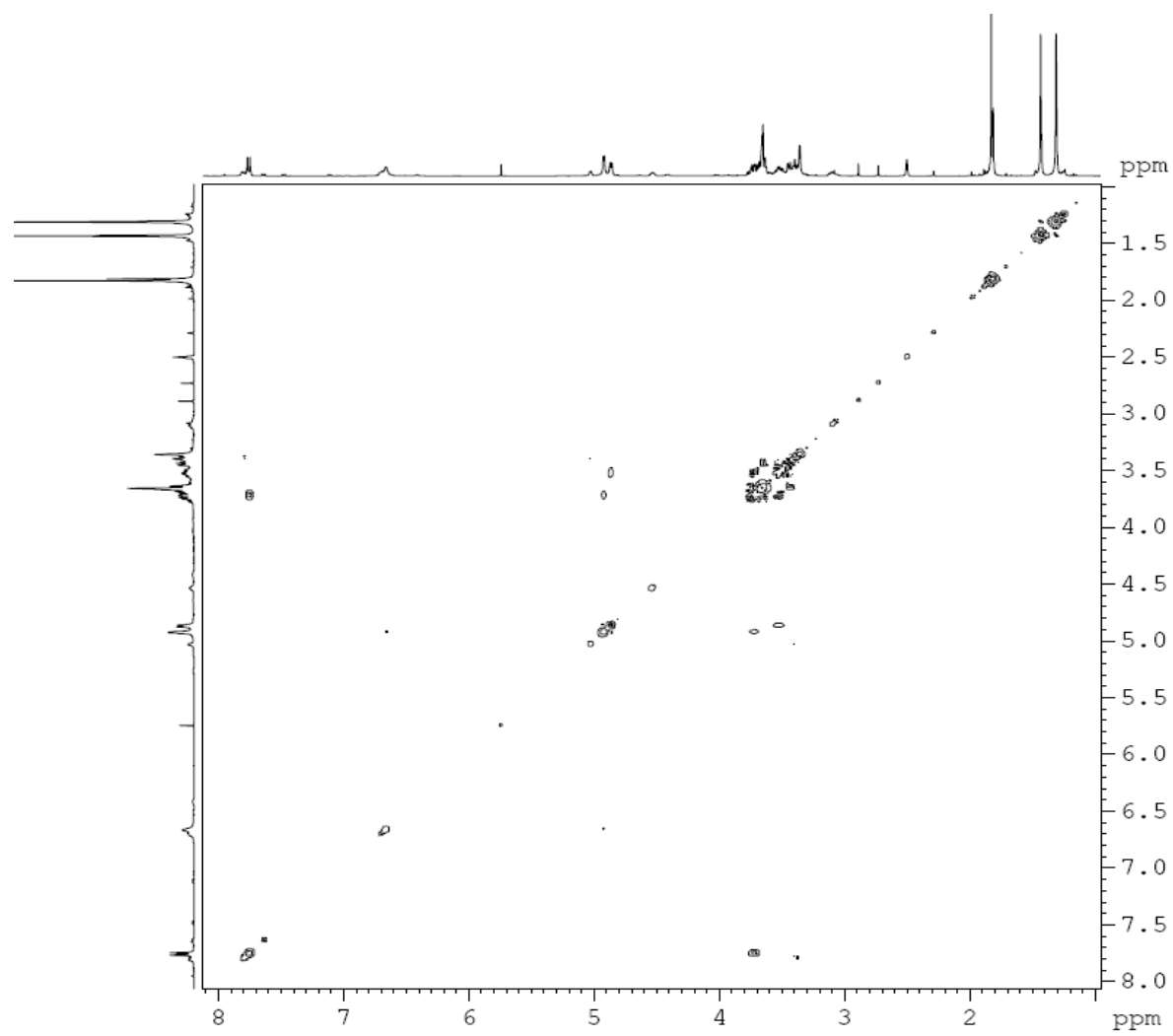
Figure 43: 400 MHz ¹H-¹H COSY spectrum of **6α/β**.

Figure 44: Mass spectrum of **6α/β**.
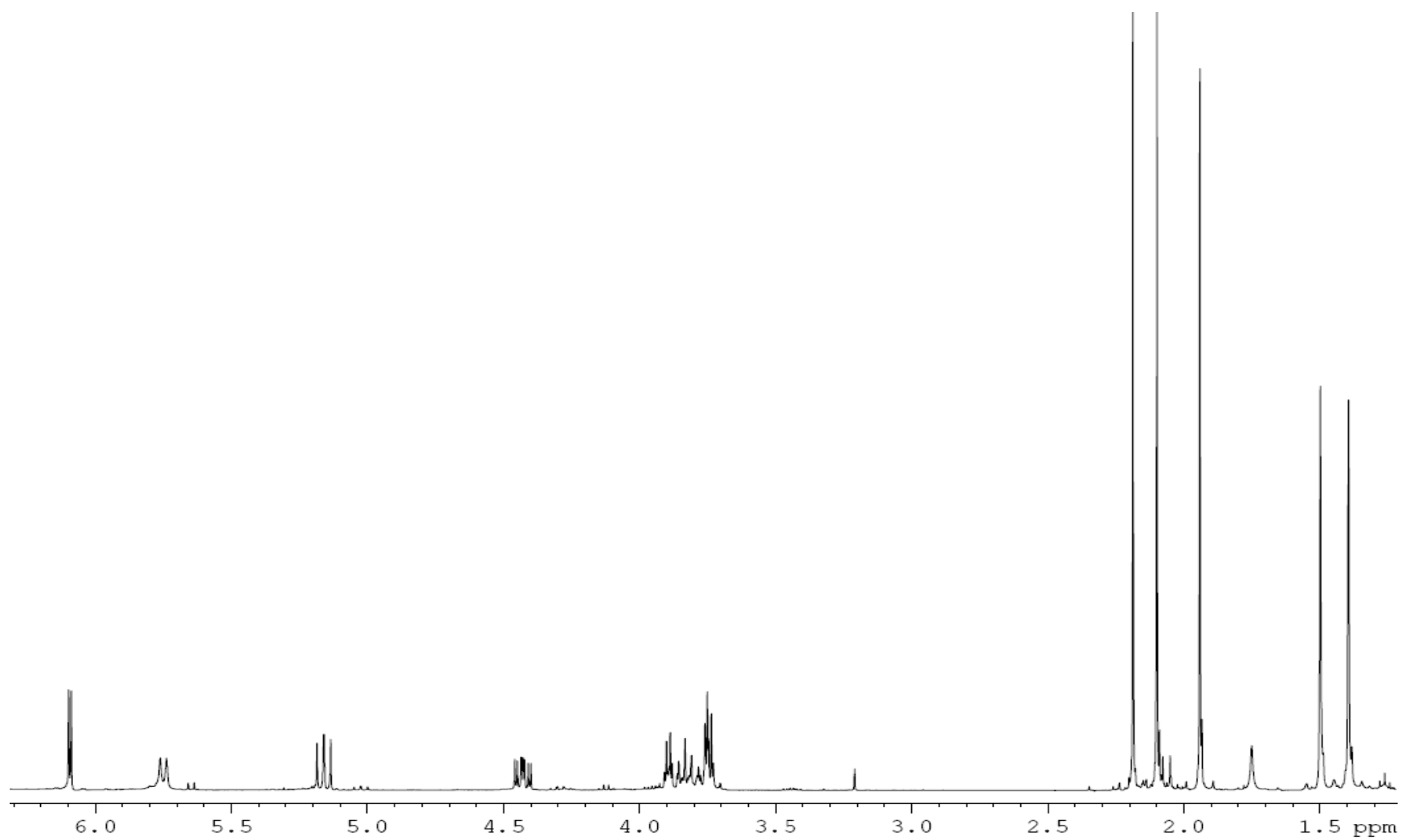
Figure 45: 400 MHz ^{1}H spectrum of **7α**.
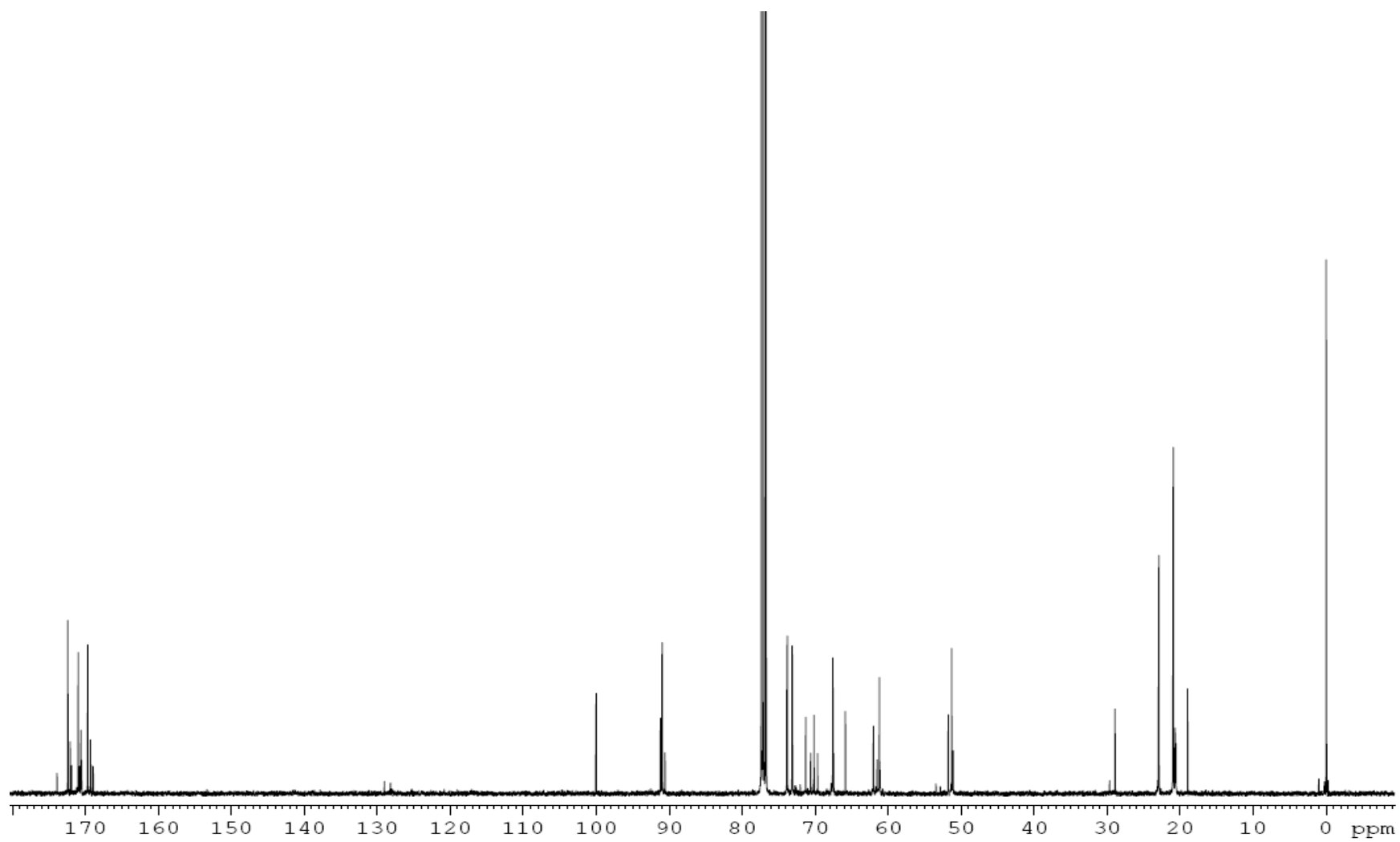
Figure 46: 100 MHz ^{13}C spectrum of **7α/β**.

Figure 47: Mass spectrum of **7α/β**.
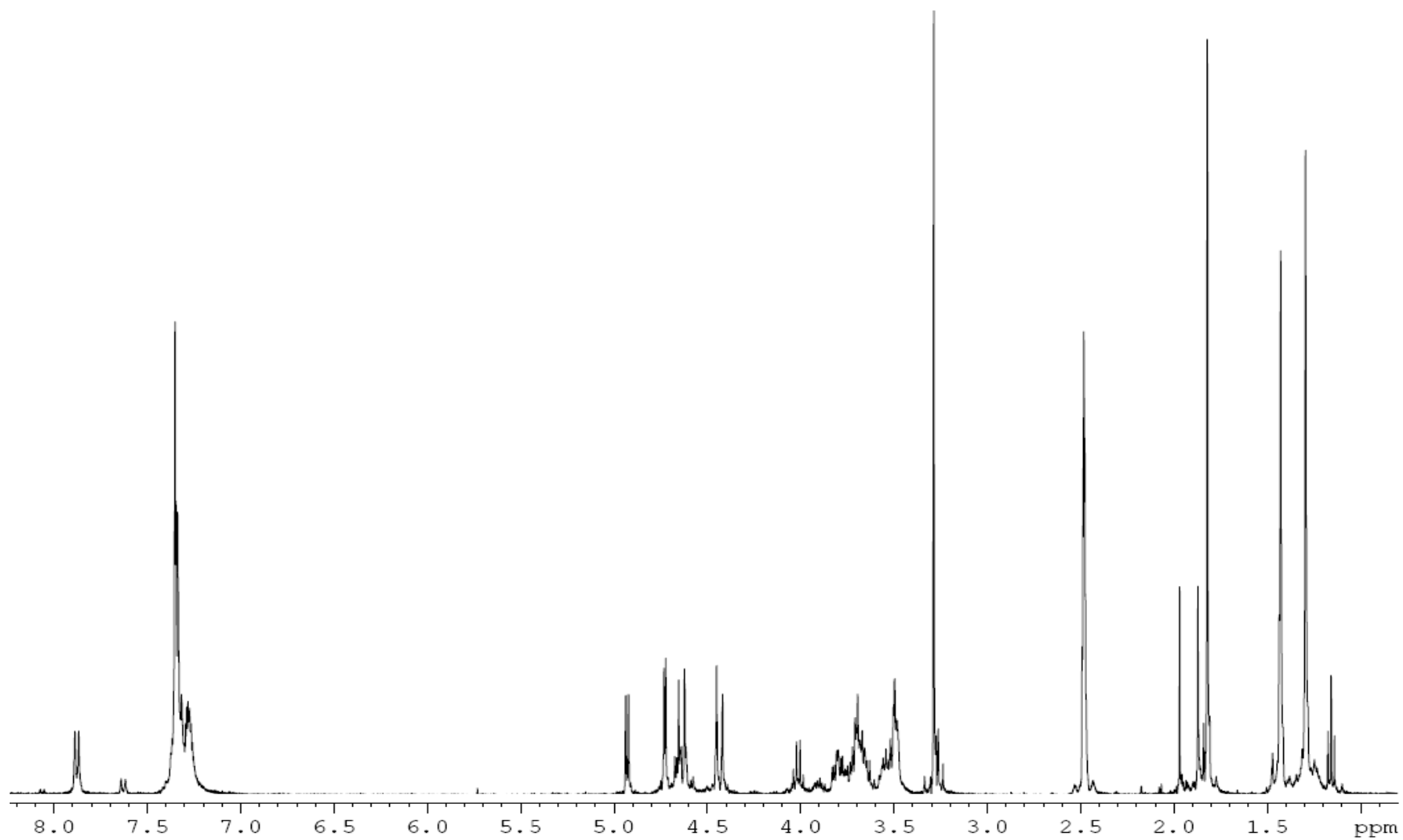
Figure 48: 400 MHz ^{1}H spectrum of **8α/β**.

Display Report

+MS

Figure 49: Mass spectrum of **8α/β**.
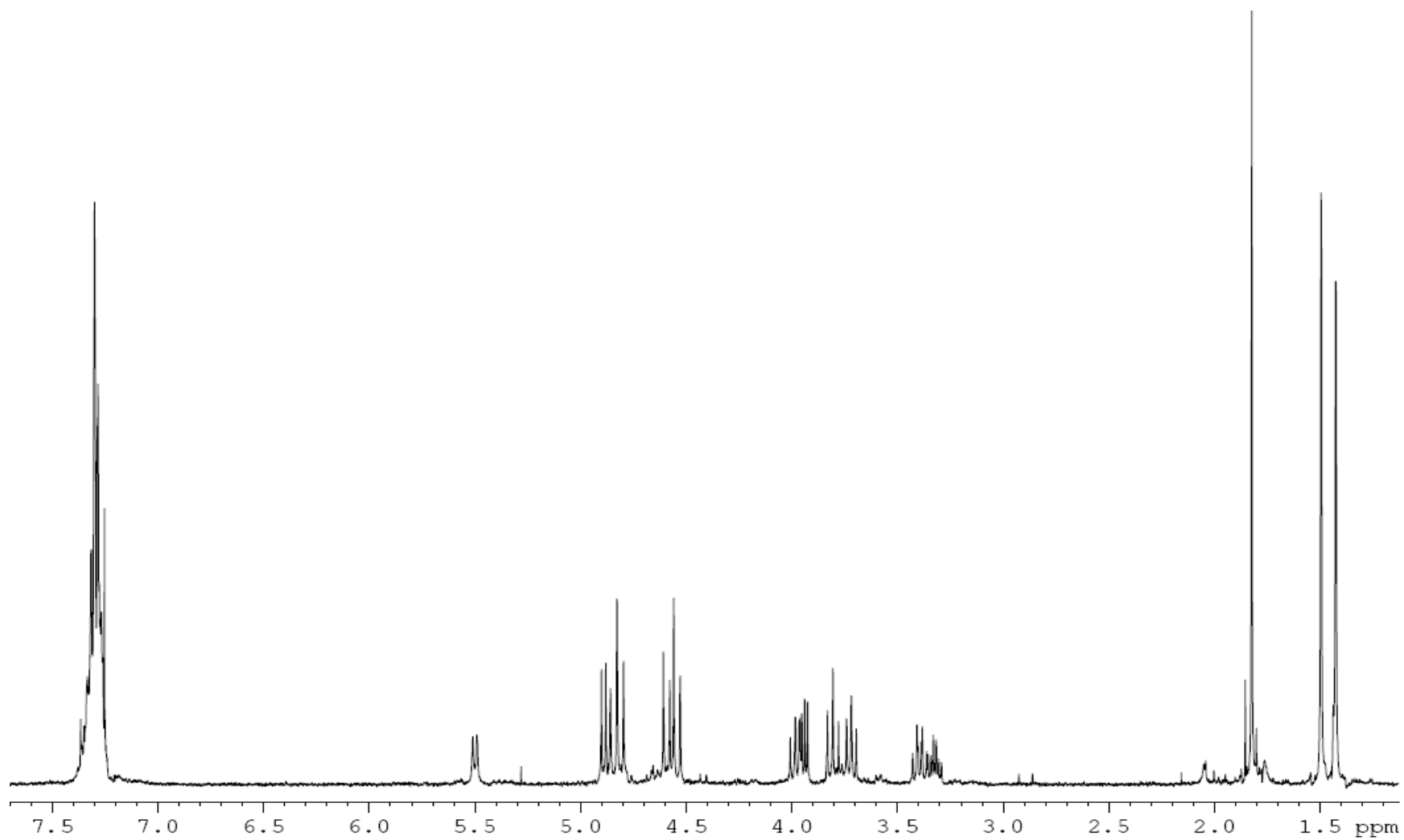
Figure 50: 400 MHz ^{1}H spectrum of **8β**.
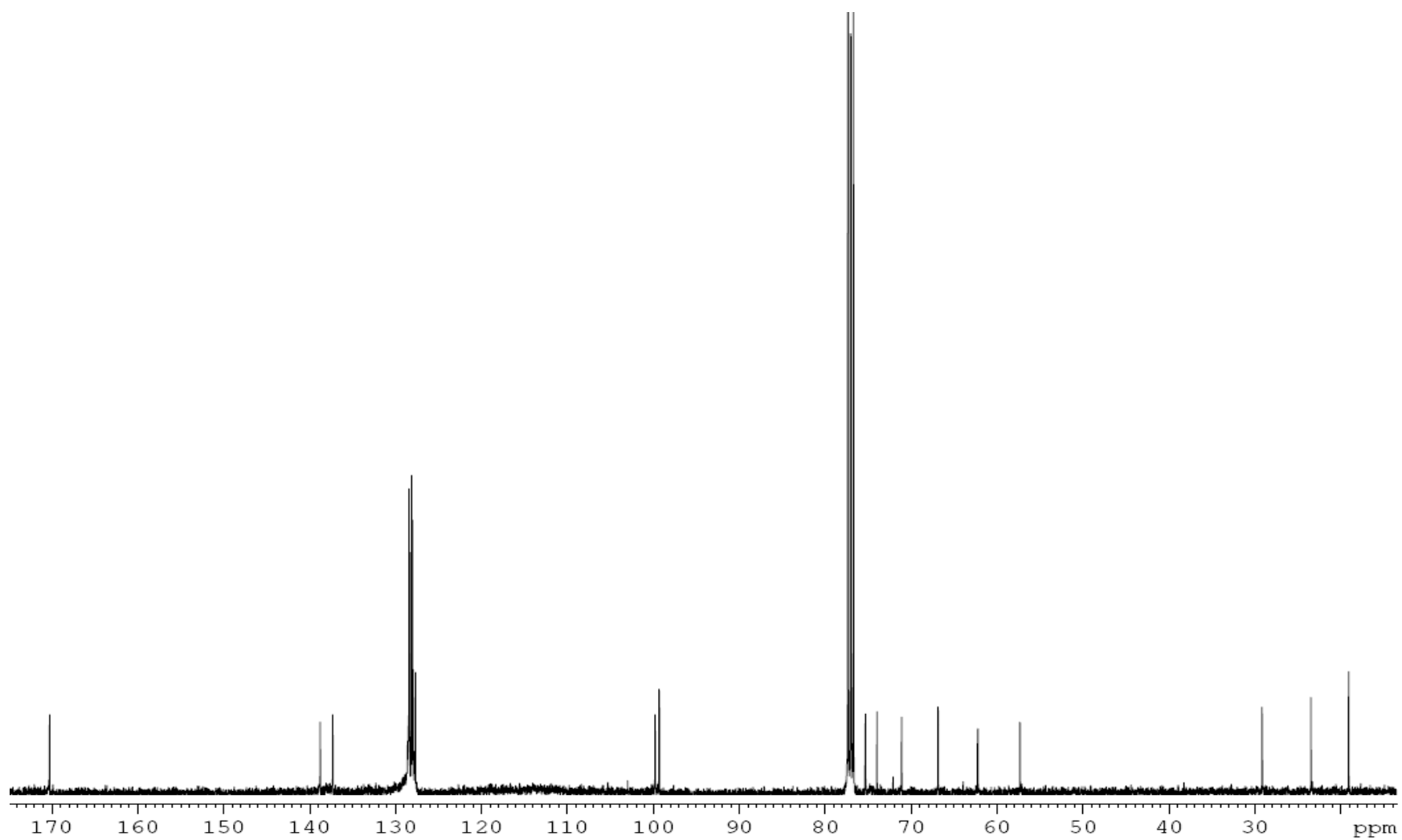
Figure 51: 100 MHz ^{13}C spectrum of **8β**.
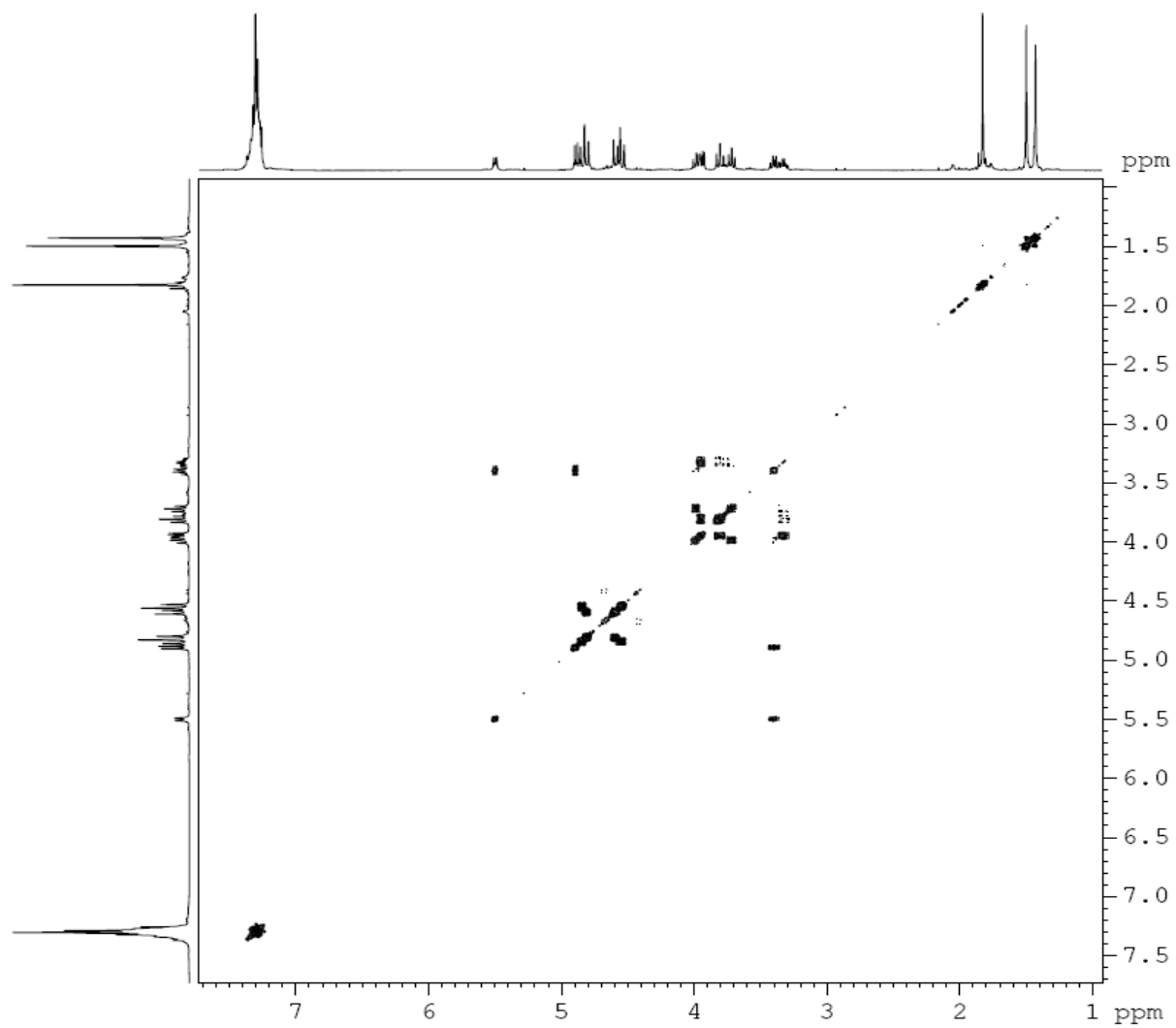
Figure 52: 400 MHz ^{1}H-^{1}H COSY spectrum of **8β**.
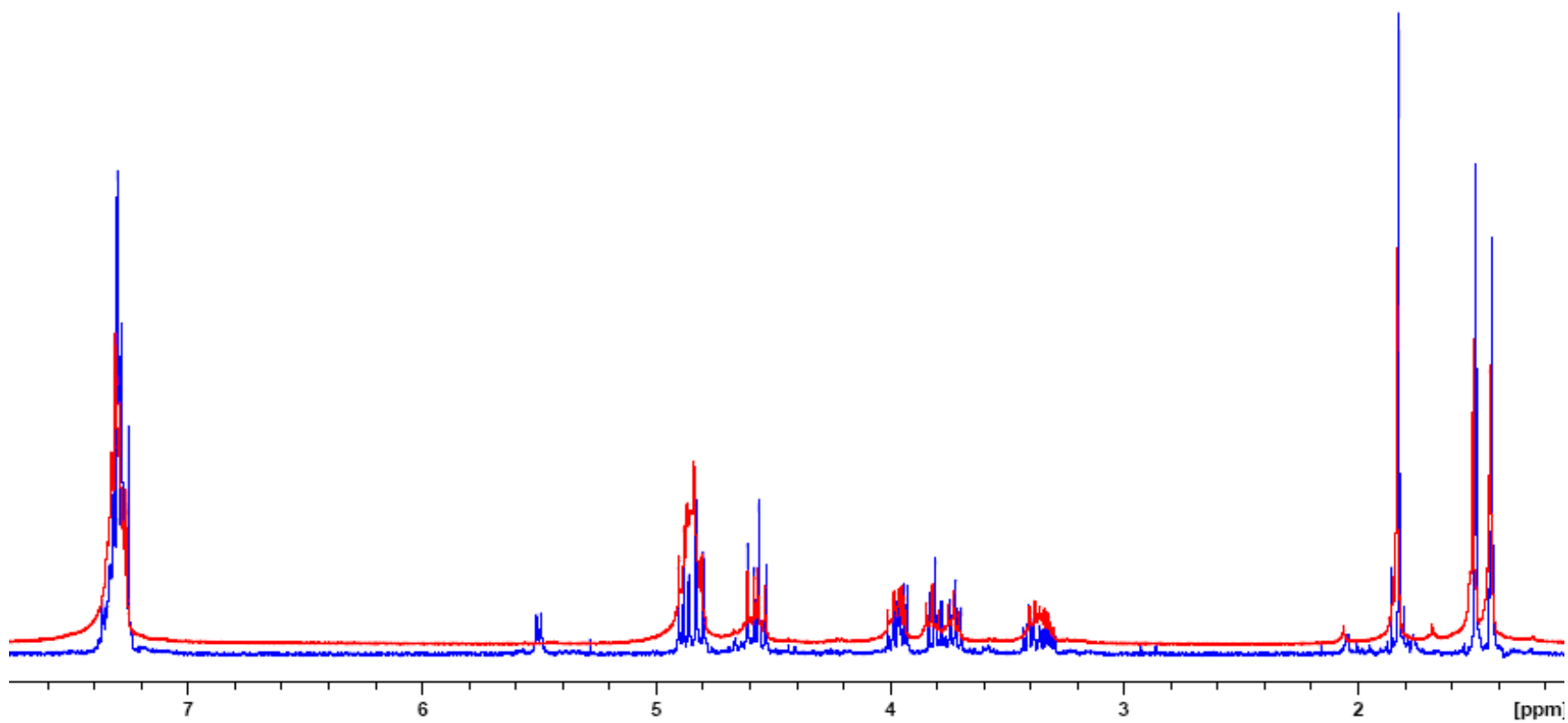
Figure 53: 400 MHz ^{1}H spectrum of **8β** with D$_2$O.

Figure 54: Mass spectrum of **8β**.
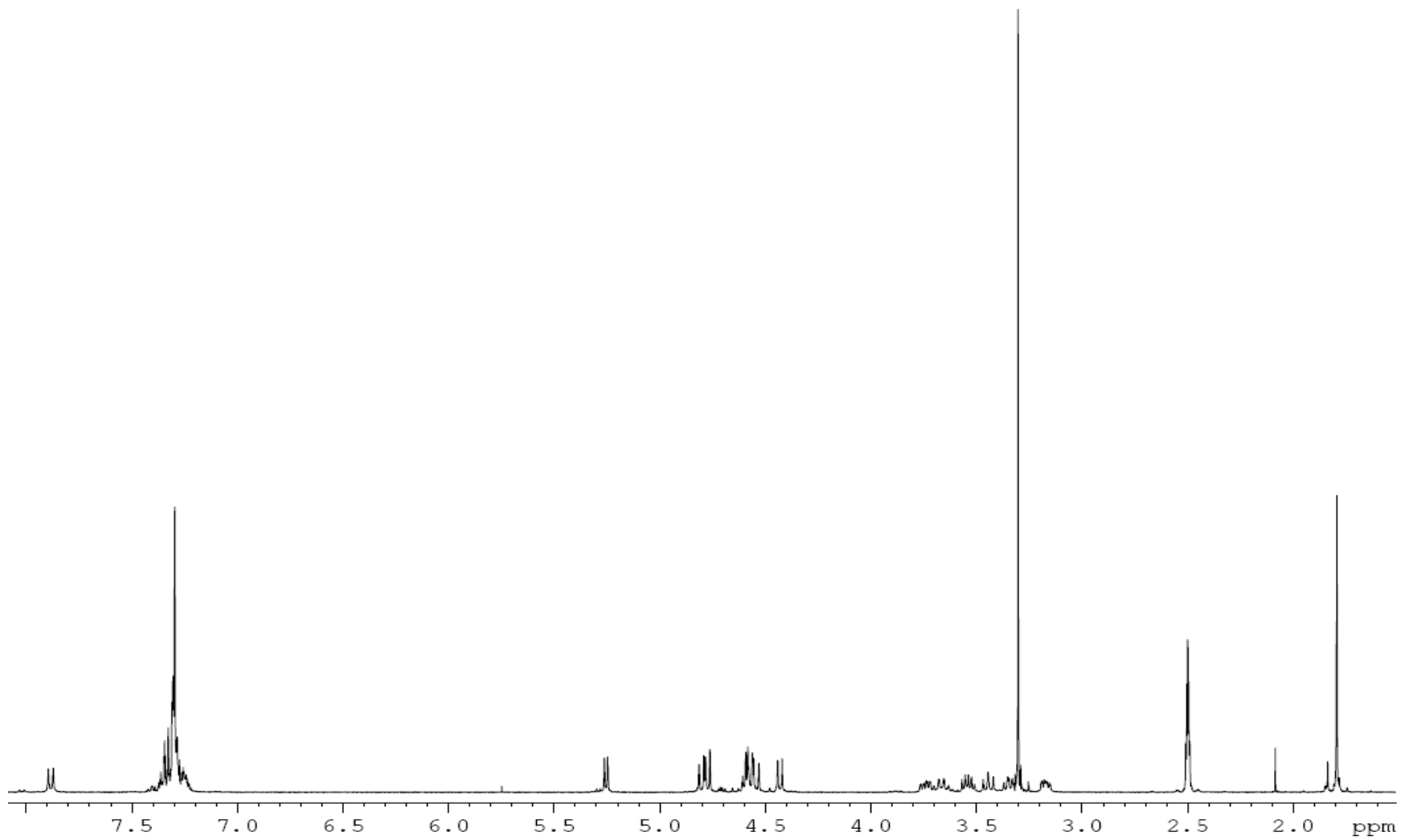
Figure 55: 400 MHz ^{1}H spectrum of **9α/β**.
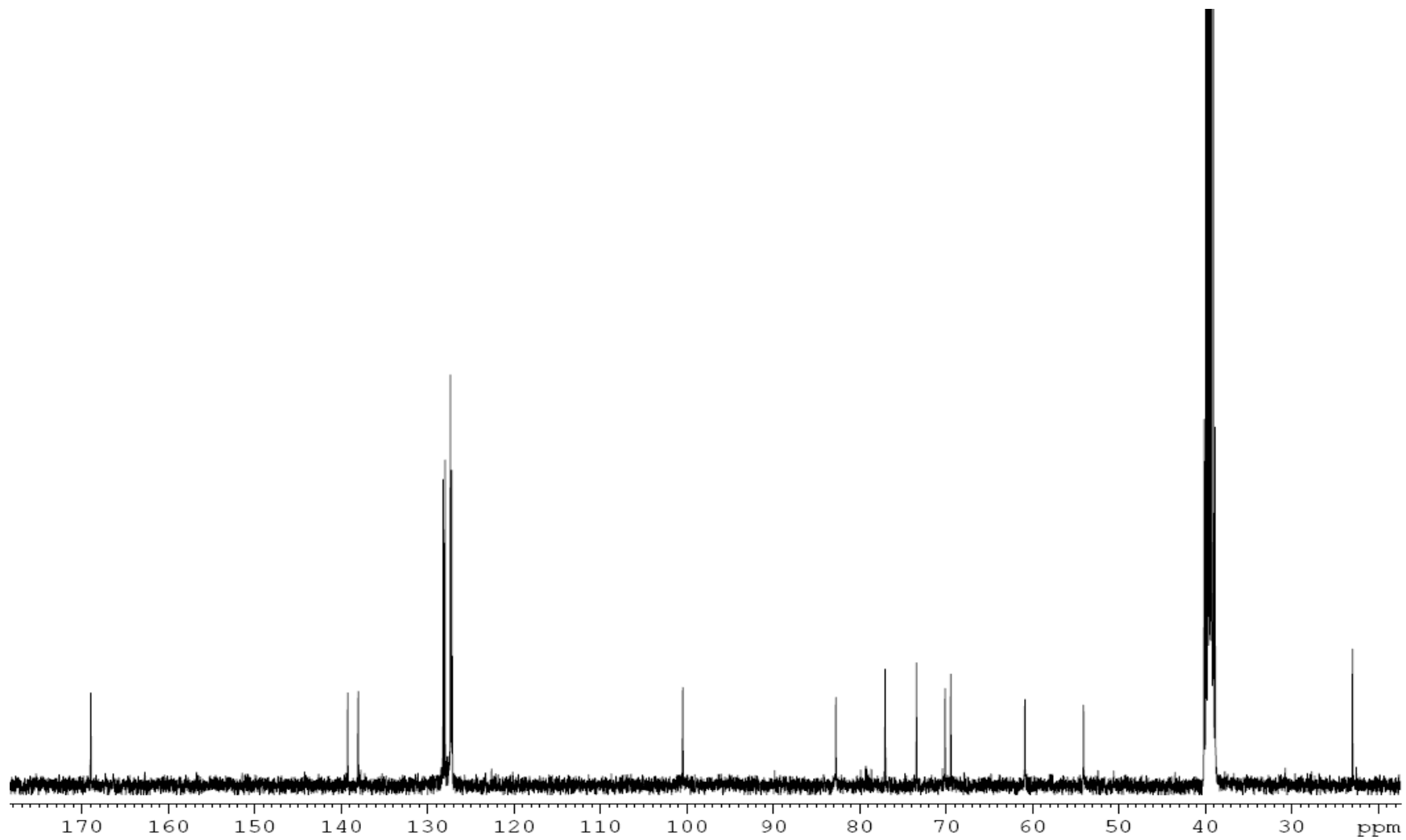
Figure 56: 100 MHz ^{13}C spectrum of **9α/β**.

Figure 57: Mass spectrum of **9α/β**.
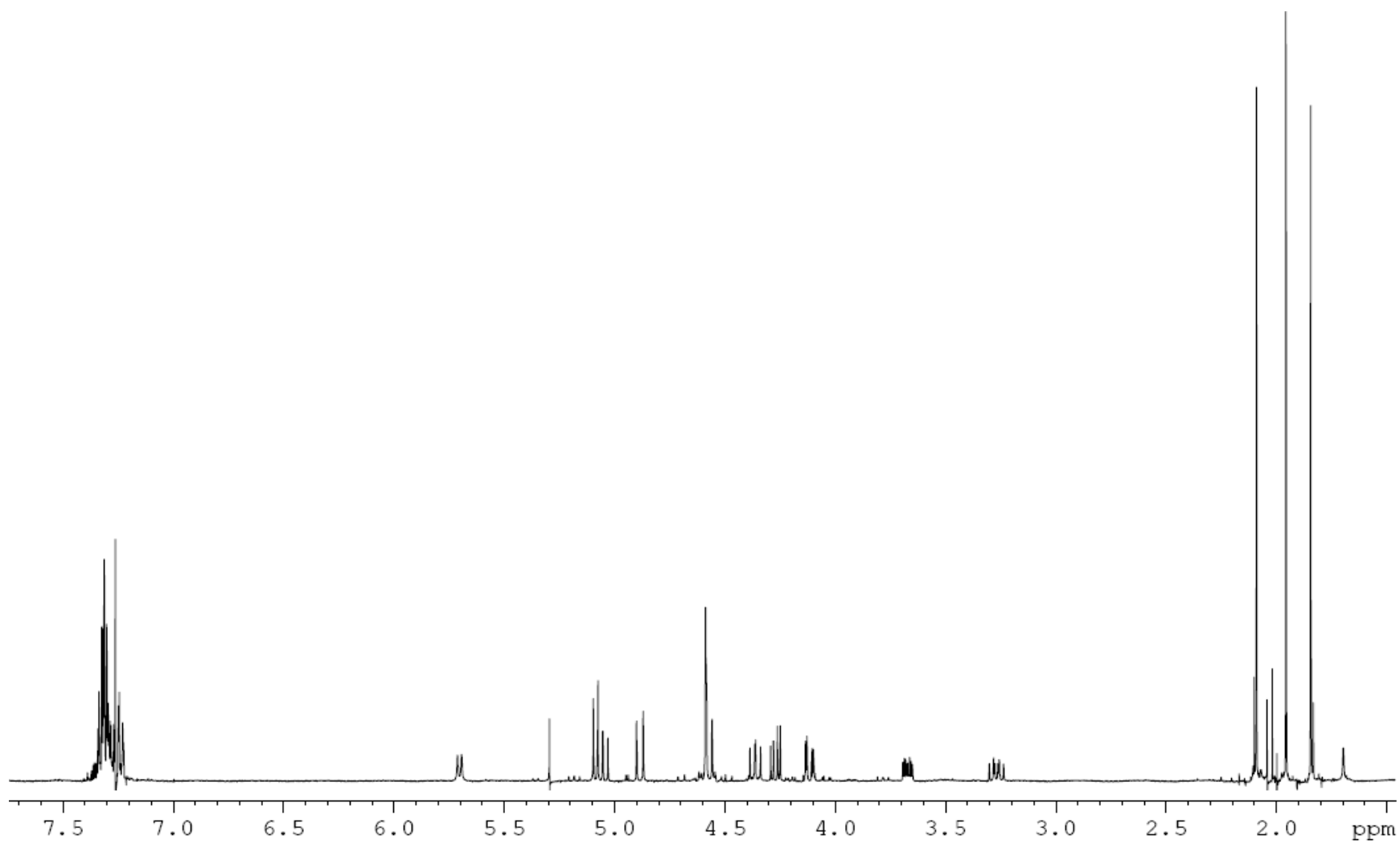
Figure 58: 400 MHz ^{1}H spectrum of **10β**.
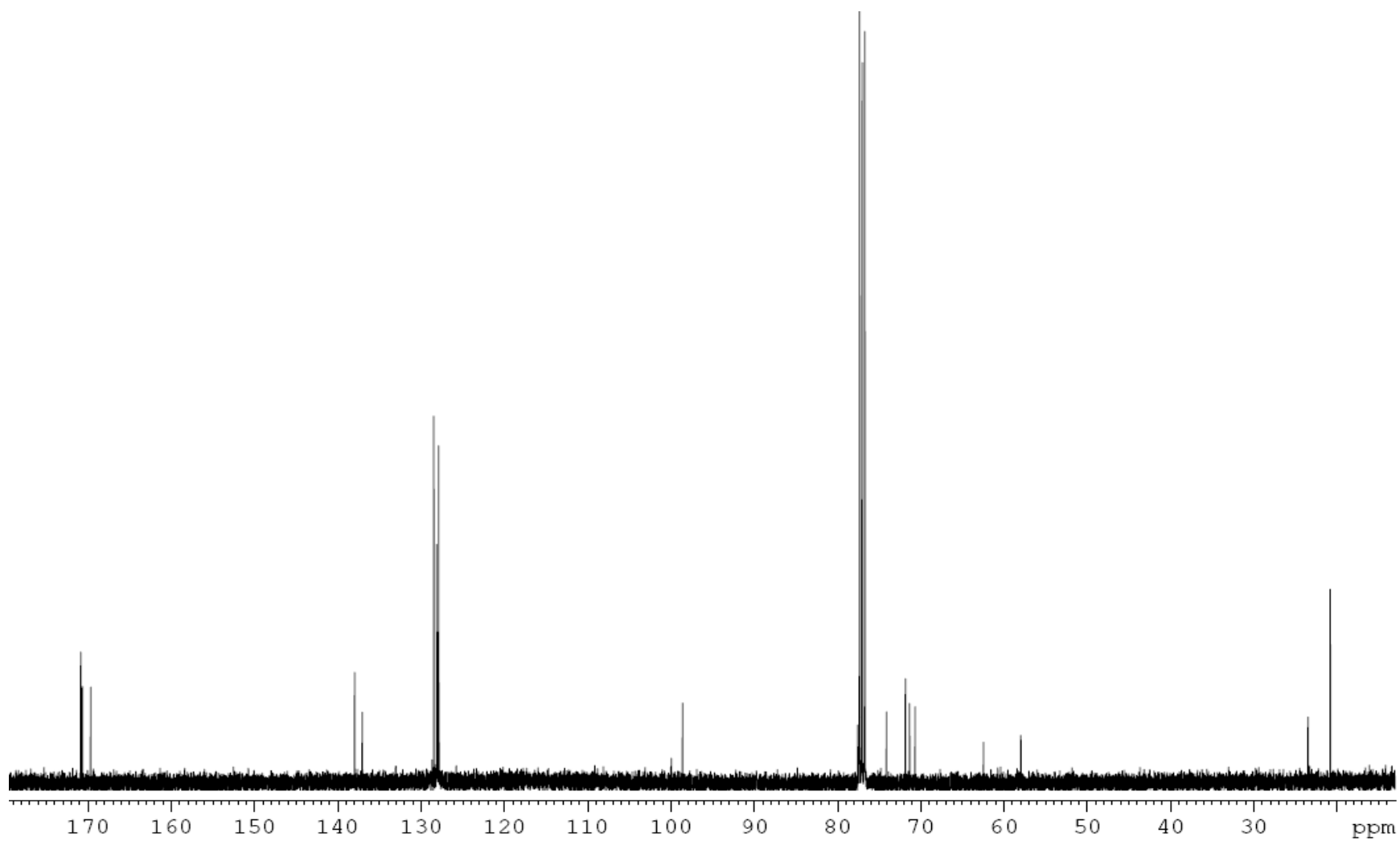
Figure 59: 100 MHz ^{13}C spectrum of **10β**.
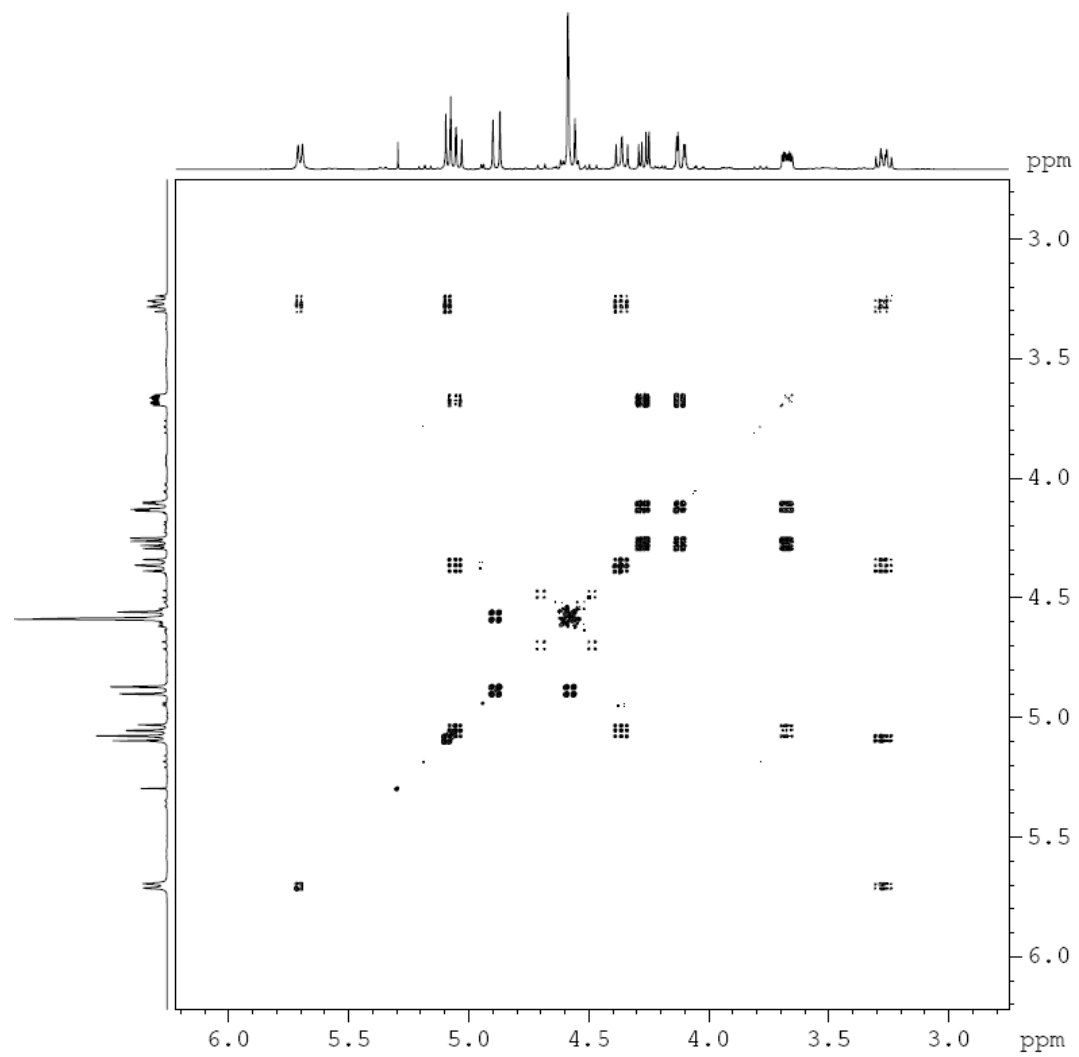
Figure 60: 400 MHz ^{1}H-^{1}H COSY spectrum of **10β**.

Display Report

Analysis Info

Analysis Name	ME2-1111.d	Acquisition Date	04/24/08 17:06:35	Operator	Administrator
Sample Name	ME-2-111	Method	XQ Default.ms	Instrument	Esquire-LC_00135
Comment	ME-2-111				

Acquisition Parameter

Ion Source Type	ESI	Mass Range Mode	Std/Normal	Ion Polarity	Positive	Alternating Ion Polarity	n/a
Scan Begin	15.00 m/z	Scan End	600.00 m/z	Averages	10 Spectra	Accumulation Time	20896 µs
Capillary Exit	119.3 Volt	Skim 1	42.5 Volt	Trap Drive	53.5	Auto MS/MS	Off

Bruker Daltonics DataAnalysis 3.0   printed: 04/24/08   17:37:06   Page 1 of 1
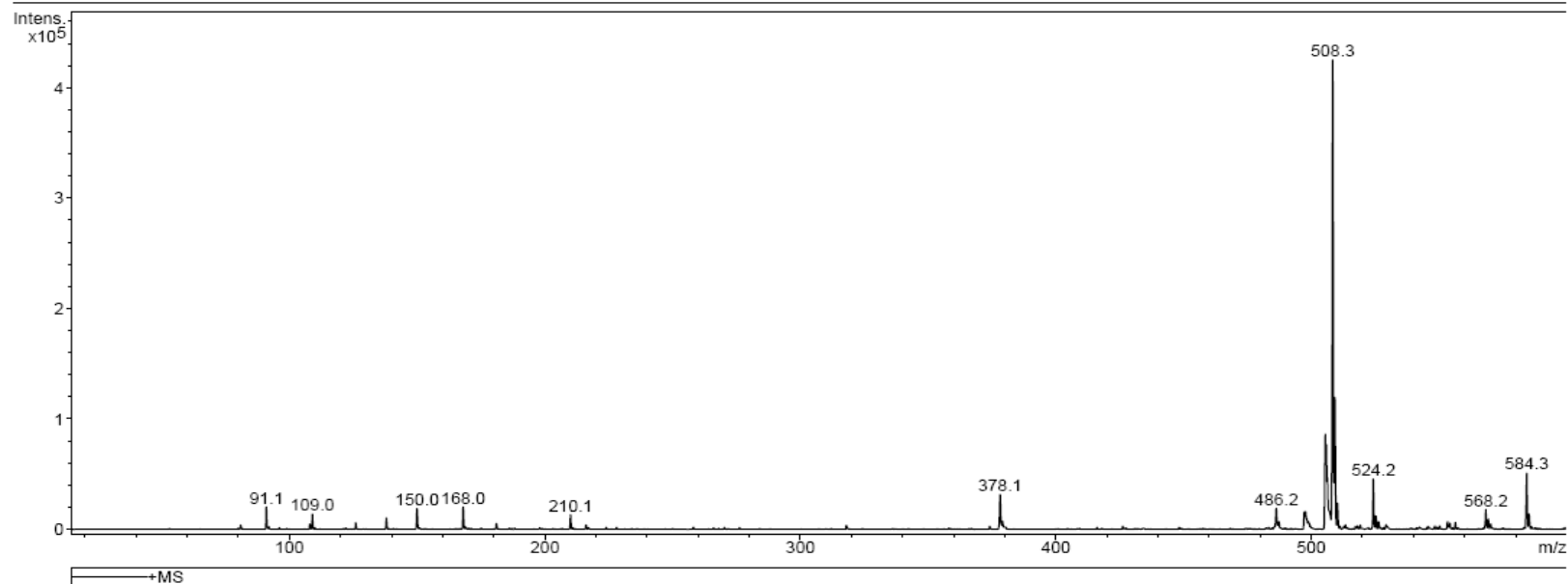
Figure 61: Mass spectrum of **10β**.
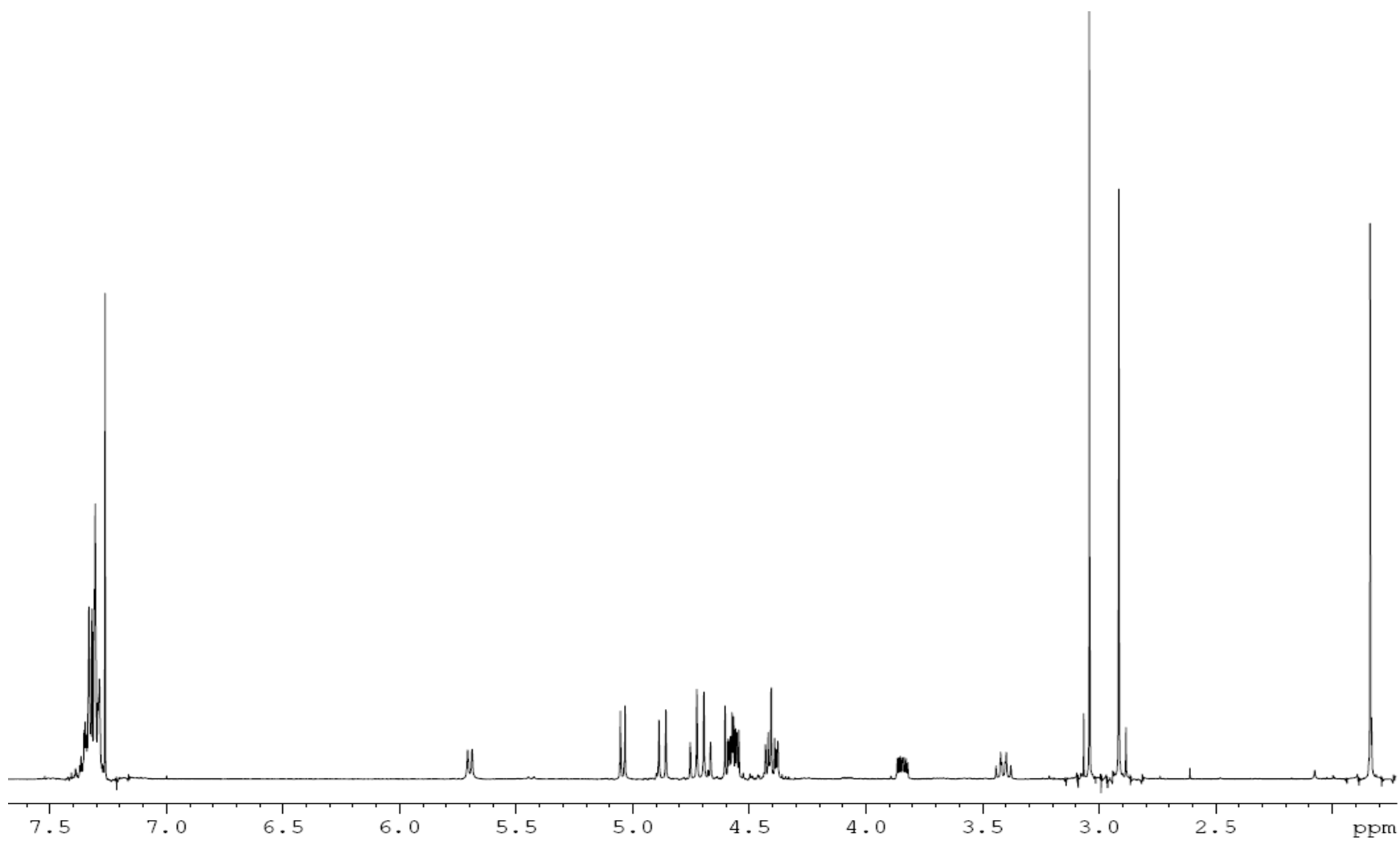
Figure 62: 400 MHz ^{1}H spectrum of **11β**.
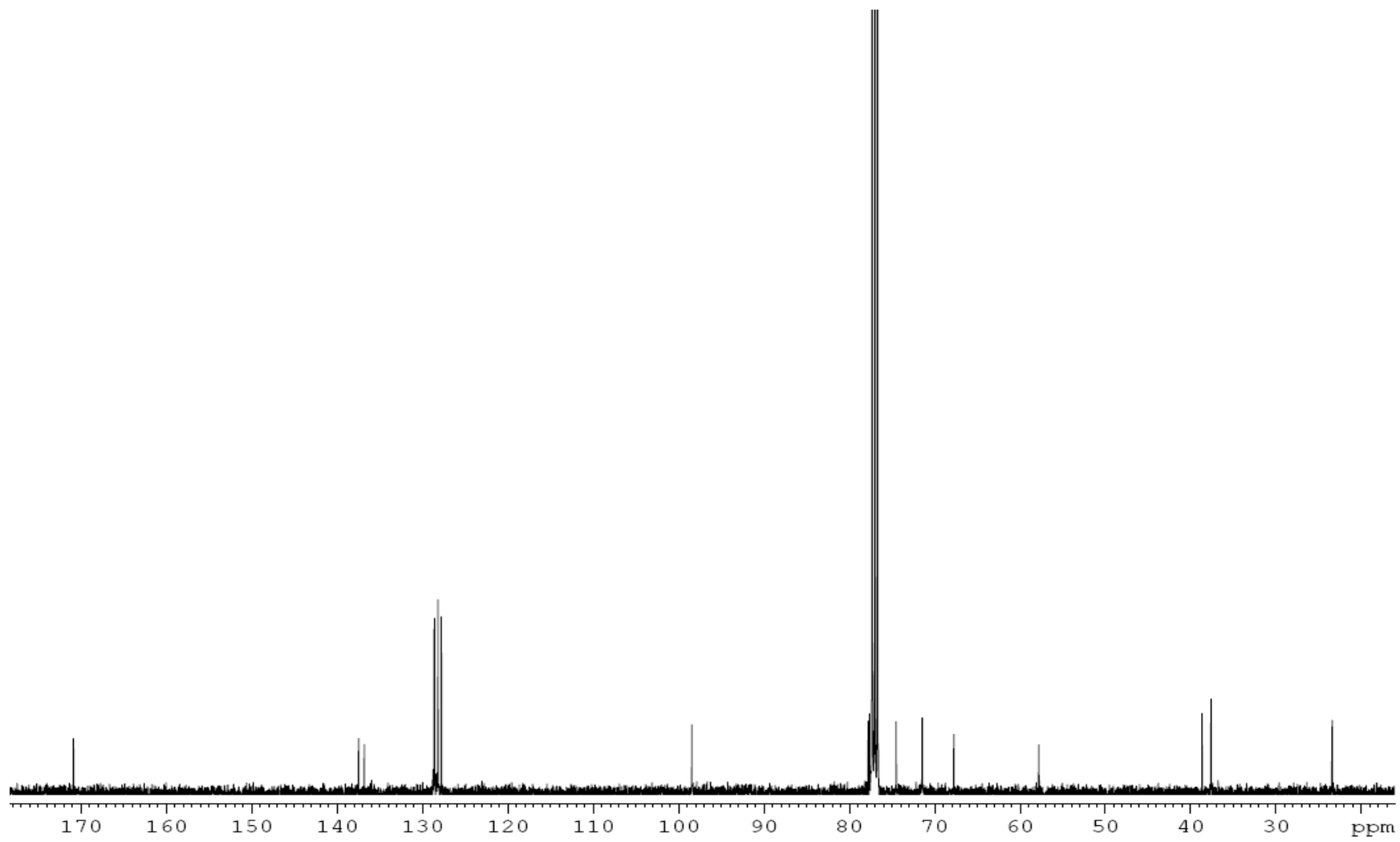
Figure 63: 100 MHz ^{13}C spectrum of **11β**.
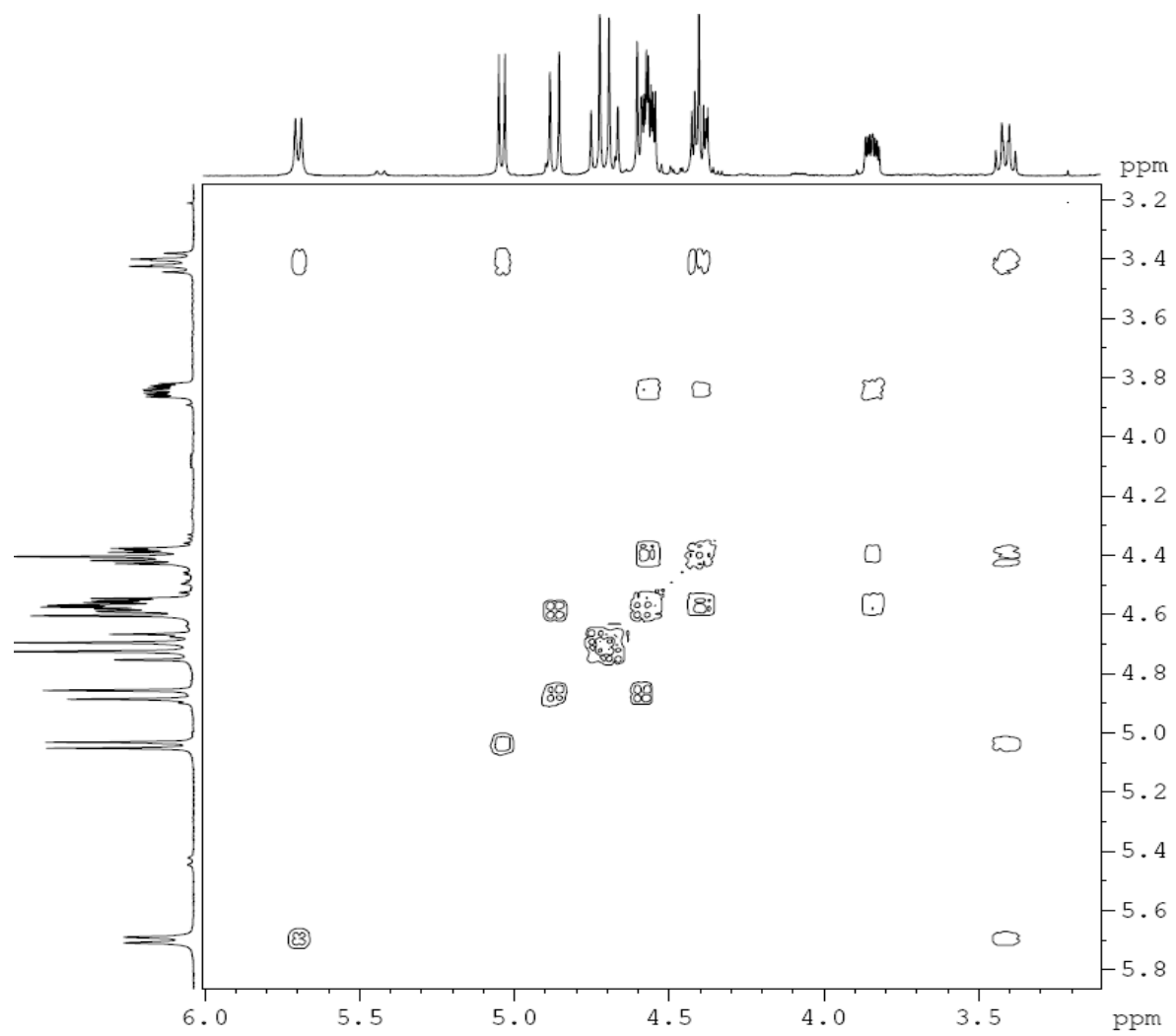
Figure 64: 400 MHz ^{1}H-^{1}H COSY spectrum of **11β**.

Figure 65: Mass spectrum of **11β**.
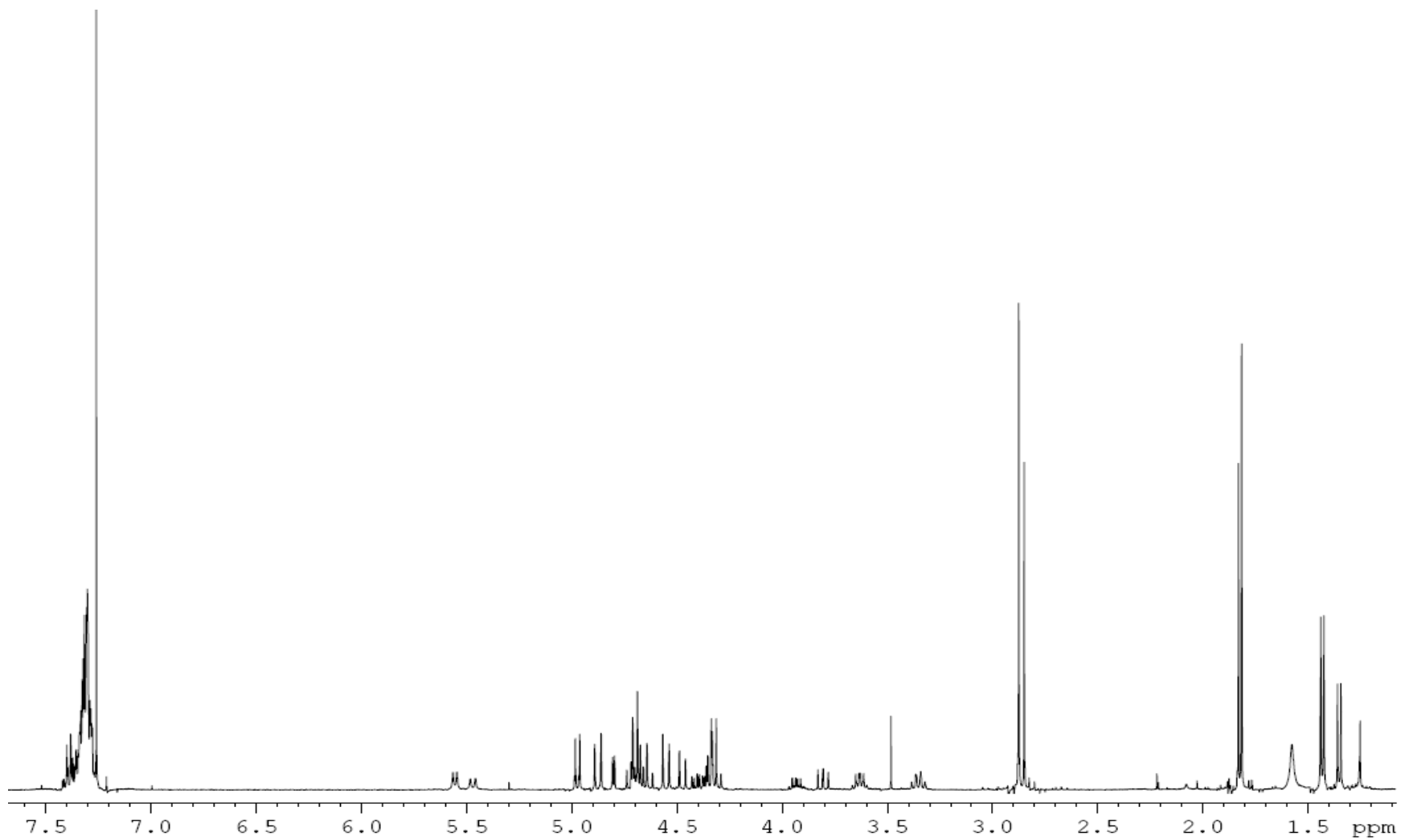
Figure 66: 400 MHz ^{1}H spectrum of **12α/β**.
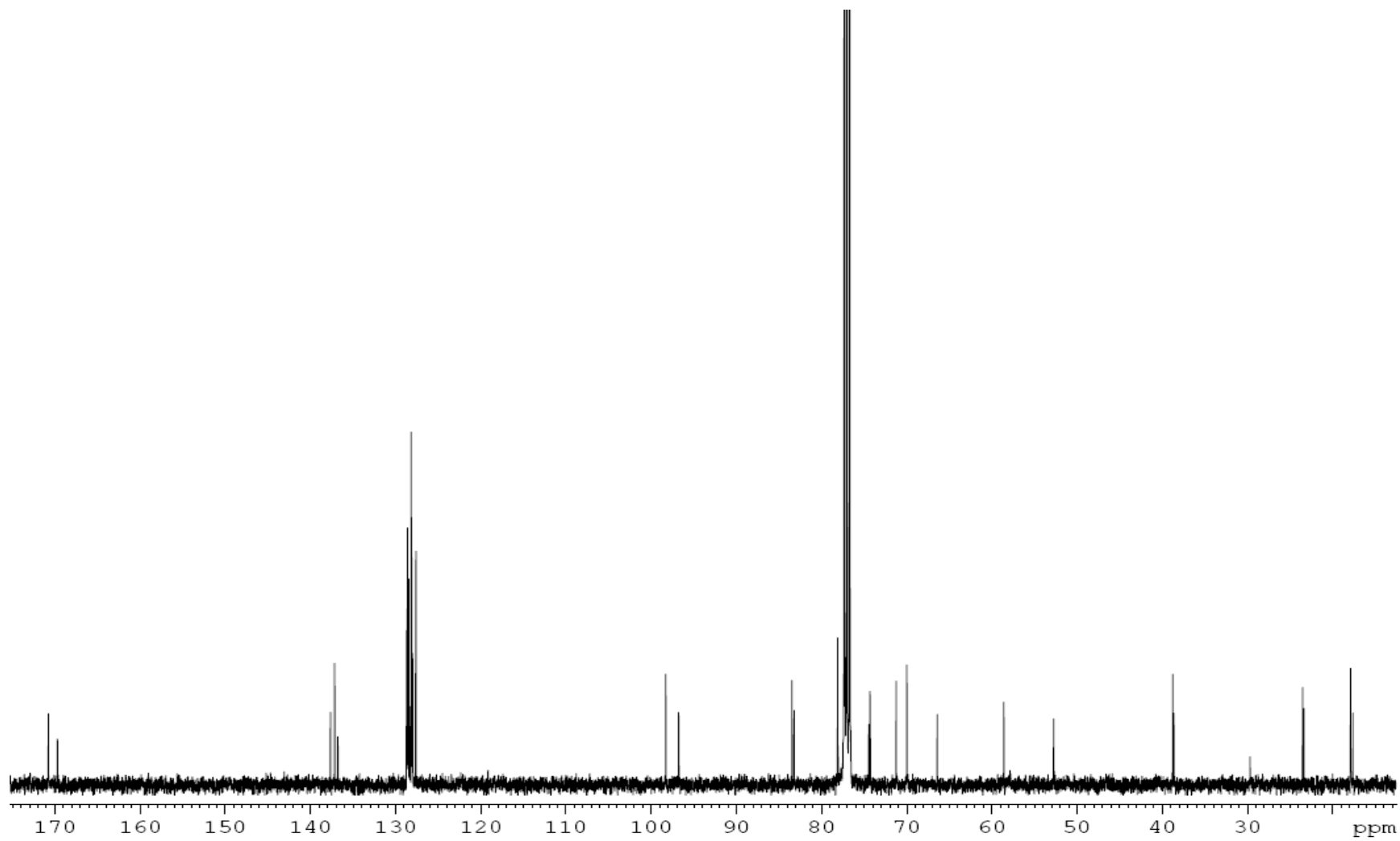
Figure 67: 100 MHz ^{13}C spectrum of **12α/β**.
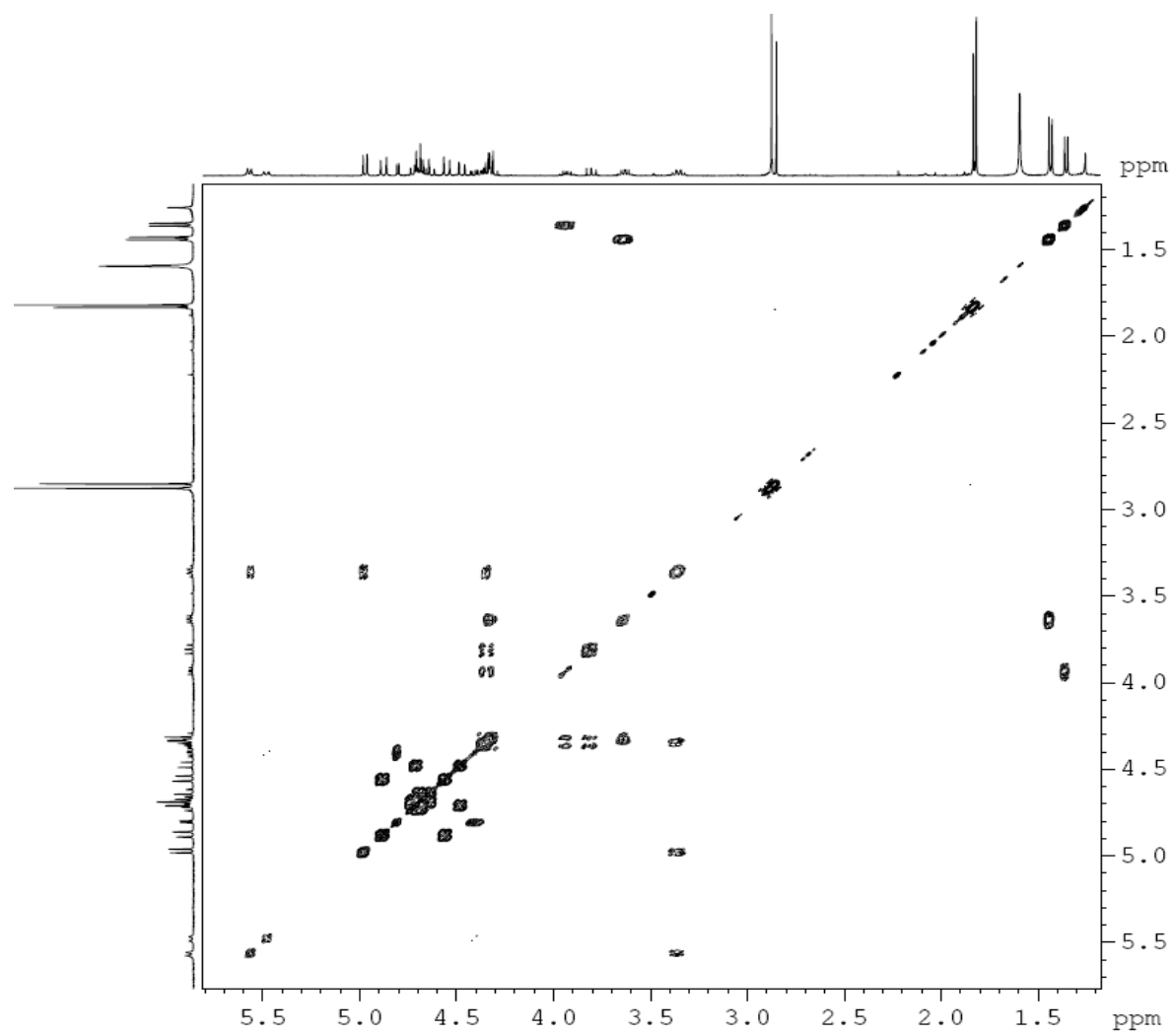
Figure 68: 400 MHz ^{1}H-^{1}H COSY spectrum of **12α/β**.

Figure 69: Mass spectrum of **12α/β**.
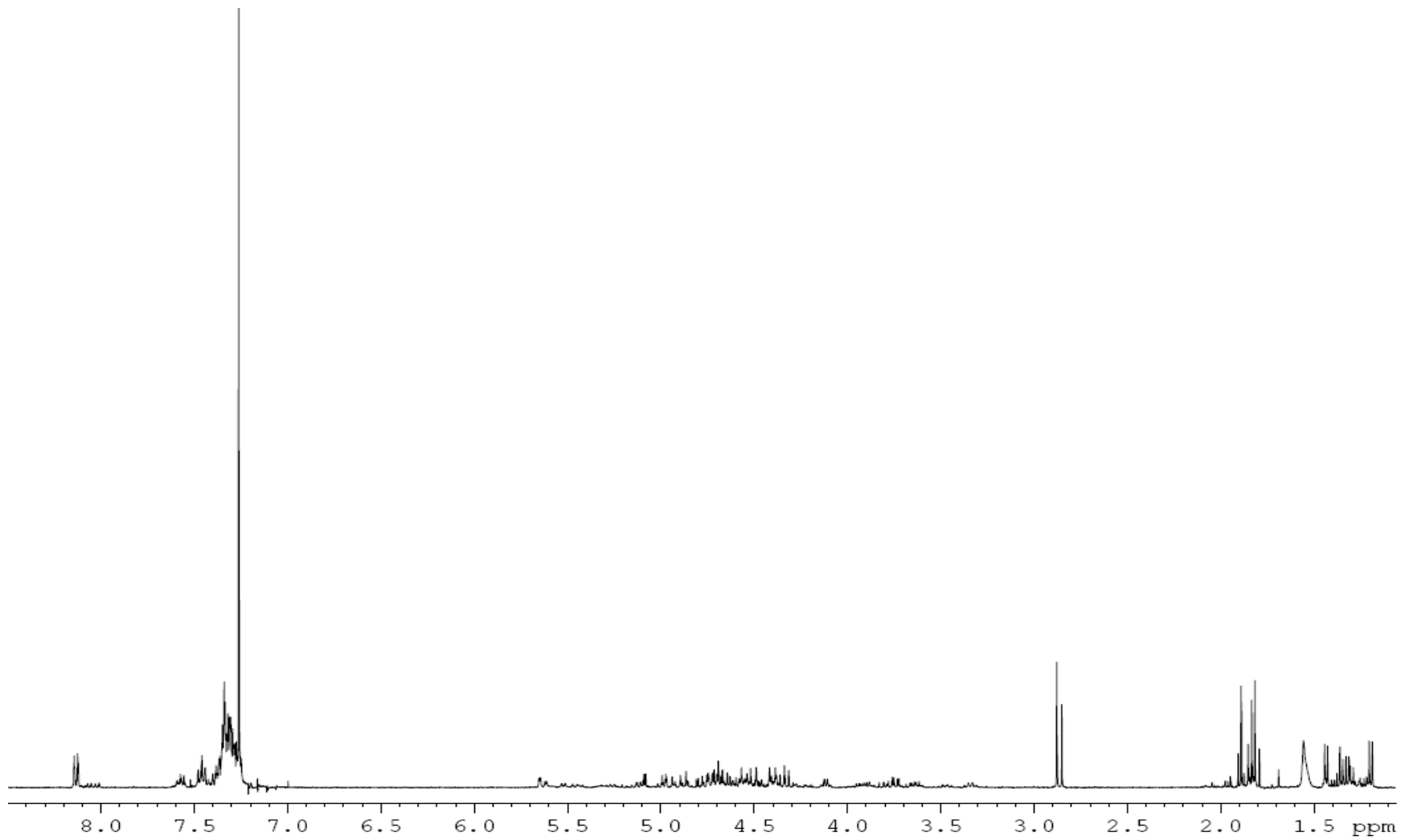
Figure 70: 400 MHz ^{1}H spectrum of **13α/β**.
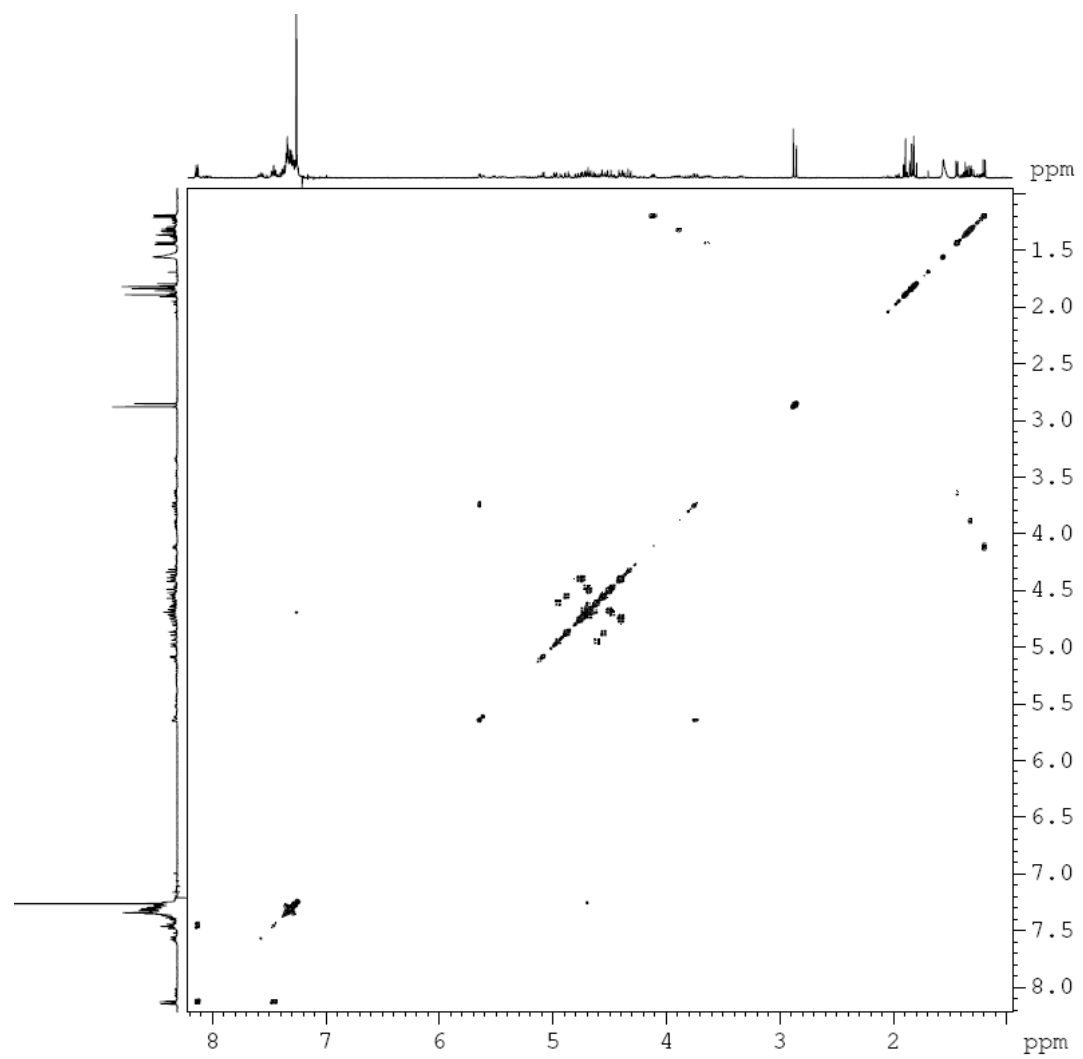
Figure 71: 400 MHz ^{1}H-^{1}H COSY spectrum of **13α/β**.
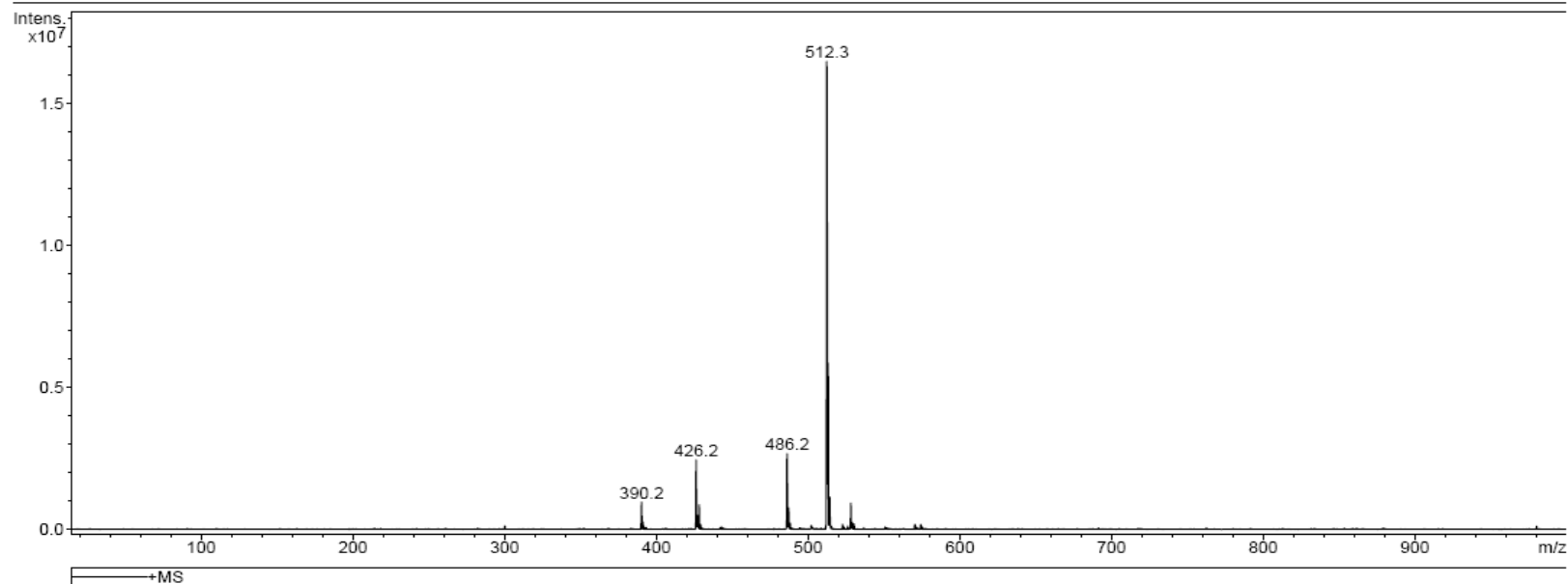
Display Report

Figure 72: Mass spectrum of **13α/β**.
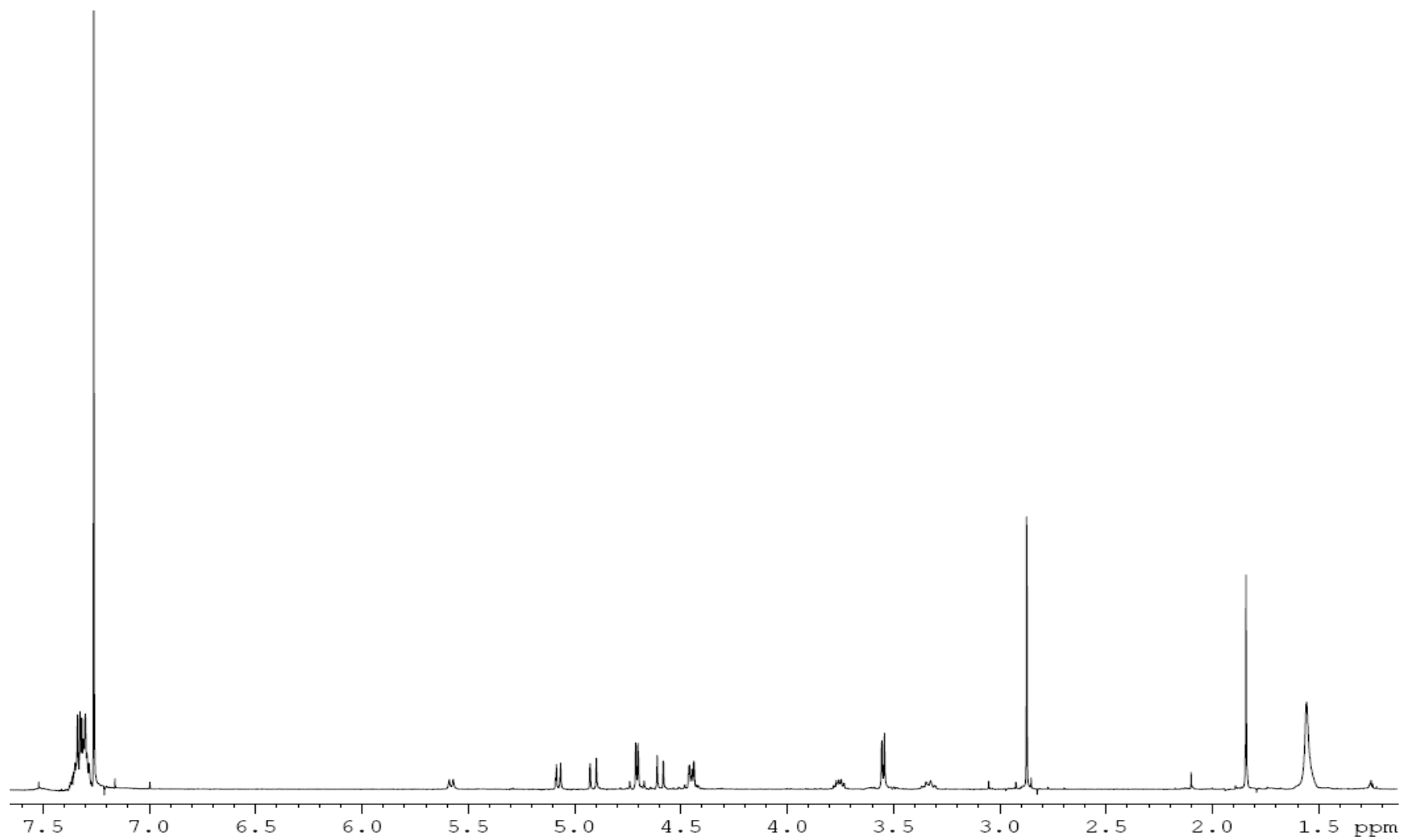
Figure 73: 400 MHz ^{1}H spectrum of **15β**.
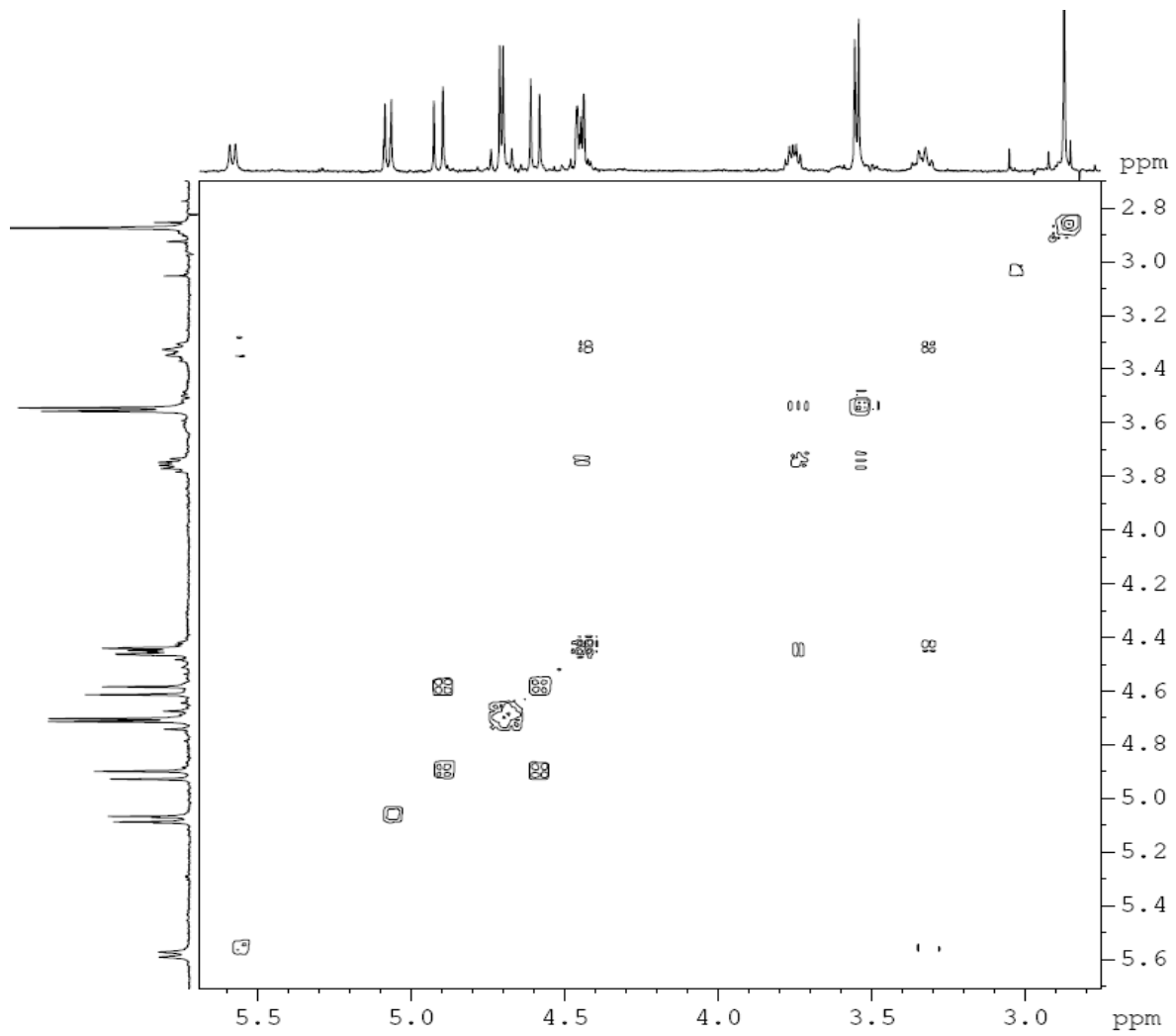
Figure 74: 400 MHz ^{1}H-^{1}H COSY spectrum of **15β**.

Figure 75: Mass spectrum of **15β**.